Chemical, molecular pharmacology and neuroprotective properties of the essential oil derived from Aloysia citrodora Palau

ABUHAMDAH, RUSHDIE,MOHAMMED,ALI,SAID

Chemical, molecular pharmacology and neuroprotective properties of the essential oil derived from *Aloysia citrodora* Palau

Rushdie Abuhamdah

A thesis submitted in accordance with the requirements for the degree of Doctor of Philosophy

School of Biological and Biomedical Sciences

Durham University

2013

Abstract

Essential oils derived from dried and fresh leaves of *Aloysia citrodora* were obtained by hydrodistillation, and were investigated for a range of pharmacological properties: receptor binding, *in vitro* acetylcholinesterase (AChE) inhibitory, antioxidant activities, and neuroprotection properties relevant to neurodegenerative diseases. Fresh leaf *A. citrodora* essential oil inhibited [^{3}H] nicotine binding to well washed rat forebrain membranes, with mean apparent IC_{50} of 0.0018 mg/ml. No significant binding activity was observed for *A. citrodora* essential oil derived from fresh or dried leaves, for $GABA_AR$ and NMDARs. *A. citrodora* essential oil, both dried and fresh, exhibited radical scavenging activity (up to 100%, IC_{50} < 0.0001 mg/ml) and iron (II) chelating properties (approx. IC_{50} = 0.05 mg/ml), and showed neuroprotective characteristics against the toxic effects of H_2O_2 (100%, 0.001 mg/ml) and β-amyloid (approx. 50%, 0.01 mg/ml) in CAD neuronal cell culture. Both EOs from dried and fresh leaves also displayed effective AChE inhibitory activity, with the dried leaves oil displaying more clear AChE inhibitory activity than fresh oil, which could be related to the higher respective levels of caryophyllene oxide. Recombinant human anticholinesterase enzyme was used for structure based *in silico* screening of *A. citrodora* essential oil constituents for AChE Inhibitors, and the top scoring hits with highest pharmacophore fit values showed common interactions with residues at the active site of that of donepezil. The top seven hits in order of fit score, were β-curcumene, curcumene bisabolene, trans-calamenene, caryophyllene oxide, β-sesquiphellandrene and geranyl acetate. This indicates that plants may yield novel effective and safe AChE inhibitors, other than alkaloids. To begin to identify the chemicals underpinning the pharmacological properties of *A. citrodora*, GC/MS analysis of the chemical composition of the essential oil from leaves of *A. citrodora* identified eighty three major chemicals, including the presence of terpenoids, monoterpenes and sesquiterpenes, and 6-methyl-5-hepten-2-one, the main constituents being limonene, caryophyllene oxide, curcumene, spathulenol, 1,8-cineole constituting 47% of the total oil. Finally, a simple, inexpensive solid phase extraction method was developed for fractionation of essential oils. Collectively, this thesis provides a better understanding of the pharmacology of the *Aloysia* essential oil and its constituents relating to its potential use in the treatment neurodegenerative disease.

List of Contents

Chapter 1

Chapter 2

Chapter 3

Cholinergic, Anti-Oxidant and Iron Chelation Properties

Chapter 4

Neuroprotective Properties

Chapter 5

Analysis and Solid Phase Fractionation

List of Abbreviations

Aβ	β-amyloid
ACh	Acetylcholine
AChE	Acetyl cholinesterase
AD	Alzheimer's disease
AMPA	2a-amino-3-hydroxy-5-methyl-4-isoxazolepropionic acid
ALS	Amyotrophic lateral sclerosis
APP	Amyloid Precursor Protein
B_{max}	Maximum number of receptors per mg protein
BSA	Bovine serum albumin
BPSD	Behavioral and Psychological Symptoms of Dementia
BZ	Benzodiazepine
CNS	Central nervous system
CO_2	Carbon dioxide
^oC	Degrees centigrade
Cl^-	Chloride ions
COX-2	Cyclooxygenase-2
CNS	Central Nervous System
DLB	Dementia with Lewy bodies
DMEM	Dulbecco's Modified Eagle Medium
DMSO	Dimethyl sulphoxide
DNA	Deoxyribonucleic acid
dH_2O	Distilled water
EC_{50}	Concentration of competitor that competes with half of the specific binding
E_{max}	Maximum response
EAAT-2	Excitatory amino-acid transporter 2
EDTA	Ethylenediaminetetracetic acid
EGTA	Ethylenebis(oxyethylenenitrilo)tetracetic acid
FCS	Foetal calf serum
Fm	Femto moles
FRET	Fluorescence Resonance Energy Transfer Technique
FLIPR	Fluorescence Imaging Plate Reader
GABA	γ-aminobutyric acid
$GABA_AR$	γ-aminobutyric acid type receptor type A
GAD	Glutamic acid decarboxylase
GAT	GABA transporters
GF/B	Glass fibre filters
GluR2	Glutamate receptor 2
GRIF-1	GABA receptor interacting factor-1
H_2O_2	Hydrogen peroxide
HCL	Hydrochloric acid
HD	Huntingdon's disease
HEK 293	Human embryonic kidney 293 cells
HEPES	N-2-Hydroxyethylpiperazine-N'-2-ethanesulphonic acid
HRP	Horseradish peroxidise
5-HT	5-hydroxy-tryptamine
IC_{50}	Concentration of ligand giving 50% inhibition of specific binding

K_D	Dissociation constant
kDa	Kilodaltons
K_I	Inhibition constant
KCC1	K^+/ Cl^- co-transporter (1)
KCC2	K^+/ Cl^- co-transporter (2)
LGIC	Ligand gated ion channel
LOX	Lipoxygenase
M	Molar
mA	Milli amps
MFA	Mefenamic Acid
µg	Microgram
MK-801	(+)-5-Methyl-10,11-dihydr-5*H*-dibenzo[a,d]cyclohepten-5,10-imine
ml	Milli-litre
mM	Milli-molar
M_1	Muscarinic acetylcholine receptors subtype1
NaCl	Sodium chloride
NADPH	Nicotinamide Adenine Dinucleotide Phosphate
$NaHCO_3$	Sodium hydrogen carbonate
NaOH	Sodium Hydroxide
Na-Az	Sodium azide
nAChR	nicotinic acetylcholine receptor
NO	Nitric oxide
NOS	Nitric oxide Synthase
n_H	Hill coefficients
nM	Nano Molar
NSAIDs	Non-steroidal anti-inflammatory drugs
NMDA	*N*-methyl-D-aspartate
O.D.	Optical density
8-OH-DPAT	8-hydroxy-2-(di-n-propylamino) tetralin
PAGE	Polyacrylamide gel electrophoresis
PD	Parkinson's disease
PBS	Phosphate buffered saline
pH	Potential of Hydrogen
PLA2	Phospholipase A2
ROS	Reactive Oxygen Species
RNA	Ribonucleic acid
RA	Rheumatoid arthritis
SAR	Structure Activity Relationship
SDS	Sodium dodecyl sulphate
TBS	Tris-buffered saline
TBPS	t- butylbicyclophosphorothionate
TE buffer	Tris-HCL, EDTA buffer
TEMED	N,N,N,´N´-Tetramethyletylenediamine
THDOC	5α-pregnane-3 α, 21-diol-20-one
Tris	Tris (hydroxymethyl) methylamine
UV	Ultra-violet
V	Volts
VD	Vascular Dementia
V/v	Volume per volume
w/v	Weight per volume

List of Figures

List of Tables

Declaration

I confirm that no part of the material presented has previously been submitted for a degree in this or any other university. If material has been generated through joint work, my independent contribution has been clearly indicated. In all other cases, material from the work of others has been clearly indicated, acknowledged and quotations and paragraphs indicated.

List of Publications

Peer reviewed original publications

- Novel anti-acetylcholinesterase inhibitor chemotypes from an essential oil derived from leaves of lemon verbena (*Aloysia citriodora* Palau): a ligand-based modelling approach. ***J Comput Aided Mol Des.*** **(in preparation).** Rushdie Abuhamdah, Georgina Uttley, Sawsan Abuhamdah, Melanie-Jayne Howes, Emke Pohl and Paul L Chazot.

- Novel Solid Phase fractionation method of Jordanian and European essential oils. ***Eur J Med Plants*** **(submitted)** Rushdie Abuhamdah, Sawsan Abuhmadah, Melanie-Jayne Howes, Michael Carroll and Paul L. Chazot.

- Pharmacological profile of an essential oil derived from leaves of lemon verbena (*Aloysia citriodora* Palau): anti-oxidant, iron chelation and neuroprotective properties. ***J Pharmacol Pharm*** **(submitted)** Sawsan Abuhamdah*, Rushdie Abuhamdah*, Melanie-Jayne R. Howes, Suleiman Al-Olimat**,** Abdel Ennaceur, Paul.L.Chazot (* equal contribution).

- Identification of a novel $GABA_A$ receptor channel ligand derived from *Melissa officinalis* and *Lavandula angustifolia* essential oils. Rushdie Abuhamdah, Mahita Mwajuma, Sawsan Abuhamdah, Melanie-Jayne Howes, Abdel Ennaceur and Paul L Chazot. **2014.** ***Eur J Med Plants*** Vol:4 issue3. (July – September).

- Phytochemical Investigations and Antibacterial Activity of Selected Medicinal Plants from Jordan. ABUHAMDAH, R., ABUHAMDAH, S., AL-OLIMAT, S. & CHAZOT, P. **2013**. ***Eur J of Med Plants*** Vol: 3, Issue: 3. (July – September).

- Effects of methimepip and JNJ-5207852 in Wistar rats exposed to an open-field with and without object and in Balb/c mice exposed to a radial-arm maze. ABUHAMDAH, R. M., VAN RENSBURG, R., LETHBRIDGE, N. L., ENNACEUR, A. & CHAZOT, P. L. **2012**. ***Frontiers in Systems Neuroscience***, Jul 16; 6:54.

Poster communications

- Won best poster in science and best poster overall, Durham Researchers' Poster Competition, on poster entitled “Medicinal Herbs for the overactive Brain” UK, **2010**.
- *Melissa officinalis L.* Essential Oil a novel Voltage-gated sodium channel blocker with anticonvulsant potential. The Physiological Society, Cross Themed Meeting, UK, **2010**.
- Medicinal plants for agitated Brain: Potential of Melissa officinalis essential oil in epilepsy. South Tees R&D Management Conference, UK, **2010**.
- *Melissa officinalis* Essential Oil in Epilepsy. Wolfson Research Institute poster competition, UK, **2010**.
- Herbal medicine for Agitation: Durham Wolfson Institute Poster Competition, Durham, UK, **2011**.
- Medicinal plants for Agitation Yorkshire and North East Hub Public Engagement, UK, **2011**.
- Potential of *Melissa officinalis L.* Essential Oil in Epilepsy and Anxiety, Development of a Novel Fractionation Protocol, BNA annual meeting, UK, **2011**.
- Pharmacological profile of essential oils derived from lemon verbena (*Aloysia citriodora Palau*) and Lemon balm (*Melissa officinalis L*.): cholinergic, anti-oxidant and iron chelation properties. E-Journal of British pharmacological society. Pharmacology, BPS annual meeting, UK, **2012**.
- Exposure of Balb/c mice to an open space anxiety test in presence of a companion from the same or different strains of mice. BNA annual meeting, UK, **2012**.
- Are pre-training habituation sessions a valid method in the study of learning and memory in rats and mice? American Society for Neuroscience, 42nd annual meeting, USA, **2012.**
- Neuroprotective activity of Aloysia citriodora essential oil versus H2O2-induced neurotoxicity in CAD catecholaminergic cells. BPS annual meeting, UK, **2013.**
- Effect of H_4R antagonism on motor and anxiety behaviours in a novel elevated platform open space test. BPS annual meeting, UK, **2013**.

Acknowledgement

I owe my deepest gratitude to my supervisor Dr Paul Chazot. Without his continuous enthusiasm, encouragement, support and patience this study would hardly have been completed. His advice, support and friendship has been invaluable on both academic and personal level, for which I am extremely grateful.

This thesis would not have been possible without the help and support of my sister Dr Sawsan Abuhamdah - University of Jordan, Dr Abdel Ennaceur - University of Sunderland, Dr Melanie-Jayne Howes - Kew Royal Botanic Gardens, Dr Michael Carroll and Dr Stephen Hobson - Newcastle university and Dr Emke Pohl Durham University.

I would like to thank my co-supervisor Dr Susan Pyner, and my thesis committee members: Dr Iakowos Karakesisoglou, Prof Colin Jahoda, and Dr Carrie Ambler, for their valuable input, discussions and encouragement.

Also I would like to acknowledge the invaluable support of all the staff in the School of Biological & Biomedical Sciences and Josephine Butler College in Durham University.

I would like also to express my appreciation, to the friendly and cheerful lab partners and fellow students, in particular, Natalie Duggett, Mwape Katebe, Natasha Lethbridge, Simon Cork, Dilwar Hussein, Georgina Uttley and Maria Anjum.

Last, but by no means least, I thank my family and friends for their enduring patience and support.

Chapter 1

Introduction

1.1 Neurodegenerative Diseases

1.1.1 Overview

Neurodegenerative diseases affect a significant number of individuals in all age groups. For the subset of disorders that affect older individuals, the number of cases is rapidly growing worldwide with increasing life expectancies. For example, approximately 18 million people currently suffer from Alzheimer's disease (AD) and that number is expected to increase to 34 million by 2025 (Thies, 2013). In addition to reduceding life expectancy and quality of life, neurodegenerative diseases inflict significant financial burdens on family members and on healthcare systems (Cuny, 2012). Neurodegenerative diseases include AD, where neurons die initially in the nucleus basalis, Parkinson's disease (PD) which affects the substantia nigra, Huntington disease where striatal medium spiny neurons are lost, amyotrophic lateral sclerosis (ALS) and prion diseases which are characterized by damage and loss of motor neurons in the brain and spinal cord. All these diseases share common features including histopathology, clinical course and molecular mechanisms of pathogenesis. A common feature of neurodegenerative diseases is an extended time course until sufficient abnormal protein accumulates, followed by a cascade of symptoms over many years with increasing disability (Jellinger, 2009). Although these conditions are characterized clinically, advances in live imaging, histological analysis, genetic studies and proteomic interrogation has refined the diagnosis (Przedborski et al., 2003). For instance, in the case of PD, radiotracer imaging can identify abnormal dopaminergic function, while newer MRI techniques can assess connectivity and microstructural damage. Volumetric analysis of regional tissue loss can be useful for differential diagnosis in dementias. In AD, specific imaging markers of abnormal protein deposition are available. Also the use of multimodal imaging,

especially when combined with other biomarkers, shows increasing promise for the detection of preclinical disease in high risk individuals (Stoessl, 2012).

Neurodegenerative diseases are often age-related, increasing in frequency with advancing age and often accompanied by four stages of microscopic signs: neuronal pathology, neuronal cell death, disappearance of neuronal cell bodies and glial proliferation (Przedborski et al., 2003).

1.1.2 Clinical Features of Neurodegenerative Diseases

Neurodegenerative diseases have a chronic clinical course that is relentlessly progressive and irreversible by any known therapy, although drug therapy or gene therapy may give marginal or temporary improvement. The major risk factor for neurodegenerative diseases is advancing age. Phenotypic variability is also commonly seen. These conditions appear to be heritable in a small percentage of cases. In the familial form of the disease, the onset occurs up to a decade before the onset of the sporadic form of the disease. Several different neurodegenerative diseases may appear together within a family. Different clinical manifestations are mediated by dysfunction of different anatomical regions of degeneration. Cognitive impairment and dementia although common, are not seen in all forms.

Neurodegenerative diseases are diagnosed primarily on the basis of history and clinical examination (Fig 1.1) (Hardiman, 2011). The most important risk factors are age, positive family history, unhealthy lifestyle, endogenous factors and exposure to toxic environment (Fig 1.2) (Farooqui, 2007) supporting the view that neural cell death is a multifactorial process (Fig 1.3). Normal aging is accompanied by a modest upregulation of excitotoxicity, oxidative stress and neuroinflammation (Facheris et al., 2004). It is not clear whether exicitotoxicity, oxidative stress or neuroinflammation are the cause or consequence of neural cell death (Andersen, 2004, Juranek and Bezek, 2005). Evidence suggests that these are closely associated with mechanisms of apoptotic cell death (Farooqui et al., 2007, Kabashi et al., 2007, Shibata and Kobayashi, 2008).

Unfortunately, effective therapies are currently lacking for the vast majority of neurodegenerative diseases. For some conditions, such as AD and PD, therapeutic agents that provide symptomatic relief are available. However, symptom alleviation is only temporary without significant alteration in the underlying disease progression. Several difficulties stand in the way of progress in the discovery and development of drugs for neurodegenerative diseases, including our undeveloped understanding of the CNS and the aetiology of these diseases (Cuny, 2012).

Neurons in general represent a vulnerable group of cells. Because they facilitate neurotransmission and maintain the metabolic needs required for long axonal projections, Neurons also have high energy requirements and are reliant on axonal transport combined with a larger surface area that make them more exposed to environmental toxins. Hence, once damaged, regeneration is difficult. The dopaminergic neurons located in the substantia nigra in PD are particularly prone to reactive oxygen species (ROS) induced injury. This selective vulnerability is believed to be driven from the fact that neurons in the substantia nigra have very high levels of iron and copper, both of which are capable of catalysing ROS formation. Additional evidence suggests that substantia nigra may have low stores of antioxidant molecules such as glutathione, thereby increasing neuronal susceptibility to the damaging effects of ROS. However, this does not explain the vulnerability of neurons associated with PD in other regions of the brain such as brainstem and spinal cord.

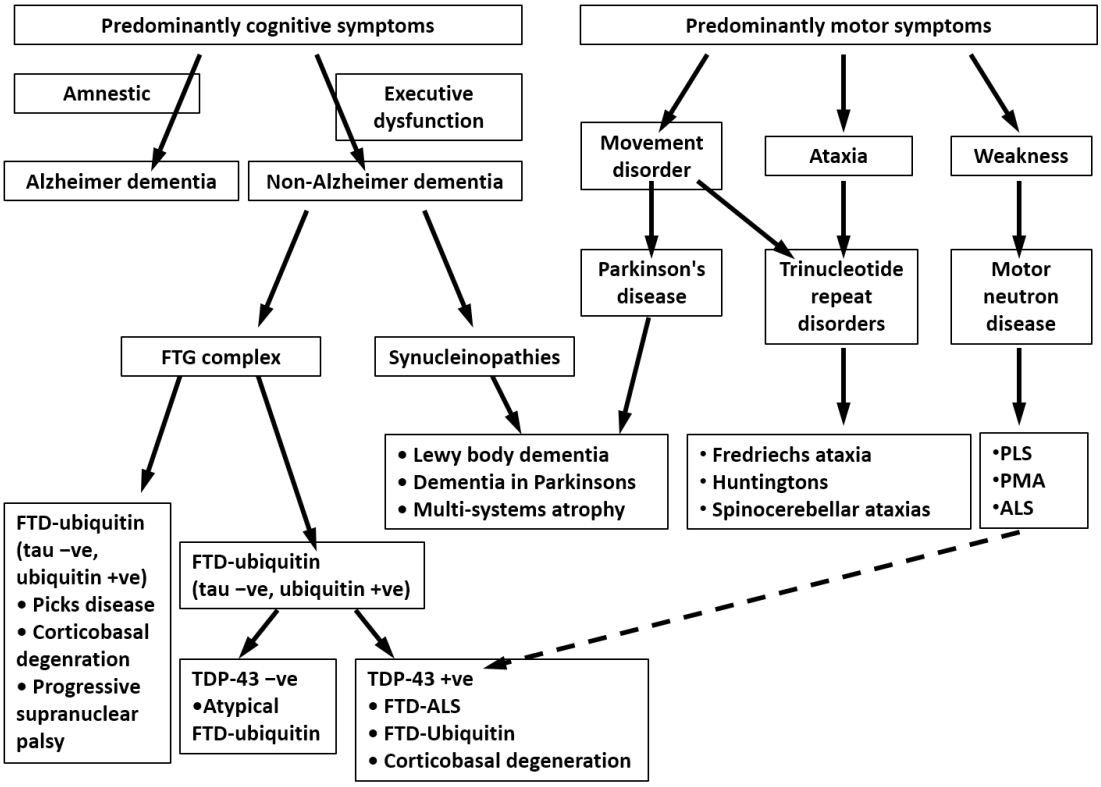

Fig 1.1

Clinical classification of neurodegenerative diseases (Hardiman and Doherty, 2011)

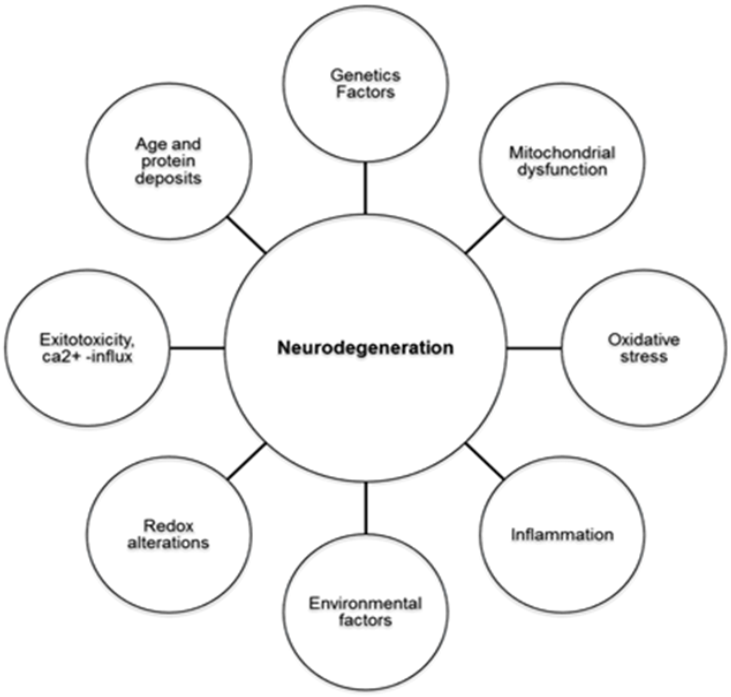

Fig 1.2

Factors effecting neurodegeneration in neurological disorders (Farooqui, 2010)

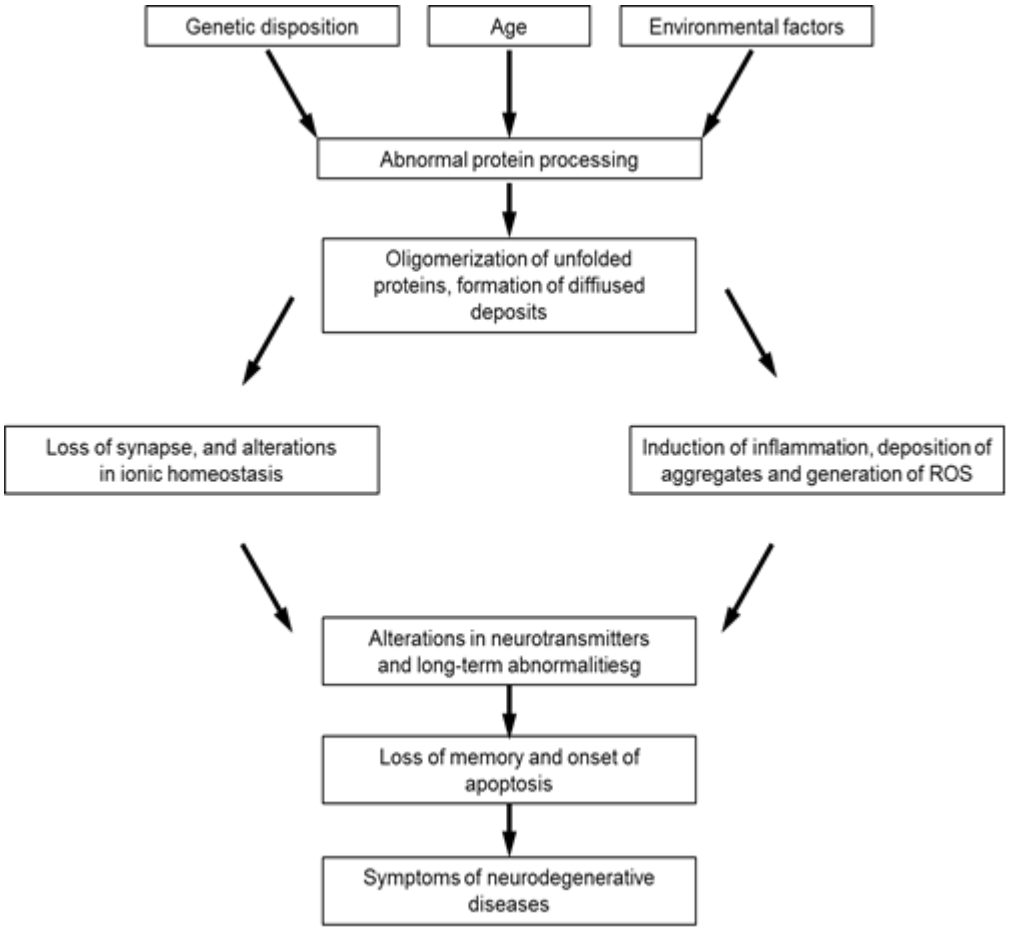

Fig 1.3

Factors associated with the pathogenesis of neurodegenerative diseases (Hardiman and Doherty, 2011)

1.1.3 **Neuropathology**

In neurodegenerative diseases only a specific neuronal population in a particular region neuronal degeneration occurs (Table 1.1) (Dwyer et al., 2005, Migliore et al., 2005) the nature of connections as well as the interactions between neurons and glial cells is essential for determining neuronal vulnerability of neurons (Farooqui et al.,2007). Despite the topographical differences in neurodegenerative diseases, histopathological findings are similar; regional atrophy with neuronal loss as well as abnormal accumulation of protein. Loss of synapses is another feature that plays an important role in loss of skilled movements, decision making, cognition, and memory related processes (Wishart et al., 2006). Tissue examination can help to identify pathological processes, also locating the site of the earliest visible alteration helps to establish the diagnosis. For example degeneration in the hippocampal and frontal lobe pyramidal neurons is associated with AD, degeneration in the dopaminergic neurons of the substantia nigra with PD, in the upper and lower motor neurons of the pyramidal system with ALS and in the medium-sized spiny GABAergic neurons of the striatum with Huntington's. On the other hand, Dementia coupled with mainly limbic atrophy suggests Alzheimer's, while mild atrophy implies Lewy body disease. Moderate cognition decline in the setting of asymmetric, motor and sensory impairment, with reduced metabolic activities, and atrophy prevailing around the central sulcus is indicative of corticobasal degeneration. To assign the most appropriate diagnosis to neurodegenerative diseases you need to identifying the sites or systems where tissue loss occurs, which may be revealed on neuroimaging during the disease progression, or on post-mortem examination; cataloguing the cells undergoing degeneration; identifying the abnormal aggregates, their cellular and topographic propensities (extracellular, cytoplasmic, or nuclear). Blood brain barrier dysfunction and hypertension may also contribute to the pathogenesis of neurodegenerative disease (Rao and Balachandran, 2002). This dysfunction is accompanied by the disruption of tight junctions, alterations in transport of molecules between blood and brain, and brain and blood, aberrant angiogenesis, vessel regression, brain hypo-perfusion and changes in inflammatory responses. All these processes leads to progressive synaptic loss and neurodegeneration (Zlokovic, 2008).

Table 1.1

Neurological diseases and selectively vulnerable cells (Hardiman and Doherty, 2011)

Disease	Vulnerable Neurons
Parkinson's disease (PD)	Dopaminergic neurons
Alzheimer's disease (AD)	Cholinergic neurons
Amyotrophic lateral sclerosis (ALS)	Upper and lower motor neurons
Frontotemporal dementia	Frontotemporal cortical neurons
Huntington disease (HD)	GABAergic neurons

1.1.4 **Genetics**

The high level of interplay between excitotoxicity, oxidative stress, and neuroinflammation in neurodegenerative diseases relies on specific genes. Neurodegenerative diseases have a small percentage of familial cases and a large percentage of apparently sporadic cases. Sporadic and familial cases are usually phenotypically and histologically indistinguishable, although the onset of familial cases tends be earlier. This suggests that genetic mutations accelerate the molecular processes that lead to late onset sporadic disease. A number of causative genes have been discovered for specific neurodegenerative disease, for example, mutations in amyloid precursor protein (APP), Presenilin 1, and Presenilin 2, which occur in early onset Alzheimer's cause altered protein production and increased aggregation of β-amyloid protein (Herl et al., 2009). Similarly, PARK 1, the first gene to be identified in PD, alters the production of the protein α-synuclein. Mutations in genes associated with oxidative stress pathways, SOD1 and DJ1, have been implicated in familial amyotrophic lateral sclerosis ALS and PD, respectively (Hardiman and Doherty, 2011).

1.1.5 **Protein Structures**

The formation of aberrant structures by more than 20 different proteins appears to underlie neurodegenerative diseases (Table 1.2). The mechanism by which the attainment of an aberrant protein structure causes disease is still unclear and may involve both the loss of a vital physiological function and/or the acquisition of toxic properties. An aberrant protein structure may bind to a specific receptor directly, causing an inappropriate activation of a cascade that initiates cellular changes, which leads to compromise of cellular function or it may acquire properties that allow them to interact with and destabilize cellular membranes or other proteins, thus causing a secondary toxicity. Moreover, accumulation of aberrant proteins may strain the normal mechanisms responsible for controlling protein folding and degradation, resulting in a generalised loss of protein homeostasis and consequent toxicity. Polymerization of aberrantly folded proteins is concentration dependent (Hardiman and Doherty, 2011). Changes in production, degradation, or clearance of native protein underlie the assembly of aberrantly folded protein and these structures are thought to be the primary event driving pathogenesis (Fig 1.4) (Hardiman and Doherty, 2011). Consequently, many of the therapies under development are designed either to remove or decrease the quantity of soluble native protein (Farooqui et al., 2007).

Disease specific proteins (tau, Aβ, α-synuclein, huntingtin), which accumulate in neurodegenerative diseases, are substrates for transglutaminase-2, a calcium-dependent cross-linking enzyme involved in the post translational modification of intra and extracellular proteins. It generates isopeptide bonds, which stabilise polymeric aggregates of accumulated proteins. This indicates the importance of transglutaminase 2-mediated cross-linking reactions (Harley et al., 2008, Wilhelmus et al., 2009, Caccamo et al., 2010). As abnormal protein aggregates cannot be degraded by cytosolic proteases, it accumulate in cells and extracellular compartments as residual debris. For example, in AD, misfolded Aβ peptide accumulates in the neuronal endoplasmic reticulum extracellularly as plaques. In contrast, in PD and dementia with Lewy bodies (DLB) abnormal accumulation of α-synuclein occurs in neuronal cell bodies, axons, and synapses. Intracellular or extracellular cerebral deposits of misfolded protein aggregates with a β-sheet

conformation, such as Aβ in AD, or α-synuclein in PD (Table 1.3) (Farooqui et al., 2007) causing extensive neurodegeneration, synaptic dysfunction, and the accumulation of advanced glycation end products (Vicente et al., 2010). Glycation facilitate misfolding, aggregation and accumulation of Aβ, tau (τ), prions, and transthyretin proteins (Chen et al., 2009, Chen et al., 2010). Advanced Glycation end products Also may cause an increase in oxidative stress and inflammation by the formation of ROS and the induction of NF-κB through their receptor, RAGE, (Vicente et al., 2010). Interactions between fragments of α-synuclein and Aβ peptide promote the aggregation of α-synuclein. In addition, under pathological conditions, interactions between Aβ and α-synuclein may initiate the formation of toxic oligomers and nanopores that increase intracellular calcium leading to induction of oxidative stress, leakage of lysosomal membranes and mitochondrial dysfunction (Crews et al., 2009).

Table 1.2

Neurological diseases associated with aberrant protein structure (Hardiman and Doherty, 2011)

Disease	Protein	Site of deposition
Parkinson disease	α-synuclein	Intracellular (Lewy neuritis and Lewy bodies)
Multiple systems atrophy	α-synuclein	Intracellular argyrophilic inclusionsin both oligodendroglia and neurons
Hereditary cerebral amyloid angiopathy	Cystatin C	Extracellular
Congophilic amyloid angiopathy	β-amyloid	Extracellular
Alzheimer's disease	β-amyloid	Extracellular (amyloid plaques)
Alzheimer's disease	Tau	Intracellular (paired helical filaments)
Frontotemporal dementia	Tau	Intracellular inclusions (paired helical filaments and Pick bodies)
Familial British dementia	ABri	Extracellular (amyloid plaques)
Familial British dementia	ADan	Extracellular (amyloid plaques)
Transmissible spongiform encephalopathies	Prion protein	Extracellular amyloid plaques
Amyotrophic lateral sclerosis	TDP43-ubiquitin	Cytoplasmic inclusions and ubiquitin-positive neuronal threads
Huntington disease	Mutant huntingtin	Nuclear and cytoplasmic inclusions
Inherited spinocerebellar ataxias	Various proteins with polyglutamine expansions	Nuclear and cytoplasmic inclusions

Table 1.3

Accumulation of various types of protein aggregates and their location in neurodegenerative diseases (Farooqui et al., 2007)

Disease	Protein	Type of aggregate	Location	References
AD	β-Amyloid	Amyloid	Extracellular	(Haass and Selkoe, 2007)
PD	α-Synuclein	Fibrillar non-amyloid	Intracellular	(Beyer, 2007) (Burke, 2004)
HD	Huntingtin	Fibrillar non-amyloid	Intracellular	(Bonilla, 2000) (Gil and Rego, 2008)
ALS	Superoxide dismutase I	Fibrillar non-amyloid	Intracellular	(Jellinger, 2009)
CJD	Prion protein	Amyloid	Extracellular	(DeArmond and Prusiner, 2003, Behrens, 2003)
Other prion diseases	Prion protein	Amyloid	Extracellular	(DeArmond and Prusiner, 2003, Behrens, 2003)

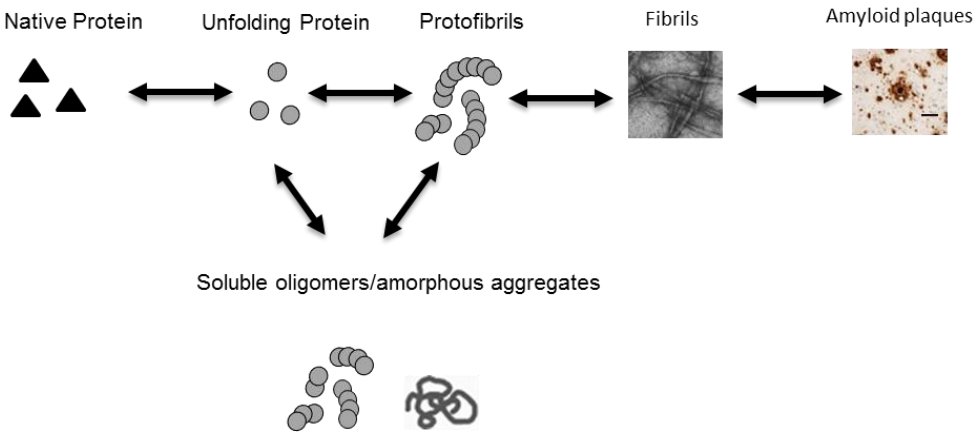

Fig 1.4

Pathways to aberrant protein structure and aggregation in amyloid related diseases

(Hardiman and Doherty, 2011)

1.1.6 **Oxidative Stress**

The Brain is the most metabolically active organ of the human body which consumes almost one-fifth of the total oxygen inspired by the individual (Cui et al., 2004) Neurons have high metabolic activity with a constant production and elimination of ROS making them more vulnerable to oxidative stress (Jenner, 2003, Emerit et al., 2004). Loss of antioxidant protection or unusual increase in ROS can lead to proteins, lipids, and nucleic acids damage. Accumulation of unrepaired damaged molecules within the cellular compartments will results in disturbed homeostasis (Le Bourg, 2001). Widespread DNA damage is clearly apparent in ALS, PD, AD and HD (Jenner, 2003, Emerit et al., 2004). Increased presence of protein carboxyl moieties indicating protein damage has been also reported in all neurodegenerative disorders (Mariani et al., 2005).

In neurodegenerative diseases, oxidative stress initially occurs at the disease specific site, for example Aβ-mediated oxidative stress in the cerebral cortex and hippocampal region of AD patients, α-synuclein induced oxidative stress in the brain stem of PD patients and glutamate receptor-mediated oxidative stress in the motor system of ALS spinal cord. ROS also activate calcium channels and deactivate calcium pumps, this leads to abnormally high intracellular levels of calcium in neurons, which increase in cytosolic Ca^{2+} levels, resulting in activation of Ca^{2+}-dependent enzymes, including nicotinamide adenine dinucleotide phosphate (NADPH) oxidase, cytosolic phospholipase A2, xanthine oxidase, and neuronal nitric oxide synthase (NOS). This activation generates more ROS, nitric oxide, and peroxynitrite, which ultimately leads to nuclear damage, mitochondrial damage, proteasome inhibition, and endoplasmic reticulum (ER) stress (Shibata and Kobayashi, 2008). NO and peroxynitrite deplete glutathione, and S-nitrosylation of many proteins, leading to more protein misfolding (Lipton et al., 2007).

Oxidative stress also stimulates astrocytes and microglia to facilitate the generation and secretion of cytokines that cause neuronal caspase-8 activation and induce glial inflammatory response (Shibata, 2008, Farooqui, 2010). The release of these mediators continue the inflammatory cycle, activating additional microglia, promoting their proliferation, and resulting in further release of inflammatory factors. The accumulation of high concentrations of these metabolites will cause further neuronal injury (Dheen et al., 2007). Moreover, oxidative DNA damage mediates the release of mitochondrial apoptosis inducing kinase, which triggers apoptosis programmed cell death.

Mitochondria are one of the major targets of ROS attacks and therefore, mitochondrial dysfunction is associated with progression of aging and manifestation of several neurodegenerative disorders (Sohal, 2002). Mitochondrial elements such as lipids, oxidative phosphorylation enzymes and mitochondrial DNA are particularly predisposed to attack by ROS due to their close proximity with the ROS production site (Pieczenik, 2007).

High concentrations of ROS generated by the oxidative phosphorylation pathway in mitochondria exposes the mitochondrial genome to oxidative stress leading to mitochondrial DNA injury. Mitochondrial dysfunction induces reduction in ATP and increased membrane permeability increasing the uptake of calcium ions, resulting in the release of cytochrome-C, which initiates the apoptotic cascade. Induction of apoptotic cell death with *in vivo* and *in vitro* studies have shown that NADPH oxidase derived from microglia play an important role in the generation of ROS. In PD, microglia-specific NADPH oxidases are involved in the production of ROS, which may contribute to the death of dopaminergic neurons. A similar process is seen in ALS, whereby oxygen radicals produced by microglial NADPH oxidase are believed to injure motor neurons. In addition, oxidation of K+ channels by ROS has been reported to be a major mechanism underlying the loss of neuronal function(Sesti et al., 2010). Redox-active transition metals contribute to oxidative stress (Bolognin et al., 2009) with increased localisation of redox-active transition metals (copper and iron) in the brain regions most affected by neurodegenerative diseases.

1.1.7 **Excitotoxicity**

Glutamate is the major excitatory neurotransmitter in the CNS, with essential roles in synaptic transmission and plasticity, key to learning and memory processes, as well as sensory and motor functions. Transmission of glutamate is mediated through three major ionotropic receptors N-methyl-D-aspartate receptors (NMDA), α-amino-3-hydroxy-5-methyl-4-isoxazoleproprionic acid (AMPA) receptors, and kainate receptors, and a range of metabotropic glutamate receptors.

The glutamate excitotoxicity hypothesis postulates that excessive synaptic glutamate causes over-activation of the postsynaptic NMDA and AMPA receptors resulting in neuronal death. High glutamate levels, which continuously activate postsynaptic receptors, may lead to increased intracellular calcium and catabolic enzyme activity. Downstream effects can include depolarization of mitochondrial membrane, activation of the caspase system, and production of ROS, all of which can culminate in cell death (Fig. 1.3). Excessive synaptic glutamate may also happen because of a fault in the cellular glutamate reuptake system. Excitatory amino-acid

transporter 2 (EAAT-2) is a glutamate transporter involved in cerebral glutamate transport. It has been postulated that some patients with ALS have decreased expression of this protein (Limpert, 2013). Patients with AD have also exhibited a reduction in EAAT-2 expression (Kong et al., 2014). It has been shown that GluA2, an AMPA glutamate receptor subunit responsible for calcium permeability into the postsynaptic cell, is not expressed in motor neurons affected by ALS patients because of a defect in the editing process for the messenger RNA encoding the GluA2 subunit (Brini et al., 2014). Absence of a functional GluA2 subunit allows calcium influx into the postsynaptic cell and results in cellular damage. Parkin, which is the gene product of PARK2, has regulatory effects on excitatory glutaminergic synapses (Dong et al., 2009). Abnormalities in parkin production can lead to enhanced synaptic activity and may even trigger an increase in the number of glutamate receptors (Dong et al., 2009). Riluzole which has a direct and indirect blocking effect on glutamate receptor activation has been proven to modestly slowdown the progression of ALS. Unfortunately, no other anti-glutamate agent has been successful thus far in disease treatment (Hardiman and Doherty, 2011).

1.1.8 **Neuroinflammation**

Neuroinflammation plays a key a key feature shared by neurodegenerative disorders. Inflammatory responses in the brain have been associated with the pathogenesis of ALS, AD and PD (Andersen, 2004, Craft et al., 2005). Chronic neuroinflammation is characterized by long-standing activation of microglia and sustained release of inflammatory mediators. This sustained release of inflammatory mediators causes an imbalance in the inflammatory cycle homeostasis by activating additional microglia, promoting their proliferation, and leading to further release of inflammatory factors (Farooqui, 2010). Microglia are CNS-specific macrophages, and enter the CNS during embryogenesis. The primary function of this subset of immune cell is to protect the brain from extrinsic pathogens and processes. During the process of activation, microglia are highly plastic and differ in morphology and phenotype, depending on the nature of the insult. Activated microglia can cause irreversible damage to tissues of the CNS. A number of factors have been identified that prime microglia to the activated state, and they may remain in the activated state

for prolonged periods. However, it is unlikely that microglial activation is the primary cause of any neurodegenerative process. It is more likely that an initial challenge induces an inflammatory cascade, which in turn initiates maladaptive processes and positive feedback loops that cause further pathological inflammation (Farooqui, 2010). Postmortem examination of brain tissue from PD patients has demonstrated activated microglia in the substantia nigra pars compacta. In AD, neuroinflammation is considered an effect of abnormal protein production. Aβ accumulation causes upregulation and activation of microglia leading to an inflammatory cascade. Also abnormal protein aggregates may trigger the expression of inflammatory mediator generating enzymes, such as phospholipase A_2 (PLA_2), cyclooxygenase-2 (COX-2) and lipoxygenase (LOX), which contributes to neurodegenerative process. Understanding the balance between protective and destructive capabilities of microglia may provide new ways of slowing neurodegeneration, by controlling neuroinflammatory processes.

1.1.9 Natural Products as Sources of Therapeutics for Neurodegenerative Diseases

Natural products are a rich source of biologically active compounds that have arisen as a result of natural selection, over perhaps 300 million years. It has been well documented that natural products have played crucial roles in modern drug development, for instance of the 520 new pharmaceuticals approved between 1983 and 1994, 39% were derived from natural products, Between 1990 and 2000, a total of 41 drugs derived from natural products were launched on the market by major pharmaceutical companies (Newman et al., 2003).

Natural product research has been the single most successful strategy for discovering new pharmaceuticals. An interesting example is the alkaloid galantamine originally isolated from the bulbs of the Amaryllidaceae family (snowdrops, daffodils), used for symptomatic treatment of AD (Scott and Goa, 2000). It is a reversible competitive inhibitor of AChE and it also interacts allosterically with nicotinic acetylcholine receptors to potentiate its action. By acting to enhance the reduced central cholinergic function associated at the early stages of this disease, significant improvements in cognition and behavioural symptoms have been observed.

The popularity of natural products, particularly those from higher plants as leads for new pharmaceuticals declined as pharmaceutical companies focused on combinatorial chemistry, coupled with very high throughput screening. Following disappointing outcomes of combinatorial chemistry, natural products research has been revived using rapid progress in molecular biology, chemistry and high throughput screening technologies along with parallel synthesis, computations and many other new techniques in medicinal chemistry of natural products.

Research of bioactive natural products spans a wide range of fields, including isolation and characterization of bioactive compounds from natural sources, structure modification for optimization of their activity and other physical properties, and total and semi-synthesis for a thorough scrutiny of structure activity relationship (SAR). In addition, synthesis of natural products also provides a powerful means of solving supply problems of natural products in bulk amounts. Structural diversity of secondary metabolites makes them valuable sources of novel lead compounds against therapeutic targets that have been newly discovered by genomics, proteomics and high-throughput screening.

Age-related loss of memory and cognitive decline has been documented for thousands of years in human history. Ancient writings which describe the cognitive decline symptoms also suggest remedies, based usually on plant extracts. For example *Ashwagandha* is mentioned in ancient Sanskrit writings from India as a promoter of learning and memory retrieval. Old European reference books (e.g. medical herbals) document a variety of other plants such as *Salvia officinalis* (sage) and *M. officinalis* (lemon balm) with memory improving properties. Some traditional herbs have anti-aging properties and they are potential candidates for the treatment neurodegenerative diseases (Luo et al., 2004, Wu et al., 2006, Chan et al., 2007, Heo et al., 2008, Zhou et al., 2008, Heo et al., 2011). Anti-aging herbs such as *Panax* (ginseng) and *Lycium barbarum* (wolfberry), are usually multi-functional and can work through different mechanisms. Increasing lines of evidence suggest that these herbs are potential candidates for the prevention or treatment of age-associated neurological disorders (Kim et al., 2007). *Rosmarinus officinalis* (Rosemary), for

example, is used by practising medical herbalists in the United Kingdom for memory problems (Moss et al., 2003). *Ginkgo biloba* is popular based on its perceived anti-ageing properties, including enhancing cerebral activity (Kleijnen and Knipschild, 1992, Perry et al., 1998, Perry et al., 1999). It has been reported to be of therapeutic value in mild to moderately affected patients with AD (Oken et al., 1998, DeKosky et al., 2008).

Volatile oils have attracted interest in recent years. One of the first findings that monoterpenes had AChE inhibitory effects was made only in the mid-1990s, in studies investigating historical records that monoterpene containing plants were 'good for the memory'. An ethanol extract *Salvia officinalis L*. (Labiatae) and *Salvia Lavandulaefolia* (Labiatae) were investigated for AChE activity and it was found that both displayed AChE inhibitory properties at quite low concentrations (Perry et al., 1996, Kennedy et al., 2005). Since the effects of the oil were superior to those of individual monoterpenes, further *in vivo* and clinical studies were carried out on the essential oils, which consist of a mixture of monoterpenes. Oral administration of *S. Lavandulaefolia* essential oil in rats decreased striatal AChE activity in both the striatum and the hippocampus compared to the control rats. Thus, it appeared that constituents of the *S. Lavandulaefolia* oil, or their metabolites, reach the brain and inhibit AChE in select brain areas, consistent with evidence of inhibition of the brain enzyme previously decribribed *in vitro* (Perry et al., 1999). The essential oil of *Salvia officinalis* (Sage) was a potent inhibitor of human AChE and consisted almost exclusively of monoterpenoids. Oral consumption leads to improved performance of secondary memory and attention tasks (Kennedy et al., 2005, Kennedy et al., 2011). *Melissa officinalis* leaf is another species that contains monoterpenes in its essential oil. It has been used as a medicinal plant for more than 2000 years and has a reputation for promoting long life and for restoring memory (Man et al., 2012). A recent randomised, placebo-controlled, double-blind, balanced crossover study showed an improvement in cognitive performance and mood in 20 healthy young participants, following treatment with dried leaf of *Melissa officinalis*. (Kennedy et al., 2003). The extract was shown by previous *in vitro* tests to be cholinergically active (Kennedy et al., 2003). In another study, an extract of *Melissa officinalis,* administered to patients with mild to moderate AD for 4 months produced a

significantly better outcome in cognitive function than placebo, although the constituents present in the extract have not been investigated (Akhondzadeh et al., 2003).

Although natural products have a long history of use for neurological symptoms, the study of the mechanisms of action of neuroactive natural products has only began relatively recently. With new technologies, researchers are now able to take a closer look at the complex molecular events associated with the therapeutic actions of natural products in neurodegenerative diseases.

A variety of natural products have been shown to have the desired effects in neurodegenerative diseases and some of these, or their derivatives, have been brought into clinical use. There are also many traditional medicinal plants used as crude extracts and mixtures with a reputation of alleviating or preventing symptoms of neurodegeneration (Bon et al., 1979, Bliss and Collingridge, 1993). In some cases, such extracts have been shown to relieve neurodegenerative symptoms in animal models or display relevant *in vitro* activity, but both the modes of action and identity of any compounds responsible have not been fully determined (Houghton et al., 2007). Some natural plant products have been shown to exert anti-inflammatory and/or antioxidant effects in a variety of peripheral systems. As increasing evidence indicates that chronic inflammatory responses play a pathological role in the central nervous system, anti-inflammatory herbal medicine and constituents have been shown to be potent neuroprotectors in various brain pathologies (Sundaram and Gowtham, 2012).

Treatment of neurodegenerative conditions presents some unique challenges as actives must penetrate into the brain either by active uptake mediated by transport proteins that bind the drug and facilitate the penetration across the blood-brain barrier, or by passive diffusion of lipophilic ones. Another concern with drugs adopted for use in neurodegenerative diseases is the potential interference of normal neurotransmission. The multifunctional properties of constituents of botanicals and their derivatives offer the possibilities for the development of effective multitarget therapeutics. The study of neuroactive natural products will indeed advance our

understanding of the nervous system, and open up exciting opportunities in drug discovery.

Identification of natural product leads follow different strategies such as bioassay guided methods; for example by spraying thin layer chromatography plates with reactive media that respond by producing a colour change in the presence of an active compound. An alternative is to use an ethnobotanical or ethnopharmacological technique, whereby the accumulated knowledge of many generations of native plant users may be used in the search for better medicines. These two techniques may be combined. The problem with any bioassay-guided technique, however, is that the inactive constituents are not identified. This represents a considerable waste, given that the plant has had to be collected, preserved, and identified. An alternative view is that it is best to extract all the constituents, with a view to screening in whichever way is appropriate, at that time or in the future. With modern high-performance liquid chromatography, it is possible to reduce a plant to its secondary metabolites, as single compounds; the products are then able to be screened in a high throughput manner in an equally short time and the compounds can be re-evaluated when new screens become available.

1.2 *Aloysia citrodora* Palau

1.2.1 Genus Aloysia

The genus Aloysia (Verbenaceae) includes approximately 200 species of herbs, shrubs and small trees. The species are mainly distributed throughout the South and Central America countries, and Mediterranean territories (Terblanché and Kornelius, 1996). Most of them are traditionally utilized as gastrointestinal and respiratory remedies (Morton, 1981). Some Aloysia species have displayed anti-malarial (Traore-Keita et al., 2000), antiviral and cytostatic activities (Lopez et al., 1979, Duscharzky et al., 2005, Reichling et al., 2009). Leaves from the majority of these species are utilized as seasoning for food preparations (Morton, 1981). The genus Lippia shows a rich genetic diversity, enabling it to synthesize a variety of essential oil constituents in plants grown in different parts of the world. However, the composition of the essential oil obtained from the same plant stock remains constant

under the same environmental conditions (Catalan and de Lampasona, 2002, Santos-Gomes et al., 2005).

1.2.2 **Synonyms**

Aloysia triphylla (L'Hér.), Britton. *Aloysia citriodora* Paláu, *Aloysia citriodora* Paláu, *Lippia citriodora* Kunth, *Lippia citriodora* Kunth, *Lippia triphylla* (L'Hér.) Kuntze

1.2.3 **Common Names**

Lemon-verbena (English), Verveine citronelle (French), Zitronenstrauch (German), Cidrão (Portuguese), Cedrón (Spanish), Melissa مليسا (Arabic). Herb Louisa, Hierba Luisa, Lemon-Scented Verbena, Verveine Citronnée, Verveine Citronnelle, Verveine des Indes, Verveine du Chili, Verveine du Pérou, Verveine Odorante, Zappania citrodora.

1.2.4 **Taxonomic Hierarchy**

Kingdom	Plantae – plants
Subkingdom	Viridae plantae – green plants
Infrakingdom	Streptophyta – land plants
Division	Tracheophyta – vascular plants, tracheophytes
Subdivision	Spermatophytina – spermatophytes, seed plants, phanérogames
Infradivision	Angiospermae – flowering plants,
Class	Magnoliopsida
Superorder	Asteranae
Order	Lamiales
Family	Verbenaceae – verbenas, verbénacées
Genus	Aloysia

Species *Aloysia citrodora* Paláu

Fig 1.5

Aloysia citrodora (Siedo and Botany, 2007)

Fig 1.6

Aloysia citrodora leaf (Grasso, 2007)

Fig 1.7

Aloysia citrodora dried leaf (Tucker, 2010)

1.2.5 **Description**

A. citrodora is a frost hardy perennial shrub which grows to 2–3 meters high (Fig 1.5). It grows well in full sun in well-drained, dry soil, and is sensitive to cold, losing its leaves at temperatures below 0 °C. It has tiny lilac or white flowers which appear within Flowering period: July to August; leaves are lemon-scented, 8 cm long, glossy, pointed, and rough to the touch (Fig 1.6 & 1.7). Spanish explorers brought this plant to Spain in the 17th century at which point it was named after Princess Louisa of Parma (genus name is a version of Louisa and the common name is Herb Louisa).

1.2.6 **Uses**

A. citrodora is a widely used herb for food and medicinal purposes and has a long history of folk uses in treating asthma, spasms, cold, fever, flatulence, colic, diarrhea, indigestion, insomnia and anxiety (Carnat et al., 1999, Santos-Gomes et al., 2005). An ethnopharmacological survey in Brazil has shown that *A. citrodora* infusion was one of the most common remedies for insommnia and anxiety (Dellacassa and Bandoni, 2003). Some pharmacological properties have been attributed to the essential oil which is spasmolytic on the guinea pig ileum (Carnat et al., 1999) and an antimicrobial (Maruzzella and Sicurella, 1960, Maruzzella and Liguori, 1958, Abuhamdah et al., 2013). Although *A. citrodora* has been approved as a herbal medicine and dietary supplement by many regulatory acts in many countries, the mechanisms of pharmacological actions of this herb are still unclear (Lai et al., 2006)

1.2.7 **Composition**

Flavones, iridoids and phenylpropanoids represent the main class of compounds of this plant, with verbascoside being the most abundant one (Funeset al. 2009; Quirantes-Pine´ et al. 2009). The strong antioxidant properties of *A. citrodora* extract have been studied in detail (Valentao et al. 2002; Liu et al. 2003; Funes et al. 2009). In addition, *A. citrodora* extract has also shown anti-inflammatory activity through different *in vitro* assays and animal models (Dı´az et al. 2004, Lee et al. 2005, Lin et al. 2006, Hausmann et al. 2007, Korkina et al. 2007). *A. citrodora* also have antispasmodic, antipyretic, sedative and digestive properties (Carnat et al., 1999,

Valentao et al., 1999, Pascual et al., 2001, Santos-Gomes et al., 2005). The essential oil from its leaves has been shown to exhibit antimicrobial activity (Duarte et al., 2005, Duschatzky et al., 2004, Lo´pez et al., 2004, Ohno et al., 2003, Sartoratto et al., 2004). Activities attributed to *A. citrodora*, include anti-genotoxic and protection against genetic damage (Zamorano-Ponce et al., 2006), neuroprotective effects (Lai et al., 2006) and hypnotic effects of the aqueous extract.

Analysis and identification of flavonoids and phenolic acids of the extracts of *A. citrodora* was performed in a number of studies (Tomaas-Barberan et al., 1987; Skaltsa and Shammas, 1988; Carnat et al., 1995, 1999; Nakamura et al., 1997; Valent et al., 1999). The leaf contains polyphenolic compounds: hydroxycinnamic derivatives with verbascoside (Lamaison et al., 1993), flavonoids, such as luteolin 7-glucoside (Skaltsa and Shammas, 1988) and luteolin 7-diglucuronide (Carnat et al., 1995). These compounds probably contribute to the antispasmodic activity. Iridoidglucosides were also reported.

1.3 Objective

In this thesis, the essential oil derived from the leaves of *A. citrodora* will be analysed and investigated for a range of pharmacological properties (focussed on receptor, AChE pharmacology, anti-oxidant and iron-chelation properties). The potential neuroprotective properties of this essential oil against oxidative stress and Aβ induced neurotoxicity was investigated using *in vitro* neuronal cell line system. A computer modelling approach was applied to identify constituents in the oil which endow AChE activity. Finally a new solid phase method was applied, as a first step, to fractionate the *A. citrodora* essential oil into its constituent neuroactive components.

Overall Hypothesis of this thesis: Based on the common traditional uses of M. *officinalis* and A. *citrodora* essential oils in treating neurological disorders, we hypothesise that they share common pharmacological properties and neuroactive components.

Chapter 2
Pharmacological Profile of *Aloysia citrodora* Palau Essential Oil: Radioligand Binding Properties

1.1 Introduction

1.1.1 Neurotransmitters in Neurodegenerative Diseases

Although the aetiology of neurodegenerative diseases is still largely unknown, for some neurodegenerative diseases there is a clear links between the disease and a deficiency of a neurotransmitters such as acetylcholine in AD, and dopamine in PD (Beal, 2005).

The major excitatory neurotransmitter in the central nervous system (CNS) is glutamate (Fonnum, 1984). Glutamate is essential for learning and memory, synaptic plasticity, neuronal survival and in early development, proliferation, migration and differentiation of neuronal progenitors and immature neurons (Ikonomidou et al., 2000). The glutamate neuronal pool is located in nerve endings. A separate pool is located in glia and serves to recycle the transmitter. Glutamate is also involved in the synthesis of the inhibitory neurotransmitter γ-aminobutyric acid (GABA). Glutamate is released from presynaptic terminals by a calcium dependent mechanism, then it is removed by uptake into the surrounding glial cells and aminated to glutamine. When released into the synaptic cleft, glutamate acts largely at postsynaptic receptors. These include the *N*-methyl-D-aspartate (NMDA), NMDA channel is normally blocked with a magnesium ion and requires depolarization of the neuron to remove the magnesium and allow the glutamate to open the channel, causing an influx of calcium, which then leads to subsequent depolarization. MK-801 an uncompetitive antagonist binds inside the ion channel of preventing the flow of ions, including an influx of calcium (Ca2+), through the channel (Foster, 1987). All receptor

subtypes for both ionotropic and metabotropic glutamate receptors have been cloned and characterized (Hollmann and Heinemann, 1994, Cao and Yao, 2013). Recently prevention of glutamate-mediated neurotoxicity has been utilised as a therapeutic mechanism in AD. Memantine, a moderate-affinity, voltage-dependent, uncompetitive antagonist of NMDA receptor, shows neuroprotective effects in patients with moderate-to-severe AD. Memantine has neuroprotective and cognition-enhanced properties, which can be combined with other treatments for AD. The efficacy and safety profile of Memantine have been reported in several clinical trials for treatment of AD and vascular dementia (Tanovic and Alfaro, 2006, Kutzing et al., 2012).

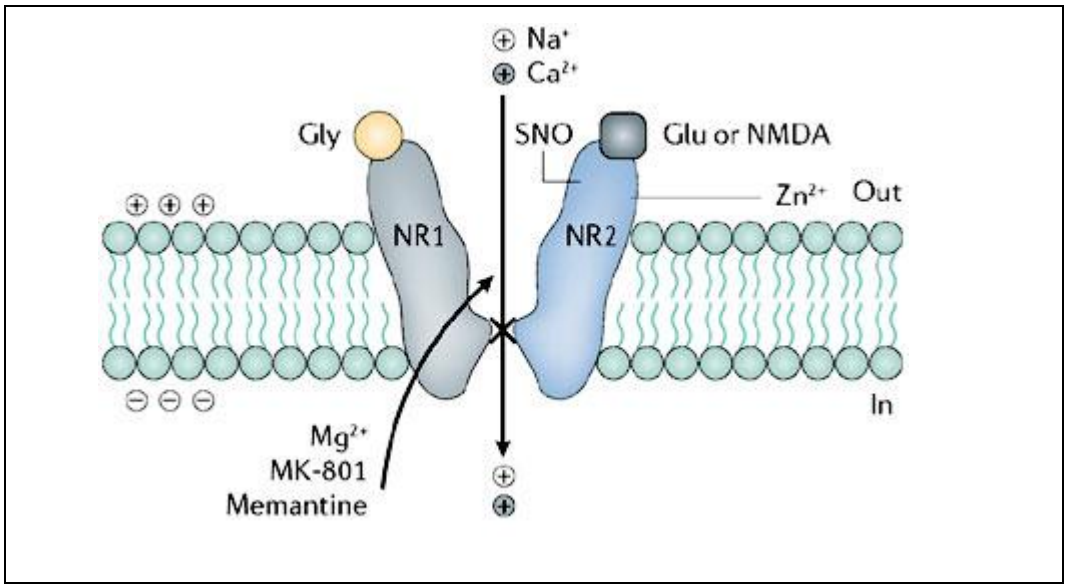

Fig 2.1

NMDA Receptor, Glycine and glutamate/N-methyl-D-aspartate (Glu/NMDA) are shown bound to their respective binding sites, and the binding site for Mg2+, MK-801 and memantine is within the ion channel pore region. The Zn2+-binding site is also highlighted. The location of the cysteine sulphydryl group (–SH) that reacts with nitric oxide (NO) species is labelled SNO. NR1, NMDA receptor subunit 1; NR2, NMDA receptor subunit 2A (Lipton, 2006).

The predominant inhibitory neurotransmitter in the central nervous system is γ-aminobutyric acid (GABA). GABA is essential for the overall balance between

neuronal excitation and inhibition. The inhibitory signal of GABA is transduced primarily by $GABA_A$ receptors. Activation of the $GABA_A$ receptor opens a Cl^- anion channel, and the resulting influx of Cl^- ions hyperpolarizes the neuron, decreasing neuronal activity. Dysfunction of $GABA_A$ receptors occurs in various neurological states, as epilepsy, PD and HD. Temporal lobe epilepsy seizures reflect excess excitation, which may result from local inhibitory circuit dysfunction. PD disrupts the input to striatal GABAergic neurons and HD destroys striatal GABAergic neurons. New drugs aimed at GABA synthesis, release and binding will offer novel and highly effective treatments for neurodegenerative diseases (Kleppner and Tobin, 2001).

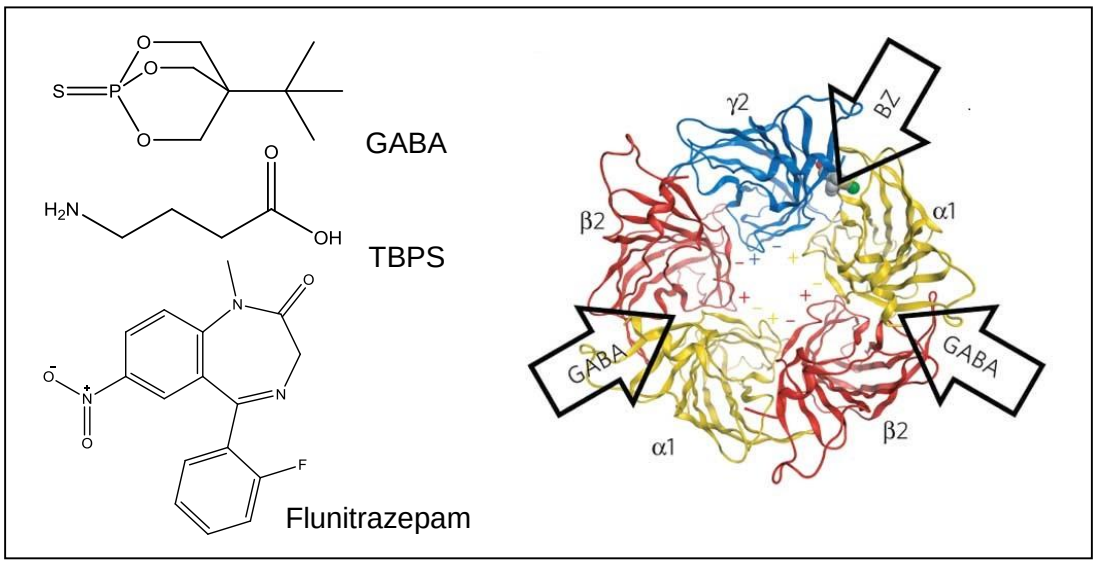

Fig 2.2
$GABA_A$ Receptor
Top view of the extracellular domain of the pentameric α1β2γ2 $GABA_AR$ in ribbon mode. The benzodiazepine-binding site (BZ) and the two GABA-binding sites are indicated by arrows. Diazepam in the benzodiazepine-binding site is depicted in space-filling mode (Richter et al., 2012). Chemical structure of GABA, TBPS and Flunitrazepam.

GABA deficiency is associated with several psychiatric disorders, such as anxiety, depression, panic and mania (Marin, 2012). GABA agonists are active in animal models for dyskinesia, epilepsy and depression, amongst others (Lloyd et al., 1982). Animal studies have shown that increasing GABA can decrease aggression (Nelson, 2007). Deficits in the central GABA system have been reported in the brains of patients with dementia (Ventriglia et al., 2013). Indirect supporting evidence for a role of GABA is provided by some of the drugs that are effective in the treatment of

agitation such as benzodiazepines. Valproic acid, which is also effective in aggressive behaviours associated with dementia, is believed to increase levels of GABA (Chindo et al., 2008). Also GABA receptors have been implicated in learning and memory (Deng et al., 2010). The formation of memory seems to require the down regulation of GABAergic transmission in neural circuits such as the amygdala, and in the hippocampus (Makkar et al., 2010). A reduction in GABAergic inhibitory transmission would allow for the activation of various intracellular cascades that are essential for the stabilization and re-stabilization of memory (Bustos et al., 2009, Luft et al., 2004). Reduced GABA transmission facilitates memory storage by increasing the release of norepinephrine and enhancing activation of β-ARs within the amygdala (Hatfield et al., 1999).

A large number of pharmacologically useful compounds interact with the $GABA_A$ receptors, including agonists and antagonists, barbiturates, neurosteroids, anesthetics and benzodiazepines.

Benzodiazepines such as Flunitrazepam enhance the effect of GABA at the $GABA_A$ receptor, resulting in sedative, hypnotic, anxiolytic, anticonvulsant, and muscle relaxant properties. Benzodiazepines do not directly activate the $GABA_A$ receptor, but positively modulate $GABA_A$ receptor mediated Cl^- conductance (Mahadik et al., 2012). The ability of benzodiazepine binding site agonists to potentiate or reduce, in the case of inverse agonists GABA-gated currents is highly correlated with the ability of GABA to increase or decrease the apparent affinity of these ligands for the benzodiazepine binding site. There appears to be a potential for new pharmacological agents for different neurodegenerative disorders based on agonist activity at inhibitory amino-acid receptors.

Nicotine is reported to have cognition enhancing effects and these may be due to nicotinic receptor stimulation but also protection against AD by other mechanisms such as inhibition of β-amyloid formation (Salomon et al., 1996), inhibition of the neurotoxic effects of excitatory amino acids (e.g. glutamate) and enhancement of the effects of nerve growth factor (NGF) (Whitehouse and Kalaria, 1995). Cytisine, another Nicotine receptor agonist is only used as a pharmacological tool because of

its strong binding affinity to nicotinic receptors, but it does not have any pharmaceutical uses because of its toxicity. Postmortem studies have shown that in AD there also appears to be a depletion of nicotinic function. Attention deficit in AD is reversed with nicotine, which is reported to up-regulate nicotinic receptors and to increase ACh release, thus enhancing cholinergic neurotransmission. Also nicotinic acetylcholine receptor (nAChR)-mediated protection against neurotoxicity induced by β amyloid (Aβ) and glutamate. nAChR stimulation blocks glutamate neurotoxicity in spinal cord motor neurons. These findings suggest that nAChR-mediated neuroprotection is achieved through subtypes of nAChRs and common signal cascades. An early diagnosis and protective therapy with nAChR stimulation could be effective in delaying the progression of neurodegenerative diseases such as AD, PD and amyotrophic lateral sclerosis (Kawamata et al., 2011).

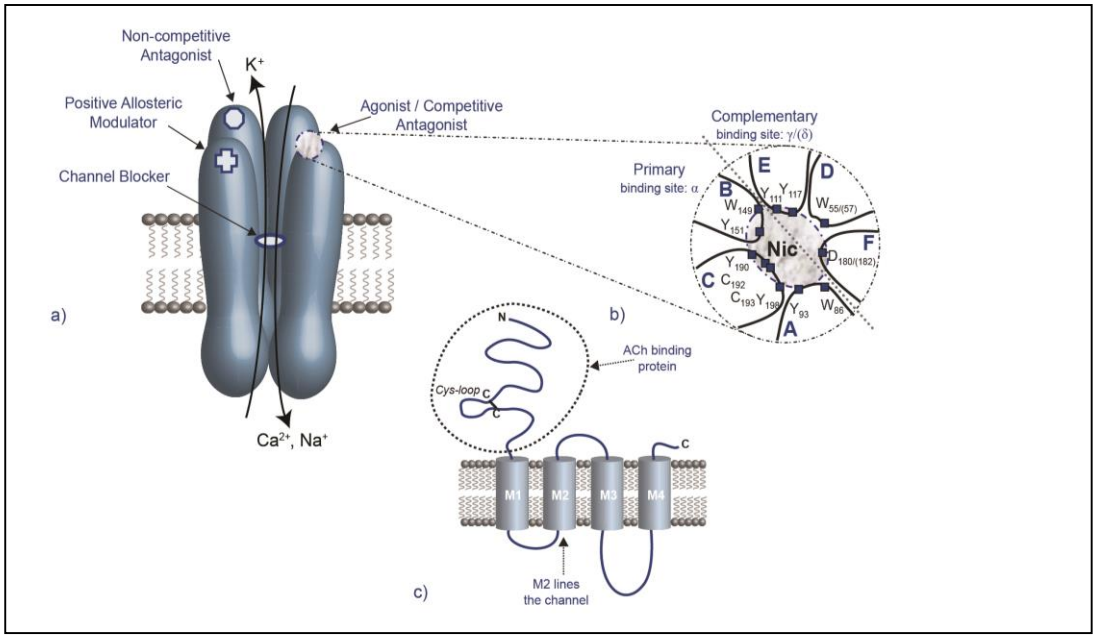

Fig 2.3
a) Schematic of a nAChR with one subunit removed to reveal the ion channel lumen. b) Agonist binding site loop model. c) The topography of a single subunit (Sharples and Wonnacott, 2001).

1.1.2 **Radioligand Binding**

Radioligand receptor binding technology has been extensively used to identify lead compounds which interact with receptors likely to be involved in neuronal, functions/dysfunctions. The first rigorous study of drug binding to receptors was that

of Paton and Rang in 1965, who investigated H-atropine binding to muscarinic receptors in smooth muscle. The use of radiolabelled drugs in radioligand binding studies is common and for many pharmaceutical manufacturers forms an essential part of the screening process, providing a rapid means of determining the affinity of new drugs for a wide range of receptors. Labelling of drugs with radioisotopes is attractive because very small quantities, often as low as 1 fmol, can be readily and accurately measured in addition to several obvious advantages to using in vitro as a first-level screen when compared to in vivo screens. Structure–activity data generated in binding assays is a direct reflection of the ligand/receptor interaction minus the complications which result from secondary events indicating bioavailability issues (Misra, 1998). In order to use these assays for plant extracts, natural products should be soluble (DMSO–H_2O) and free of salts as well as acids; otherwise false positives can be produced since the assay is pH dependent. Also, natural products must be free of proteins which may interfere with the assay.

A pharmacological screen of *A. citrodora* essential oil was carried out using a range of radioligand binding assays targeting major ligand-gated ion channel receptors (NMDA, nicotinic and $GABA_A$Rs), the rational for which is described in section 2.1.1. Four different oil concentrations [0.0001, 0.001, 0.01 and 0.1 mg/ml] of both dry and fresh essential oil were tested.

1.2 Materials and Methods

1.2.1 Chemical Materials

[^{3}H] Flunitrazepam (specific activity 91.0 Ci mmol-1), [^{3}H] nicotine (specific activity 77 Ci mmol-1) and [^{3}H] MK-801 (specific activity 25 Ci mmol-1) were all provided by Amersham Biotech (Little Chalfont, UK). [^{35}S]-t butylbicyclophosphorothionate (TBPS; specific activity 80 Ci mmol^{-1}) was from Perkin Elmer Life Sciences (Waltham, USA). Dimethylsulphoxide (DMSO), GABA, glutamate, ketamine, and all other chemicals were purchased from Sigma (St. Louis, USA).

1.2.2 *A. citrodora* Essential Oil Protocol

Fresh leaves of *A. citrodora* were collected from University of Jordan Faculty of Agriculture Botanic garden, spring 2011, when growth rate was maximal. The plant was authenticated by Prof. Suleiman Al-Olimat from the Faculty of Pharmacy, University of Jordan, where the voucher specimen (herbarium number AC-V1) is kept. Leaves were dried carefully in the shade at room temperature and then homogenized to fine powder and kept within tight bottles.

1.2.3 Rat Forebrain Membrane Protocol

Wistar strain adult male rats (200–300 g) were maintained under a 12 h light, 12 h dark cycle at 23 °C and 65% humidity, with water and standard laboratory food available ad libitum. Animal treatment and husbandry were performed in accordance with approved use of animals in scientific procedures regulated by the Animals (Scientific Procedures) Act 1986, UK. Animals were sacrificed humanely using Schedule 1 procedures by stunning followed by decapitation. The head of the rat was removed and placed on ice. Excess tissue from neck, up to the base of the skull was trimmed with a pair of large scissors. Using a scalpel or blade, a midline skin incision was made along the top of the skull (from between the eyes to the base of the skull) and pulled back to expose the bone. With the points of the small scissors two lateral cuts in the bone at the base of the skull were made to enable this (flap) to be removed with the forceps. The small scissors were then used to carefully cut up the side of the skull, removing the one covering the top of the brain with forceps. Again, using the small scissors, a midline cut was made through the nasal sinuses and this bone was removed. With a small spatula, the brain was carefully scooped

out rinsed with physiological buffer, to remove any remaining blood, hair, meningeal or bone fragment, the required tissue (forebrain) dissected immediately and kept frozen at -20ºC until use. The tissue was then homogenized in ice-cold homogenisation buffer containing 320 mM sucrose, using a dounce glass/glass homogenizer. The homogenate was centrifuged at 1000 × g, 4 °C for 10 min, the supernatant was stored in ice, and the pellets was re-homogenized in ice-cold buffer again, re-centrifuged at 1000 × g, 4 °C for 10 min. The supernatant from the first and second centrifugation steps were pooled together and centrifuged at 12,000 × g, 4 °C for 30 min. The supernatant was discarded and the pellet resuspended in 50 mM Tris containing 5 mM EDTA and 5 mM EGTA, pH 7.4 (5 ml/g of original tissue), and frozen at −20 °C until use.

1.2.4 Well-Washed Rat Membranes Freeze/thaw Protocol

The $GABA_AR$ binding assays were performed with well-washed rat membranes prepared by a five-step freeze-thaw protocol (Enna, 1978, Rezai et al., 2003). Briefly the unwashed membranes, prepared as described above, were thawed, resuspended in 50 volumes of homogenization buffer (50 mM Tris–HCl, pH 7.4, containing 5 mM EDTA, 5 mM EGTA and 320 mM sucrose) and were snap frozen in liquid nitrogen, centrifuged 12,000 × g, 4 °C for 30 min. The pellets were washed four additional times by resuspension in 50 volumes of ice-cold homogenization buffer, snap frozen in liquid nitrogen followed by centrifugation at 12,000 × g, 4 °C for 30 min. Finally, the pellets were suspended in homogenization buffer (pH 7.4). The tissue was then homogenized using a dounce glass/glass homogenizer, aliquots into (1 ml) samples and were then frozen and stored at −20 °C.

1.2.5 Determination of Protein Concentration in Well-Washed Rat Membranes

The protein concentration was determined using the method of Lowry (Lowry et al., 1951) employing Bovine Serum Albumin (BSA) as the standard protein. A stock solution of BSA (1 mg/ml) was serially diluted in water, to give a range of standard BSA concentrations from 0 to 100 µg/ml. Lowry reagent A (2% (w/v) sodium carbonate, 0.1M sodium hydroxide and 5% (w/v) SDS.), Lowry reagent B (2% (w/v) sodium potassium tartrate) and Lowry reagent C (1% (w/v) copper sulphate) were

mixed in a volume ratio of A (50): B (1): C (1). To both the BSA standards and the unknown protein samples (5 µl protein + 95 µl dH20, and 10µl protein + 90 µl dH_20) 0.5 ml of the mixture of reagent A, B and C was added, each sample was vortexed and incubated at room temperature for 10 minutes. All samples were assayed in triplicate. On the addition of 50 µl of Folin-Ciocalteau phenol reagent (1 M, 1:1 mix of Folin reagent and water) each sample was mixed and incubated at room temperature for 30 minutes. The reaction was terminated by the addition of 500 µl of water. The O.D. at λ = 750 nm was determined for each sample using a Jenway-Genova spectrophotometer. A calibration curve was plotted of O.D. at λ = 750 nm for the BSA samples. This was then used to determine the unknown protein concentration for any prepared well washed rat membranes samples.

1.2.6 **Binding Assay Protocol**

Each assay was performed in triplicate. All binding assays were carried out in 4 ml polystyrene tubes. Ligand stock was diluted in assay buffer to a concentration tenfold the desired final concentration. Solutions of test compounds were prepared at tenfold the desired final concentration. 80 µl assay buffer were added to the first three tube set (which represents total binding) and 60 µl assay buffer for all other tubes in the experiment.20 µl of the 10 x test compound were added to the tubes, except the total and non-specific binding sets. 20 µl of the 10x non-specific agent were added to the second three set of tubes for determination of non-specific binding. 100 µl of membrane preparation or cell homogenate were added to all the tubes. 20 µl of the 10x [^{3}H] or [^{35}S] ligand were added to all the tube. The samples were vortex-mixed and incubated until binding equilibrium was achieved. For many ligands, 1 hr at room temperature is sufficient to reach equilibrium. At the end of the incubation, the assay mixtures were harvested onto pre-soaked (0.2% polyethyleneimine) GF/B filters using Brandel cell harvester and wash subjected to three quick washes with ice-cold 10 mM sodium phosphaste buffer pH 7.4. The filters were transfered into 3 ml scintillation vials, each incubated with 1 ml scintillation cocktail, left for 16-24 hr at room temperature. Membrane bound readioactivity was determined by liquid scintillation counter (Beckman LS 500 CE). All tested compounds were dissolved at 100 mM in DMSO and serial dilutions were made with respective assay buffer. GABA, (-)-Nicotine hydrogen tartrate salt, and Ketamine stocks (10^{-2} M) were made

in assay buffer. Diazepam stocks (10^{-2} M) were prepared in absolute ethanol. Picrotoxinin stocks (10^{-2} M) were prepared in DMSO. No effect of solvents on radioligand binding assays was seen at concentrations below 0.1% (v/v) DMSO or 0.1% (v/v) ethanol.

1.2.7 **[^{3}H] Flunitrazepam Binding Assay**

[^{3}H] flunitrazepam binding assays were performed as previously described (Rezai et al., 2003). Briefly, well-washed rat forebrain membranes prepared by five-step freeze-thaw protocol were thawed, centrifuged and the supernatant was discarded. The pellets were resuspended again in fresh buffer (50 mM Tris-HCl, 5 mM EDTA, 5 mM EGTA, pH 7.4) to yield a final protein concentration in the assay of 1 mg/ml. An amount of 100 µg membrane protein was incubated with [^{3}H] flunitrazepam (approximately 1 nM) for 1 h at 4 °C with a range of test concentrations (10^{-11} to 10^{-4} M). Non-specific binding was defined in the presence of 100 µM diazepam.

1.2.8 **[^{3}H] Muscimol Binding Assay**

[^{3}H] muscimol binding assays were performed as previously described in Bohme et al., (2004). Briefly, well-washed rat forebrain membranes prepared by five-step freeze-thaw protocol were thawed, centrifuged and the supernatant was discarded. The pellets were resuspended again in fresh buffer (50 mM Tris-HCl, pH 7.4) to yield a final protein concentration in the assay of 1 mg/ml. An amount of 100 µg membrane protein was incubated with [^{3}H] muscimol (approximately 10 nM) for 1 h at 4 °C with a range of test concentrations (10^{-11} to 10^{-4} M). Non-specific binding was defined in the presence of 100 µM GABA.

1.2.9 **[^{35}S]-t-butylbicyclophosphorothionate (TBPS) Binding Assay**

[^{35}S] TBPS binding was performed essentially as described in Im et al., (1994). Briefly, well-washed rat membranes prepared by a five-step freeze-thaw protocol were, on the day of experiment, centrifuged and the supernatant was discarded. The pellets were resuspended in fresh buffer (50 mM Tris-HCl, containing 0.2 M NaCl, pH 7.4) to yield a final protein concentration in the assay of 1 mg/ml. An amount of 100 µg membrane protein was incubated with [^{35}S] TBPS (approximately 20 nM) for 90 min at 25 °C with a range of test concentrations (10^{-11} to 10^{-4} M). Non-specific binding was defined in the presence of 100 µM picrotoxinin.

1.2.10 [^{3}H] MK-801 Binding Assay

[^{3}H] MK-801 binding assays were performed as previously described (Chazot et al., 1993). Briefly, well-washed rat forebrain membranes prepared by five-step freeze-thaw protocol were thawed, centrifuged and the supernatant was discarded. The pellets were resuspended again in fresh buffer (25 mM sodium phosphate buffer pH 7.4) to yield a final protein concentration in the assay of 1 mg/ml. An amount of 100 µg membrane protein was incubated with [^{3}H] MK-801 (approximately 1 nM) and 10 µM glutamate for 2h at 22 °C with a range of test concentrations (10^{-11} to 10^{-4} M). Non-specific binding was defined in the presence of 10 mM ketamine.

1.2.11 [^{3}H] Nicotine Binding Assay

[^{3}H] Nicotine binding assays were performed as previously described in Wake et al., (2000). Briefly, well-washed rat forebrain membranes prepared by five-step freeze-thaw protocol were thawed, centrifuged and the supernatant was discarded. The pellets were resuspended again in fresh buffer (50 mM Tris buffer containing 8 mM $CaCl_2$ pH 7.4) to yield a final protein concentration in the assay of 1 mg/ml. An amount of 150 µg membrane protein was incubated with [^{3}H] Nicotine (approximately 4 nM) for 1 h at 25 °C with a range of test concentrations (10^{-11} to 10^{-4} M). Non-specific binding was defined in the presence of 100 µM (-)-Nicotine hydrogen tartrate salt.

1.2.12 Radio Ligand Binding Assay Analysis

Results from the radioligand binding assays were analysed using GraphPad Prism 5 Software program (GraphPad Software, San Diego, CA). For competition assays non-linear least squares regression was used, curves were best fitted to a one- or two-site binding model. The EC_{50} and IC_{50} values are the concentrations for half-maximal enhancement and displacement, respectively. Data were analysed using a Student's unpaired t-test, with levels of significance set at $p < 0.05$.

The IC_{50} values for competition curves fitted to a one-site competition model, were calculated from the following equation: $$y = \frac{A + (B - A)}{1 + 10^{(x - \log IC_{50})}}$$

Where:

A and B = the minimum and maximum percentage specific binding respectively.

Y = specific binding at a fixed concentration of displacing drug

X = $\log_{10}$ concentration of the displacer

IC_{50} = concentration of the displacer which inhibits 50% of the specific binding of the radioligand.

The IC_{50} values for competition curves fitted to a two-site competition model were calculated from, $Y = \frac{A + (B - A)}{\left(\frac{Fraction1}{1 + 10^{(x - \log IC_{50}1)}}\right) + \left(\frac{1 - Fraction1}{1 + 10^{(x - \log IC_{50}2)}}\right)}$

Where: A, B, X and Y are as above, (1) and (2) = the high and low affinity sites for the one-site and two-site binding models, the apparent inhibition constants (KI) were calculated using the Cheng-Prusoff equation (Yung-Chi and Prusoff, 1973),

Where:

IC_{50} = concentration of ligand giving 50% of the specific binding.

[L] = [^{3}H] Radioligand concentration.

K_D = dissociation constant from saturation binding of [^{3}H] radioligand to the respective receptor.

1.3 Results

1.3.1 Effects of *A. citrodora* Essential Oils on the Benzodiazepine Binding Site of the $GABA_A$ labelled by [^{3}H] Flunitrazepam in rat forebrain membranes

To validate the [^{3}H] flunitrazepam binding assay, two control compounds were used, GABA & diazepam. It is known that the binding sites for GABA and benzodiazepines are allosterically coupled; this is demonstrated by the ability of GABA to enhance the binding of [^{3}H] flunitrazepam as shown in Fig 2.4. GABA significantly enhanced specific binding of [^{3}H] flunitrazepam to native forebrain preparation in a concentration-dependent manner, yielding a mean Emax = 153 ± 4% and apparent EC_{50} = 31 ± 2 nM, respectively. GABA enhancement of [^{3}H] flunitrazepam observed in our study was in the range of that observed for well-washed rat cerebral cortical membranes by (Ghiani et al., 1996). Diazepam significantly displaced specific binding of [^{3}H] flunitrazepam in a concentration-dependent manner. Data were best fit to sigmoidal model yielding a mean apparent IC_{50} = 19.4 ± 1.5 nM. (Fig 2.5) shows the results from three independent experiments, each performed in triplicate for each membrane preparation. The potency of diazepam to displace [^{3}H] flunitrazepam is in good agreement with the literature data obtained for the displacement of the same radioligand from brain membranes (Massotti et al., 1991).

The effects of *A. citrodora* essential oil on radioligand binding to benzodiazepine site of $GABA_A$ were studied using [^{3}H] flunitrazepam binding assay with four different oil concentrations [0.0001, 0.001, 0.01 and 0.1 mg/ml] of both dry and fresh extract. Specific [^{3}H] flunitrazepam binding was defined using diazepam (100 µM). *A. citrodora* essential oil (both fresh and dry) did not alter the equilibrium binding of [^{3}H] flunitrazepam to $GABA_A$ receptors in adult rat forebrain membranes as shown in figures 2.6 and 2.7

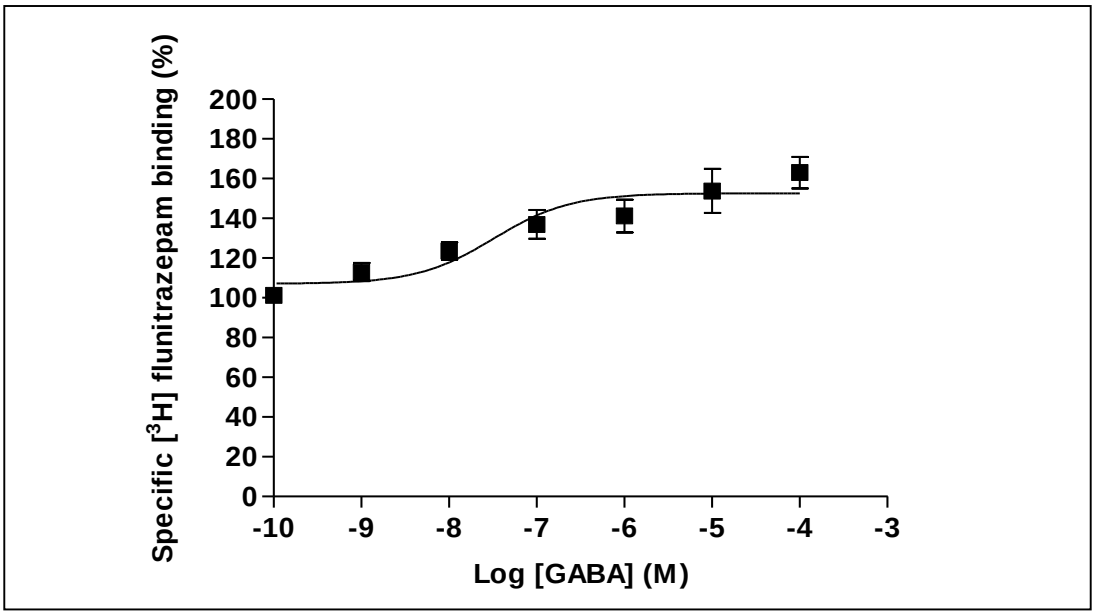

Figure 2.4
Effect of GABA upon [^{3}H] Flunitrazepam binding to adult rat forebrain membranes. Results are mean ± SD for three independent experiments each performed in triplicate.

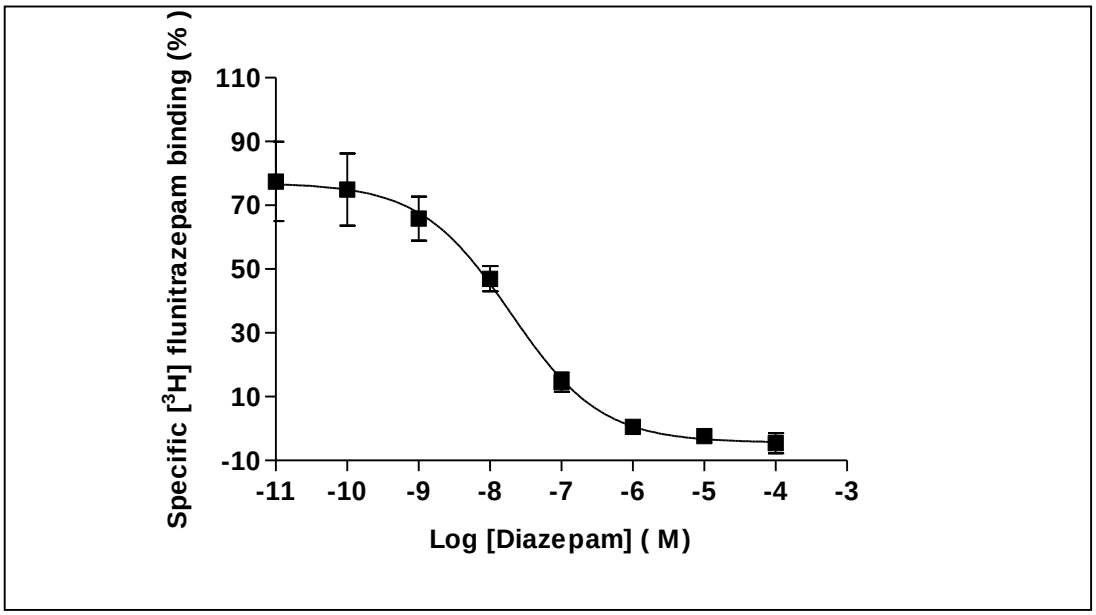

Figure 2.5
Effect of diazepam upon [^{3}H] flunitrazepam binding to adult rat forebrain membranes. Results are mean ± SD for three independent experiments each performed in triplicate.

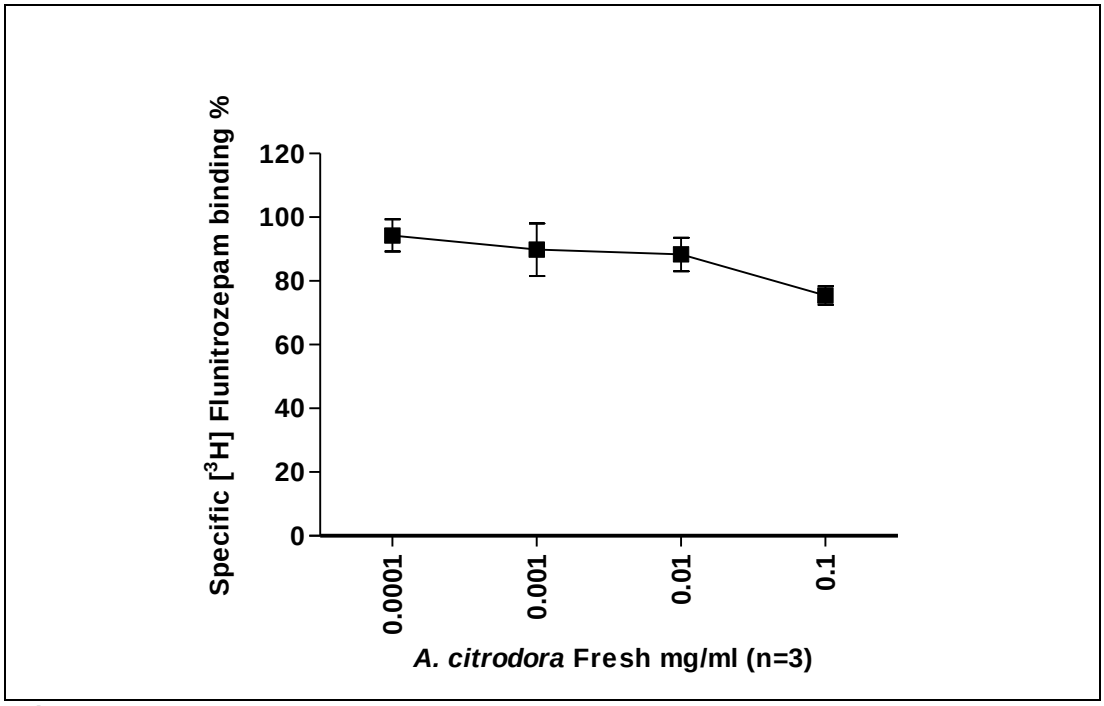

Fig 2.6

Effect of Fresh *A. citrodora* essential oil upon [^{3}H] flunitrazepam binding to adult rat forebrain membranes. Results are mean ± S.D for three independent experiments each performed in triplicate.

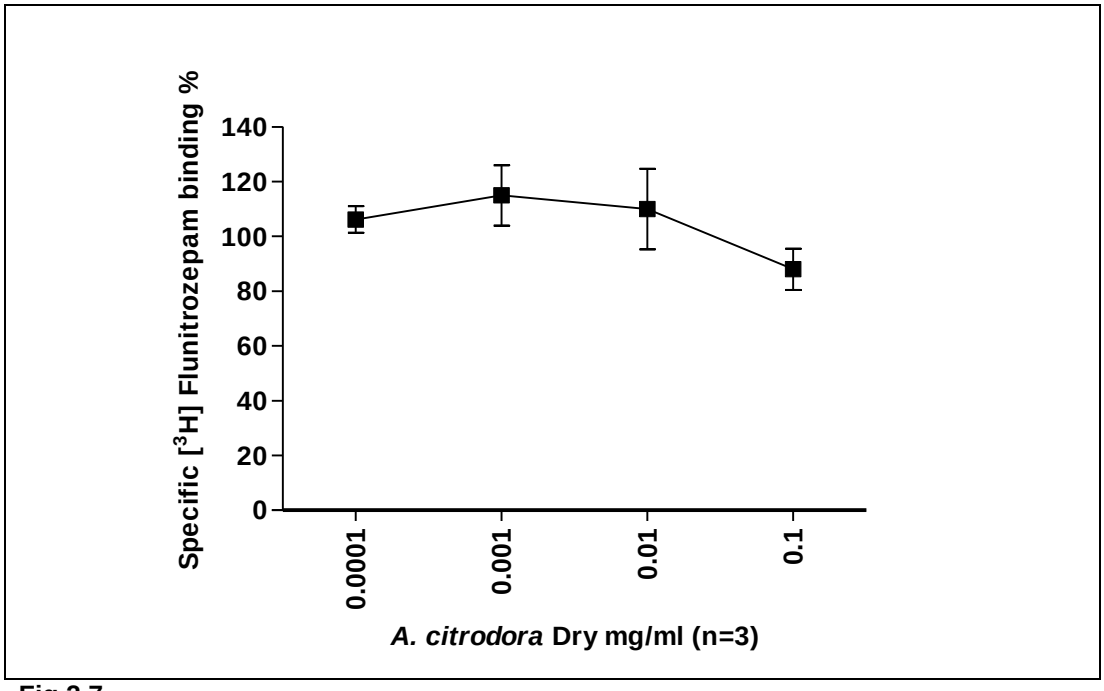

Fig 2.7

Effect of Dry *A. citrodora* essential oil upon [^{3}H] flunitrazepam binding to adult rat forebrain membranes. Results are mean ± S.D for three independent experiments each performed in triplicate.

1.3.2 Effects of *A. citrodora* EO on the Agonist Binding Site of the $GABA_AR$ labelled by [^{3}H] Muscimol in rat forebrain membranes.

A control experiment of [^{3}H] muscimol binding to well washed rat forebrain in the presence of different concentrations of GABA was carried out to validate the assay. GABA significantly displaced specific binding of [^{3}H] muscimol in a concentration-dependent manner. Data were best fit to sigmodial model variable slope with a pseudo-Hill coefficient, close to unity (n_H = 0.72 ± 0.06) with an apparent IC_{50} = 106 ± 1 nM. (Fig 2.8) shows the results from three independent experiments, each performed in triplicate for each membrane preparation. The observed potency of GABA for inhibiting [^{3}H] muscimol binding is also in good agreement with the binding affinity of this drug for recombinant α1β2γ2 $GABA_AR$ reported by (Baur and Sigel, 2003).

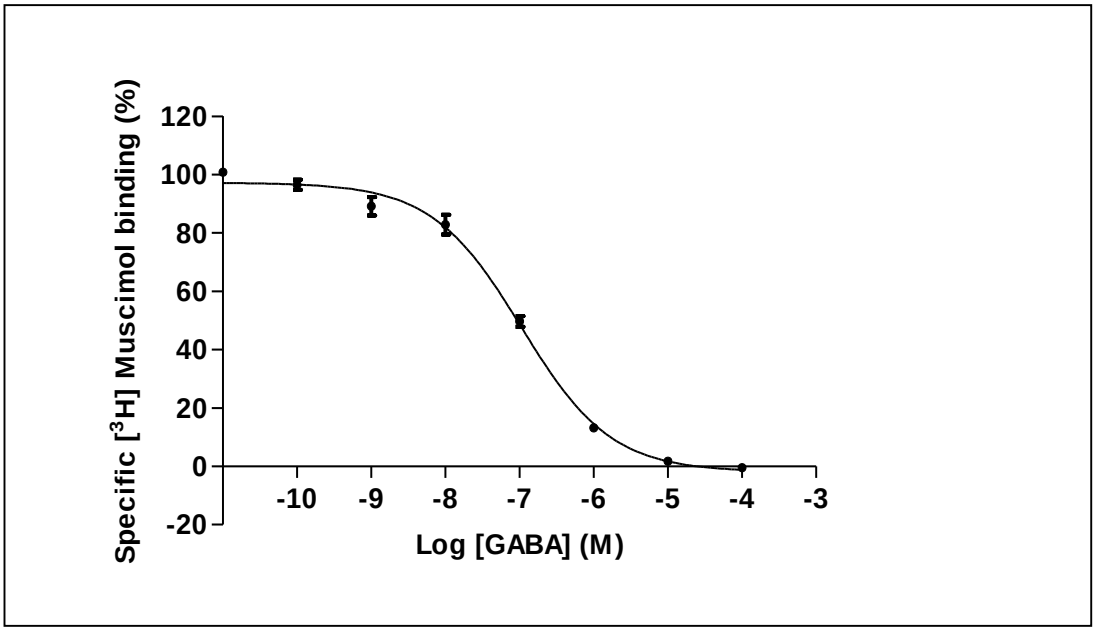

Fig 2.8
Effect of GABA upon [^{3}H] muscimol binding to adult rat forebrain membranes. Results are mean ± SD for three independent experiments each performed in triplicate.

The effects of *A. citrodora* essential oils on radioligand binding of $GABA_AR$ were studied using [3H] muscimol binding assay with concentrations [0.0001, 0.001, 0.01 and 0.1 mg/ml] of both dry and fresh extract. Specific binding was defined using 100 µM GABA. *A. citrodora* essential oil did not alter the equilibrium binding of [3H] muscimol to $GABA_A$ receptors in adult rat forebrain membranes as shown in figures 2.9 and 2.10.

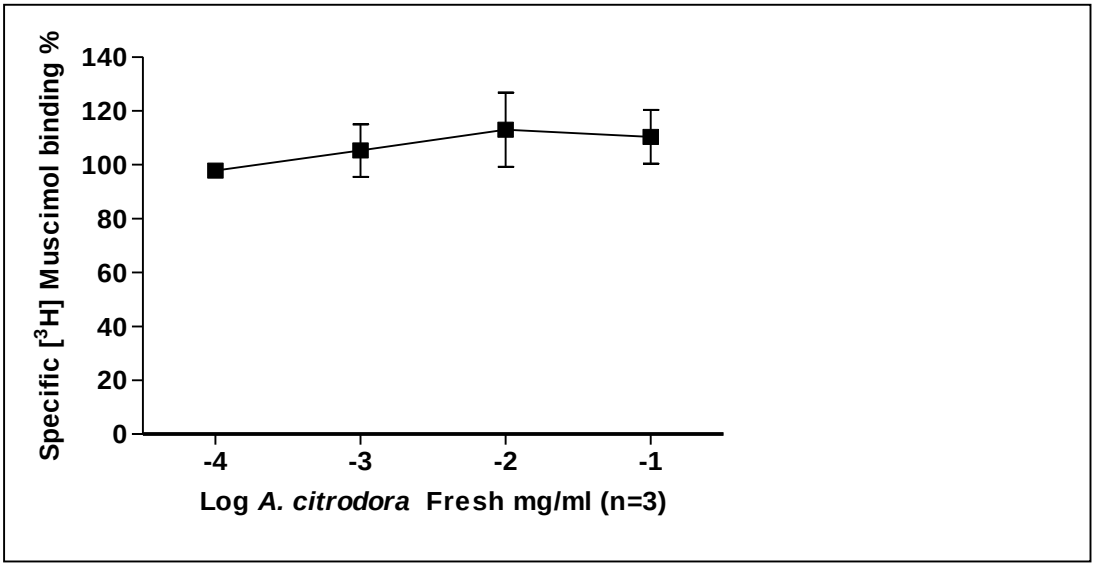

Fig 2.9
Effect of fresh *A. citrodora* upon [^{3}H] muscimol binding to adult rat forebrain membranes. Results are mean ± SD for three independent experiments each performed in triplicate.

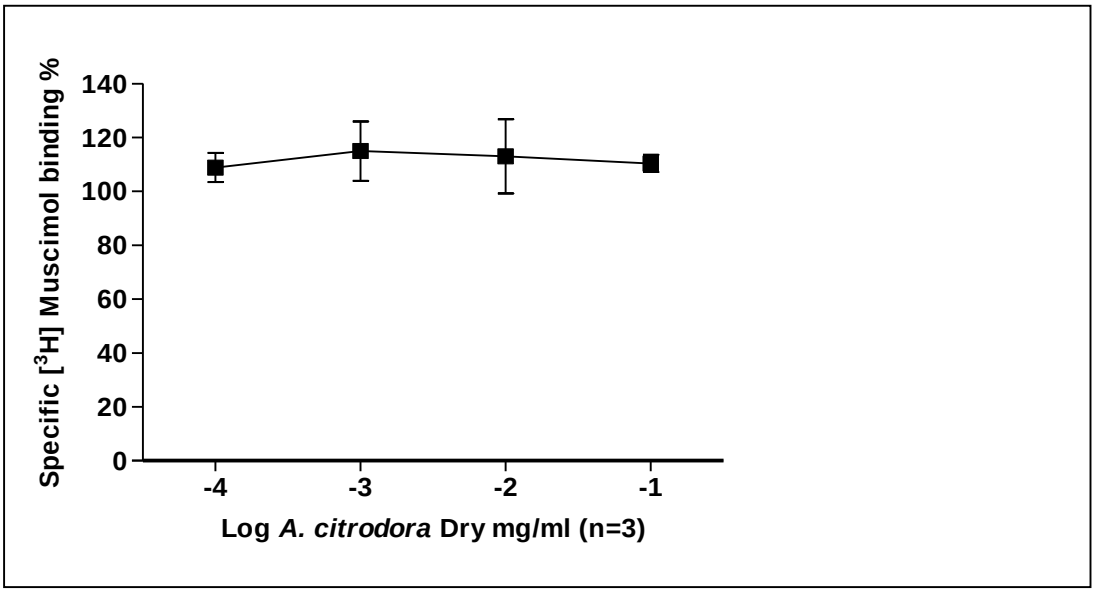

Fig 2.10 Effect of dry *A. citrodora* upon [^{3}H] muscimol binding to adult rat forebrain membranes. Results are mean ± SD for three independent experiments each performed in triplicate.

1.3.3 Effects of *A. citrodora* EO on the Channel Binding Site of the GABAAR Labelled by [^{35}S] TBPS in Rat Forebrain Membranes

Two control compounds were used to validate [^{35}S] TBPS (t-butylbicyclophosphorothionate) binding assay, picrotoxinin and diazepam. Picrotoxinin displayed a steep monophasic inhibition of [^{35}S] TBPS binding with Hill slope close to unity nH = 1.3 ± 0.2 with an apparent IC_{50} = 309 ± 1 nM. Fig 2.11 shows the results. The observed IC_{50} appears to be in close agreement with the published literature (257 ± 12 nM) (Wang et al., 1999). Consistent with pervious published data (Ghiani et al., 1996), diazepam significantly enhanced specific binding of [^{35}S] TBPS in a concentration-dependent manner, data were best fit to sigmoidal model, yielding a mean Emax = 157 ± 3% and apparent EC_{50} = 4.3 ± 0.5 nM, respectively. Fig 2.12 shows the results from three independent experiments, each performed in triplicate. However, it is known from the literature that diazepam had a bidirectional modulatory effect on [^{35}S] TBPS binding. At low concentrations diazepam enhanced the specific binding of [^{35}S] TBPS whereas, at high concentrations it elicited an inhibitory effect. The observed apparent EC_{50} values obtained are similar to the literature (Ghiani et al., 1996).

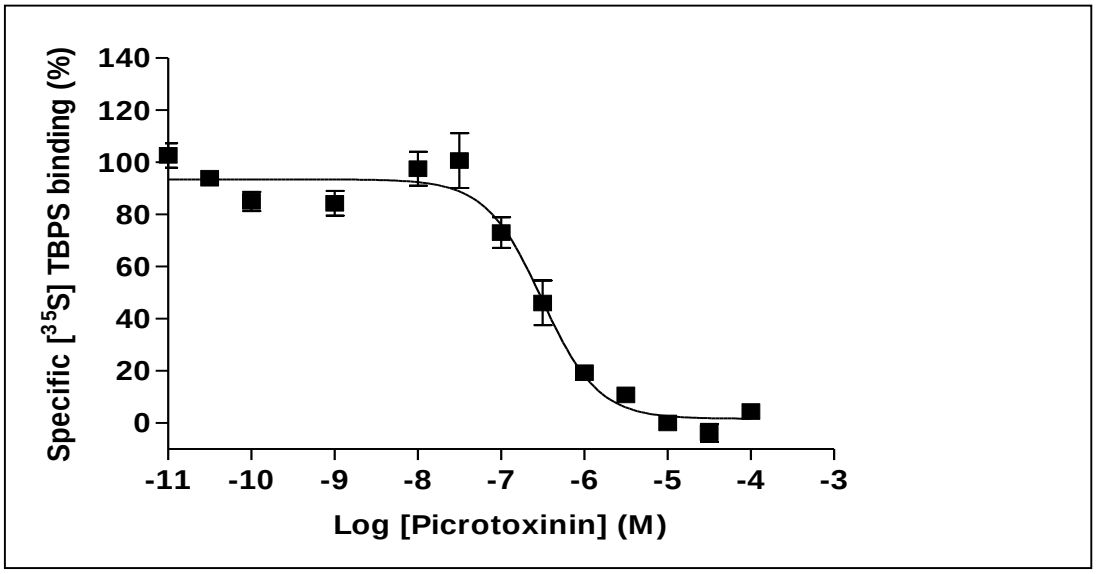

Fig 2.11
[^{35}S] TBPS competition binding to well-washed adult rat forebrain membranes in the presence of picrotoxinin. Results are mean ± SD for three independent experiments each performed in triplicate.

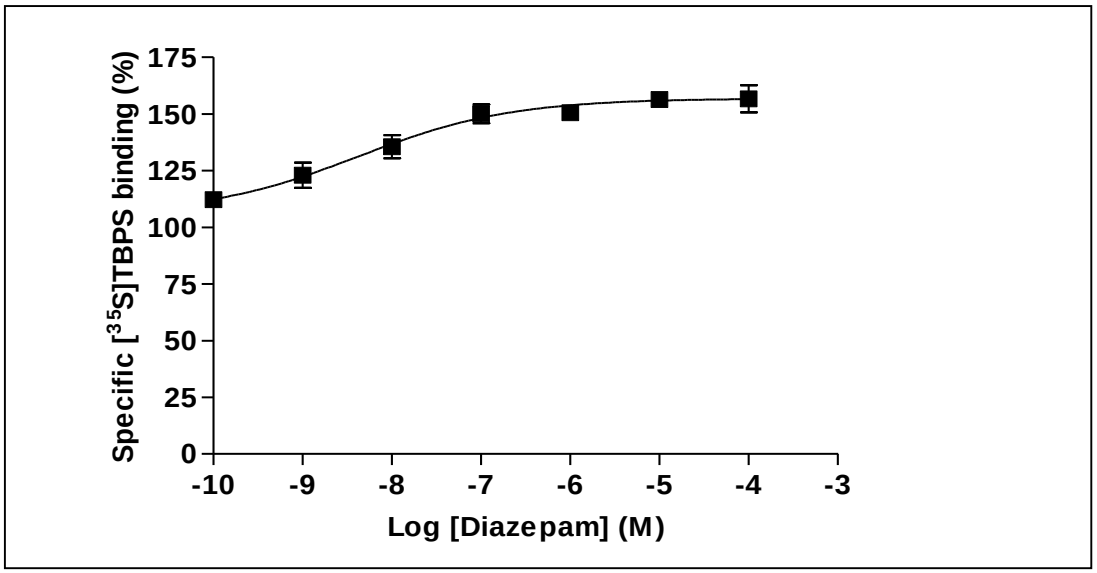

Fig 2.12
[^{35}S] TBPS competition binding to well-washed adult rat forebrain membranes in the presence of diazepam. Results are mean ± SD for three independent experiments each performed in triplicate.

To investigate the effect of *A. citrodora* essential oils on the channel site of $GABA_A$ receptor [^{35}S] TBPS binding activity was carried to well-washed to adult rat forebrain, using four different oil concentrations [0.0001, 0.001, 0.01 and 0.1 mg/ml] of both dry and fresh oil extract. Specific binding was defined using 100 µM picrotoxinin. *A. citrodora* essential oil both fresh and dry did not alter the equilibrium binding of [^{35}S] TBPS to $GABA_A$ receptors in adult rat forebrain membranes as shown in figures 2.13 and 2.14.

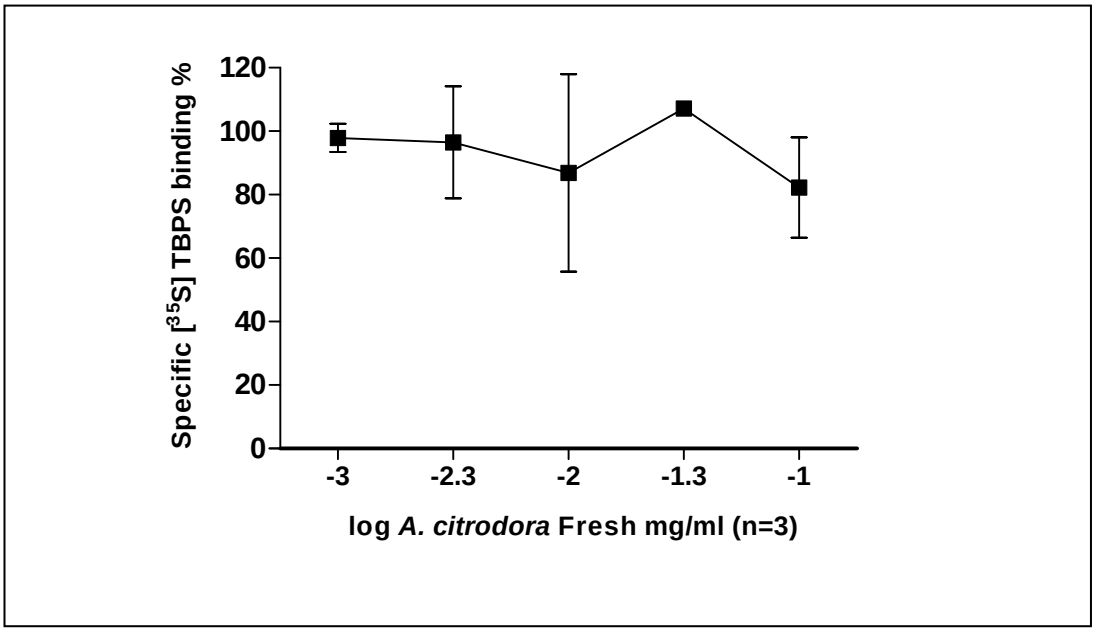

Figure 2.13
[^{35}S] TBPS competition binding to well-washed adult rat forebrain membranes in the presence of fresh *A. citrodora* oil. Results are mean ± SD for three independent experiments each performed in triplicate.

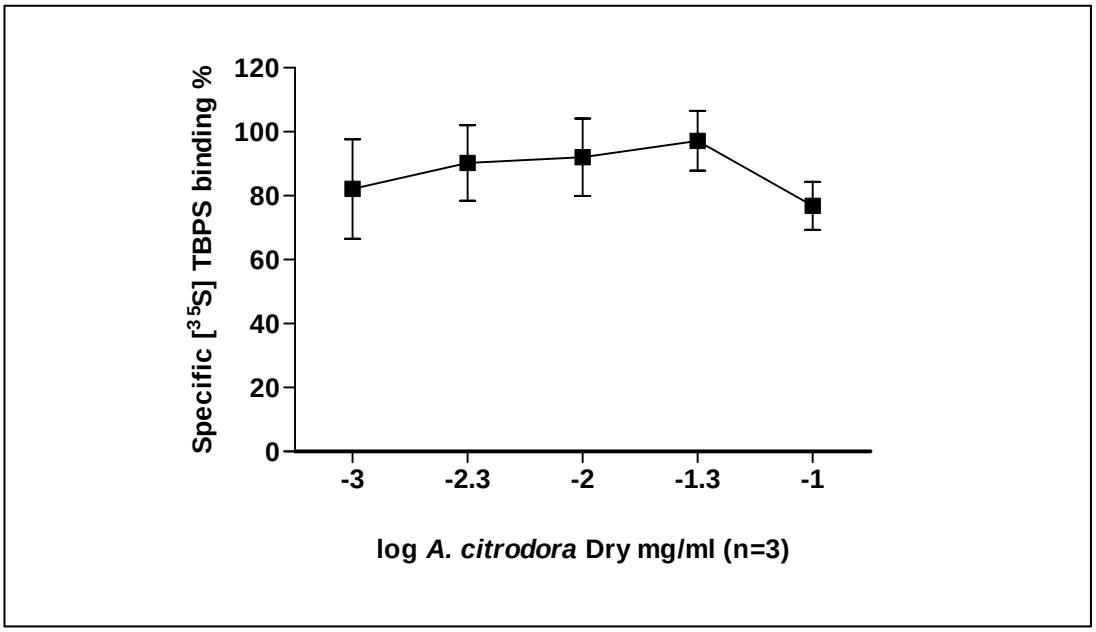

Figure 2.14
[^{35}S] TBPS competition binding to well-washed adult rat forebrain membranes in the presence of dried *A. citrodora* essential oil. Results are mean ± SD for three independent experiments each performed in triplicate.

1.3.4 Effects of *A. citrodora* EO on the [^{3}H] MK-801 Binding to Rat Forebrain Membranes

A control experiment of [^{3}H] MK-801 (uncompetitive antagonist of the NMDA receptor) binding to adult rat forebrain in the presence of different concentrations of ketamine was carried out to validate the assay. Ketamine significantly displaced specific binding of [^{3}H] MK-801 in a concentration-dependent manner in native preparation. Data were best fit to one site model yielding a mean of apparent IC_{50} = 2 ± 1 mM. Fig 2.15 shows the results. The observed IC_{50} value appears to be similar to the literature value (Wang et al., 1999).

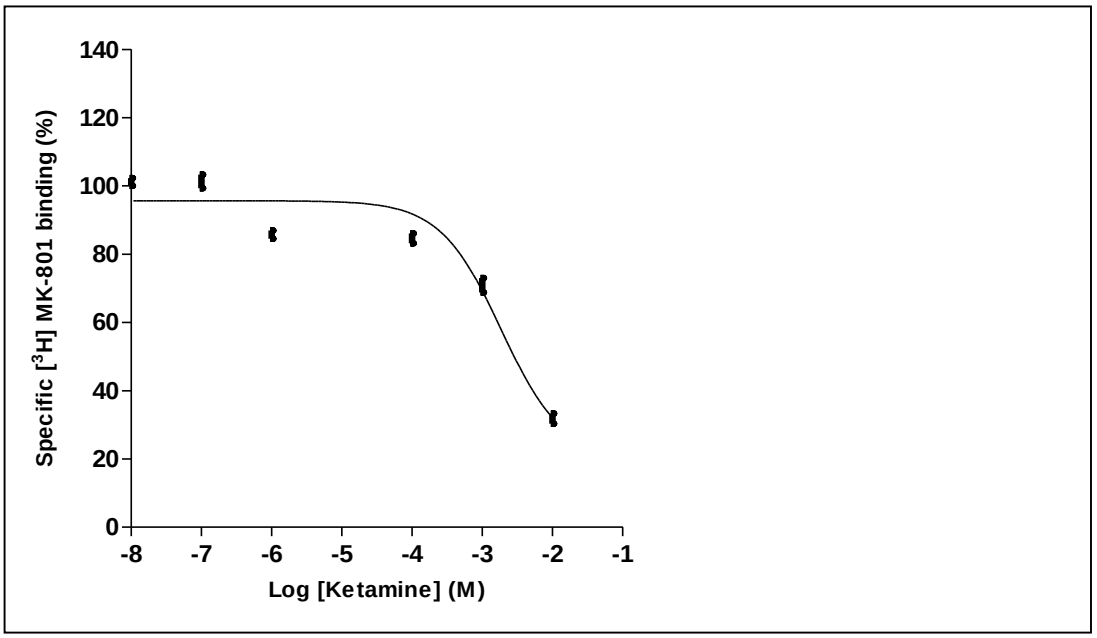

Fig 2.15 [^{3}H] MK-801 competition binding to adult rat forebrain membranes in the presence of ketamine. Results are mean ± SD for three independent experiments each performed in triplicate.

The effects of *A. citrodora* Essential Oils on radioligand binding was assayed at the excitatory ligand gated ion channels gated by NMDA using [^{3}H] MK-801 binding assay with four different oil concentrations [0.0001, 0.001, 0.01 and 0.1 mg/ml] of both dry and fresh extract. Non-specific binding was defined in the presence of 10 mM ketamine. *A. citrodora* Essential Oils both fresh and dry did not alter the equilibrium binding of [^{3}H] MK-801 binding to rat forebrain membranes. (Fig 2.16 and 2.17) show the results.

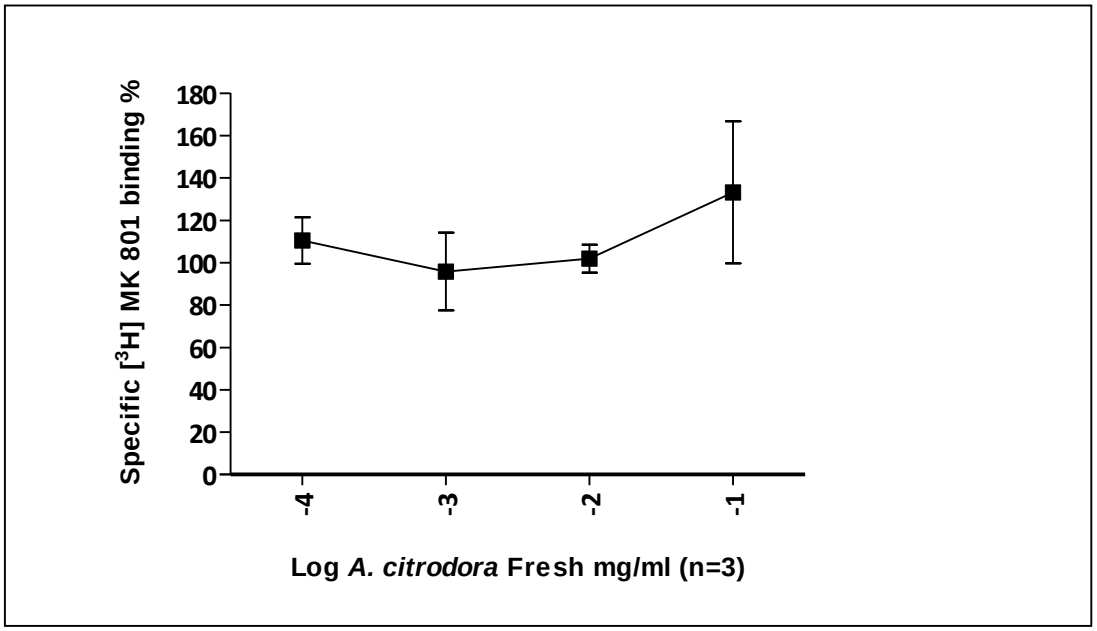

Fig 2.16 [^{3}H] MK-801 competition binding to adult rat forebrain membranes in the presence of fresh *A. citrodora* essential oil. Results are mean ± SD for three independent experiments each performed in triplicate.

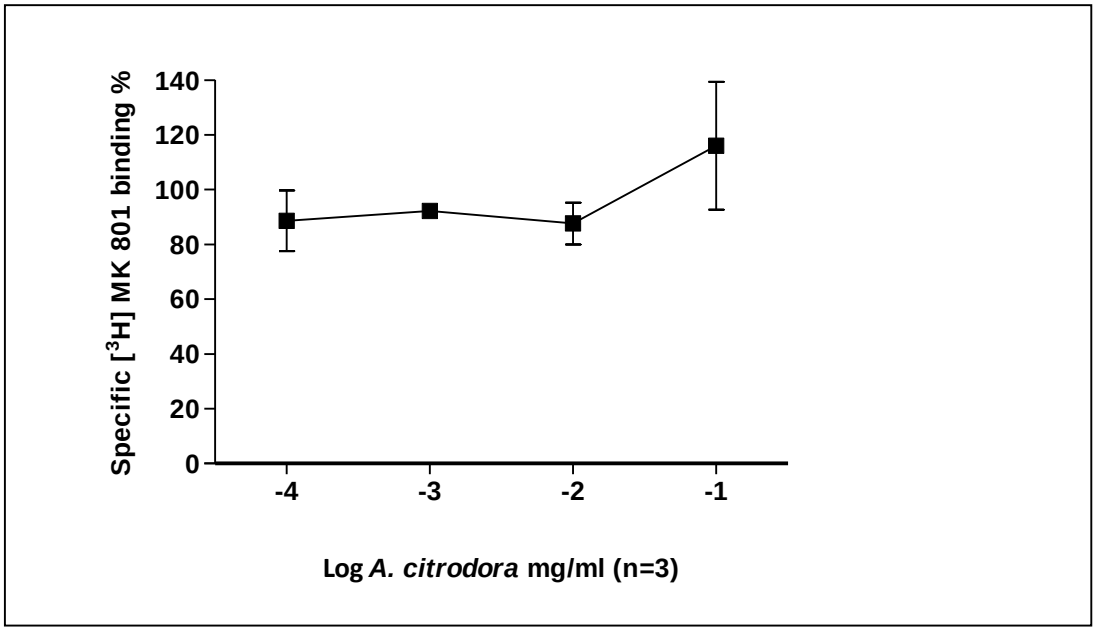

Fig 2.17 [^{3}H] MK-801 competition binding to adult rat forebrain membranes in the presence of dried *A. citrodora* essential oil. Results are mean ± SD for three independent experiments each performed in triplicate.

1.3.5 Effects of *A. citrodora* EO on [^{3}H] Nicotine Binding to Rat Forebrain Membranes

A control experiment of [^{3}H] nicotine binding to adult rat forebrain, in the presence of different concentrations of nicotine, was carried out to validate the assay. Fig 2.18 shows the results. Nicotine produced a concentration dependent inhibition of [^{3}H] nicotine binding, data was best fit to two site competition model, comprising high and low affinity binding sites in the ratio 74: 26 (high: Low % , SD ± 6). Site one apparent IC_{50} 4.5 nM, site two apparent IC_{50}= 3.5 µM. Nicotine binds to the α4β2 nAChR with high affinity (4.5 nM) whereas the α7 is 1000-fold less sensitive (3.5 µM). This selectivity profile is consistent with the published literature (Xiao et al., 1998).

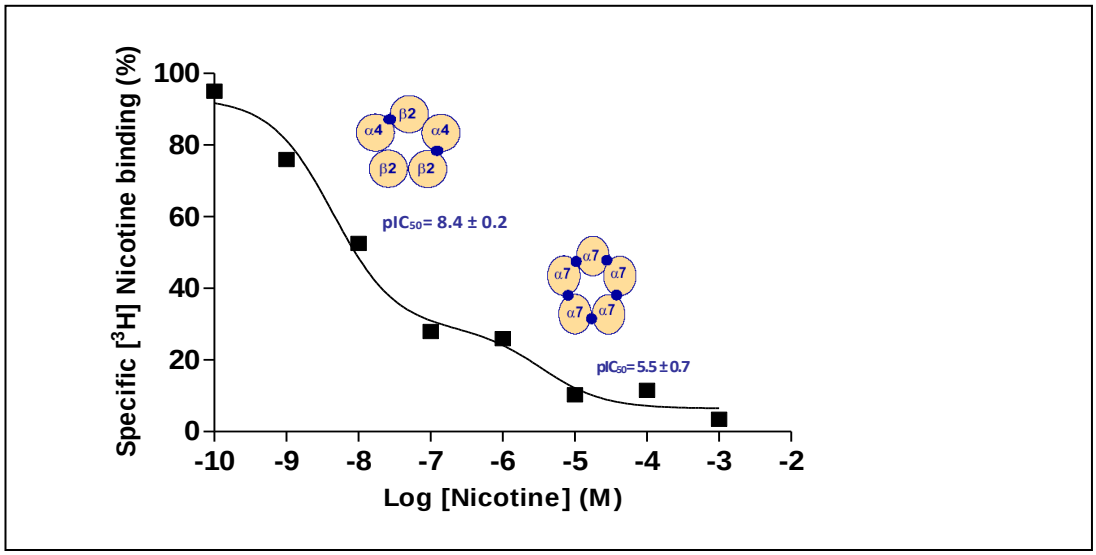

Fig 2.18 [^{3}H] nicotine competition binding to adult rat forebrain membranes in [^{3}H] nicotine competition binding to adult rat forebrain membranes in the presence of nicotine. Results are mean of three independent experiments each performed in triplicate.

The effects of *A. citrodora* essential oils on neuronal nicotinic receptors using [^{3}H] nicotine binding assay with four different oil concentrations [0.0001, 0.001, 0.01 and 0.1 mg/ml] of both fresh and dried extract. Only fresh extract inhibited from [^{3}H] nicotine binding to well washed rat forebrain membranes at concentrations of 0.001mg/ml and above, with mean apparent IC_{50} of 0.0018 ± 0.0008 mg/ml (Fig 2.19).

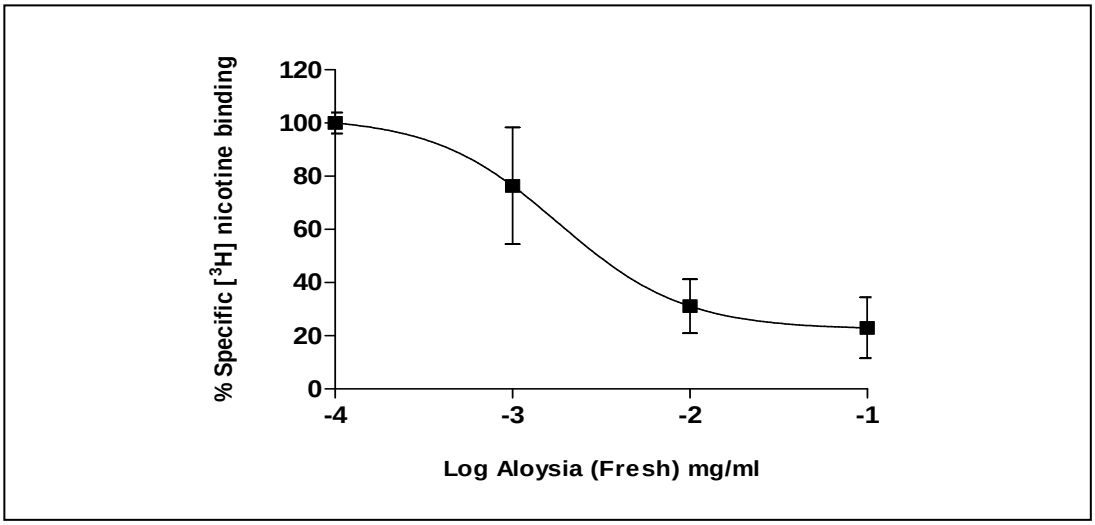

Fig 2.19
[^{3}H] Nicotine competition binding to well-washed adult rat forebrain membranes. Results are expressed as mean % specific [^{3}H] nicotine binding ± S.D. for three independent experiments

1.4 Discussion

In this chapter, we have characterized the radioligand binding profile for the essential oils (EO) derived from freshly prepared and dried *A. citrodora* focussing on the binding sites of major CNS ligand gated ion channel $GABA_A$, NMDA and nicotinic receptors. A series of control experiments were initially performed to validate the assays employed.

The major finding was that fresh *A. citrodora* essential oil inhibited [^{3}H] nicotine binding in a concentration-dependent manner (IC_{50} = 0.0018 mg/ml) with no significant effects on the other major ligand gated ion channels (up to 0.1 mg/ml) which were tested. This is in marked contrast to our previous published findings with the essential oils derived from the European Melissa (*M. officianalis*) essential oil in which displayed no apparent effects upon nicotinic receptors, but showed a dose dependent inhibition of [^{35}S] TBPS binding to $GABA_A$ receptor with apparent IC_{50} 0.040 mg/ml (Huang et al., 2008)

Many medicinal plants have nicotinic agonist activity (Polya, 2003). For instance Lobeline from *Lobelia inflate* interacts with the nicotinic receptor (Decker et al., 1993) and could also be exploited to influence cholinergic function in AD. Other alkaloids such as sophoramine and cytisine, found in members of the Leguminosae, have nicotinic actions (Brahmachari 2012). Cytisine is only used as a pharmacological tool because of its strong binding affinity for nicotinic receptors, but not used for any pharmaceutical purposes because of its toxicity (Brahmachari 2012). The root of *Withania somnifera* is one of the most highly regarded herbs in Ayurvedic medicine and has cognitive enhancing properties, by augmenting learning acquisition and memory in both young and old rats (Ghosal et al., 1989). The mechanisms to explain this effect involve the modulation of cholinergic neurotransmission. The root extract enhanced AChE activity in the lateral septum and globus pallidus areas of the brain and also enhanced muscarinic M1 receptor binding in cortical regions, but as with *A. citrodora* essential oil it did not affect $GABA_A$, benzodiazepine receptor binding, nor NMDA or AMPA glutamate receptor subtypes (Schliebs et al., 1997).

Neuronal nicotinic acetylcholine receptors represent novel targets for CNS therapeutics, and may have substantial roles in mediating antinociception, as well as modulating cognitive performance. Much of the current pharmacological approaches for treating neurodegenerative disorders are mainly directed at correcting neurotransmitter specific deficiencies. This significantly contributes to the deterioration in cognitive function seen in AD patients (Birks, 2006). Furthermore, the reduced number of nicotinic acetylcholine receptors in the hippocampus and cortex of AD patients, as compared to age-matched controls, results in reduced nicotinic cholinergic excitation which may not only impair postsynaptic depolarization but also presynaptic neurotransmitter release and Ca^{2+} dependent intracellular signalling, including transcriptional activity. The most common approach to correct the nicotinic cholinergic deficit in AD is the application of cholinesterase inhibitors. The use of nicotinic acetylcholine receptors agonists may represent another means for activating viable cholinergic receptors in the AD brain. (Maelicke and Albuquerque, 2000).

Nicotinic agonists can increase tau immune reactivity and alter its phosphorylation state (e.g., increased both tau phosphorylated and dephosphorylated levels probably via activation of nicotinic acetylcholine receptors (Rubio et al., 2006). Chronic nicotine treatment results in decreased plaque load and reductions in cortical β-amyloid concentrations in the Tg mice carrying the Swedish mutation of human APP (Hellstrom-Lindahl et al., 2004), but not in 3xTg-AD mice (Oddo et al., 2005).

Approximately half of the cortical tyrosine kinase receptor A (TRkA) is lost in the early stages of AD progression (Counts et al., 2004). Nicotine treatment of Wistar rats increased the expression of TrkA in the hippocampus (Jonnala et al., 2002). In the cholinergic neurons of the basal forebrain from AD patients, TrkA was found to serve as a receptor for the NGF a critical trophic factor for the survival of neurons.

New evidence that the cholinergic system has a specific pathogenic role in the neurodegenerative alterations of aged and, especially, demented patients is fast accumulating. Both in vivo and in culture, nicotine protects striatal, hippocampal and cortical neurons against the neurotoxicity induced by excitotoxic amino acids as well

as the toxicity caused by β-amyloid, the major component of senile plaques. Further support for the implication of nicotinic receptors in brain ageing has arisen from recent studies on transgenic animals lacking nicotinic receptor subtypes, which has shed light on the mechanisms of nicotine neuroprotection and neurotoxicity (Zanardi et al., 2002).

A. citrodora essential oil constituent(s) responsible for this activity needs to be identified. An initial attempt will be described later in Chapter 5. The next two chapters will investigate whether the *A. citrodora* essential oils display any anti-cholinesterase, or anti-oxidant or neuroprotective properties along with its nicotinic binding profile.

Chapter 3

Pharmacological Profile of *Aloysia citrodora* Palau Essential Oil: Cholinergic, Anti-Oxidant and Iron Chelation Properties

3.1 Introduction

3.1.1 Acetylcholinesterase Inhibitors in Neurodegenerative Diseases

According to the cholinergic hypothesis, AD is caused by reduction in the synthesis of acetylcholine in cholinergic neurons of basal forebrain and loss of cholinergic neurotransmission in the cerebral cortex. The decrease in acetylcholine significantly contributes to the deterioration in cognitive function seen in AD patients (Birks, 2006). Cholinesterase enzymes hydrolyze acetylcholine. The selective inhibition of AChE reduces the breakdown of acetylcholine and increases availability of acetylcholine at the synapse resulting in restoration of cognitive and memory function. AChE inhibitors are currently the pharmacological mainstay therapy for AD. They include donepezil, galantamine, and rivastigmine (Bond et al., 2012).

3.1.2 Oxidative Stress in Neurodegenerative Diseases

Oxidative stress results from excessive levels of ROS generated through imbalance of normal biochemical processes. These oxygen radicals can then damage all types of macromolecules, disrupting normal cellular functions and, ultimately, cause cell death. The brain has the highest metabolic rate of any tissue and has an obligate requirement for aerobic metabolism. This, combined with endogenously high concentrations of Cu^{+} and Fe^{+} metal ions increase the vulnerability of brain to oxidative stress. The vast majority of biochemical radicals and ROS arise from the redox chemistry of metals. Redox-active metals become

available for ROS and radical generation when they either escape their chaperones (usually because the concentration of metal is too high to be completely chaperoned), or because of an accumulation of a damaged metalloprotein that inappropriately permits reaction of the metal with oxygen. The hydroxyl radical generates a variety of oxidative damage observed often in neurodegenerative disorders, including AD and PD.

The primary ROS implicated in oxidative stress is the hydroxyl radical, whose damage is dependent upon its diffusion capacity over nanometre distances from its generation site. Although peroxynitrite also appears capable of hydroxyl-like activity, most hydroxyl radicals reflect the Fenton reaction between reduced transition metals (usually iron II or copper I) and H_20_2. Re-reduction of iron III and copper II can be performed by superoxide or other cellular reductants such as ascorbate.

In addition to their role in redox processes, transition metals may contribute to neurodegeneration, along with redox-inactive metal ions, through their deleterious effects on protein and peptide structure, such as a pathological aggregation phenomenon. In such cases, transition metals can sometimes exert dual neurotoxic effects. In contrast, there are also a number of normal antioxidant defence mechanisms to combat the effects of ROS through both enzymatic and none enzymatic pathways in mammalian cells. Cytosolic copper-zinc superoxide dismutase (CuZnSOD) and mitochondrial manganese superoxide dismutase (MnSOD) are two such important players in the antioxidant defense system. These enzymes convert reactive superoxide to harmless O_2 and H_2O_2. The latter is then removed by catalase and peroxidases, which are abundant throughout tissues. In addition, there are a number of proteins closely tied to metal induced redox activity. These include proteins involved in metal transport and those which do not normally have a metal-binding function, but are able to bind metals for neuroprotection (Zatta, 2003).

3.1.3 Iron in Neurodegenerative Diseases

Free iron has long been implicated in neurodegenerative disease through its redox transitions *in vivo*. The consequential generation of oxygen free radicals can further induce oxidative stress in tissues. Abnormally high levels of iron and oxidative stress have been found in most neurodegenerative disorders (Sayre et al., 2000, Smith et al., 2010). Oxidative stress, under these conditions, has been associated with levels of free iron. An increased level of total iron does not necessarily signify increased oxidative stress if it is accompanied by a concomitant increase in iron storage proteins, which keep iron in a redox-inert state. Two classes of iron-related neurodegenerative disorders can be distinguished; the first due to iron accumulation in specific brain regions, and the second resulting from defective iron metabolism and perturbation of iron homeostasis (Zecca et al., 2004). As life expectancy increases and, as a consequence, brain iron accumulates, we would expect the occurrence of iron-related neurodegenerative diseases to inexorably increase (Robert Crichton, 2013).

The aim of this chapter is to screen the essential oil derived from the leaves *A. citrodora* for potential anti-oxidant and iron chelation properties, in addition to AChE inhibitory activity.

3.2 Materials and Methods

3.2.1 Acetylcholinesterase Inhibitory Assay in 96-well Plate

AChE inhibitory activity was determined using a 96-well plate format Ellman's colorimetric method (Ellman et al., 1961) with slight modification as previously described by (Oinonen et al., 2006). 25 µl of plant extract dissolved in 50 mM Tris buffer (pH 8), was added to the wells in a 96-well plate, followed by 25 µl of 15 mM acetylthiocholine iodide in H_2O, 125 µl of 3 mM 5,50-dithiobis (2-nitrobenzoic acid) in 50 mM Tris buffer containing 0.1 M NaCl and 0.02 M $MgCl_2$ (pH 8) and 50 µL of 50 mM Tris buffer containing 0.1% (w/v) bovine serum albumin (BSA). The absorbance at 412 nm was measured on 15 occasions over a 15 min period (spontaneous hydrolysis) using BioTek ELx800 microplate reader, USA. Then, 25 µL of 0.22 U/ml AChE in 50 mM Tris buffer containing 0.1% (w/v) BSA was added to initiate the reaction and the measurement was repeated. The absorbance readings were corrected by subtracting the spontaneous hydrolysis values. AChE inhibitory effect of the sample was estimated in terms of percentage change in average absorbance compared to the blank, which is referred to as percentage inhibition. Galantamine hydrobromide (0.67 µM) was used as the reference standard.

3.2.2 DPPH (2,2-diphenyl-1-picrylhydrazyl) Assay

Radical scavenging capacity was determined according to the technique reported by (Loizzo et al., 2009). An aliquot of 1.5 ml of 0.25 mM 2,2-diphenyl-1-picrylhydrazyl (DPPH) solution in methanol and 12 µl of essential oil at concentrations ranging from 0.0001 to 1 mg/ml were mixed. The mixture was shaken vigorously and allowed to reach a steady state at room temperature for 30 min. Decolourization of DPPH was determined by measuring the absorbance at λ=517 nm with a SpectroScan80D spectrophotometer. The DPPH radicals scavenging activity was calculated according to the following equation: Scavenging activity % = $[(A_0 - A_1) /A_0] X100$. Where A_0 is the absorbance of the control (blank, without extract) and A_1 is the absorbance in the presence of the extract. The results

were compared to that of butylated hydroxyanisole (BHA) employed as the standard control.

3.2.3 Ferrous Ion-Chelating Effect

The ferrous ion chelating activity of EOs was assessed by the ferrozine assay as described by (Yamaguchi et al., 2000). Briefly, 200 µl of different concentrations of EOs prepared in methanol were added to 740 µl methanol and 20 µl of $FeCl_2.4H_2O$ solution (2 mM) and left for incubation at room temperature for 5 min. The reaction was initiated by adding 40 µl of ferrozine (5 mM), into the mixture which was then; shaken vigorously and left to stand at room temperature for 10 min. Absorbance of the solution was then measured spectrophotometrically at 562 nm. The percentage inhibition of ferrozine Fe^{2+} complex formation was calculated using the formula: (%) = $[A_0 - A_1) /A_{0]} X 100$**.** Where A_0 is the absorbance of the ferrozine–Fe^{2+} complex and A_1 is the absorbance of the test compound. EDTA (0.1%) was used as a positive control.

3.2.4 Materials

Ethylenediaminetetraacetic acid (EDTA), AChE (Type-VI-S, EC 3.1.1.7), acetylthiocholine iodide, 5,5′-dithiobis-2-nitrobenzoic acid (DTNB), Tris-HCl, bovine serum albumin, galantamine, Ferrozine , iron (II) chloride tetrahydrate.

3.2.5 Statistical Analysis

All the experiments were performed in triplicate and statistical analysis of the data were performed using GraphPad Prism 5.0 program. A probability value of $p<0.05$ was considered statistically significant.

3.3 Results

3.3.1 Anti-cholinesterase Activity

Both EOs from dried and fresh leaves elicited as effective AChE inhibitory activity as the positive control galantamine, but with higher potency for the dried leaf oil compared to fresh leaf oil.

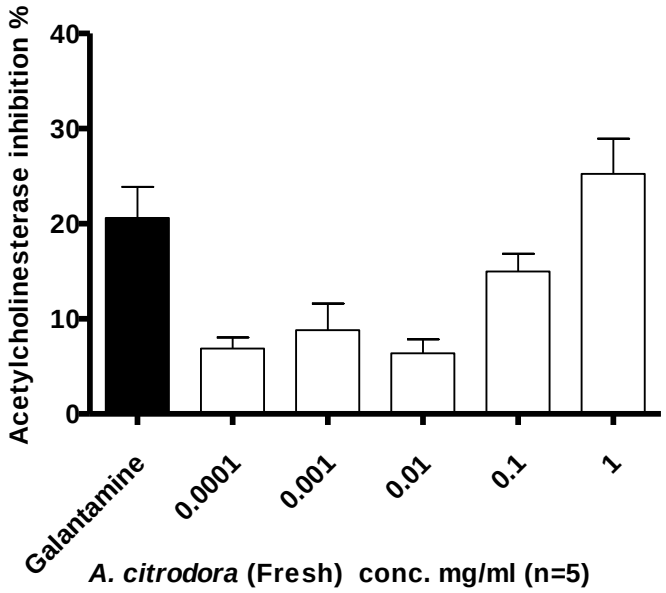

Fig 3.1

Percentage inhibition of AChE by fresh *A. citrodora* essential oil compared to standard, galantamine (1.93e-4 mg/ml). Values are means ± SD, from at least three separate experiments. All concentrations of oil displayed significant activity Vs baseline, $p < 0.001$.

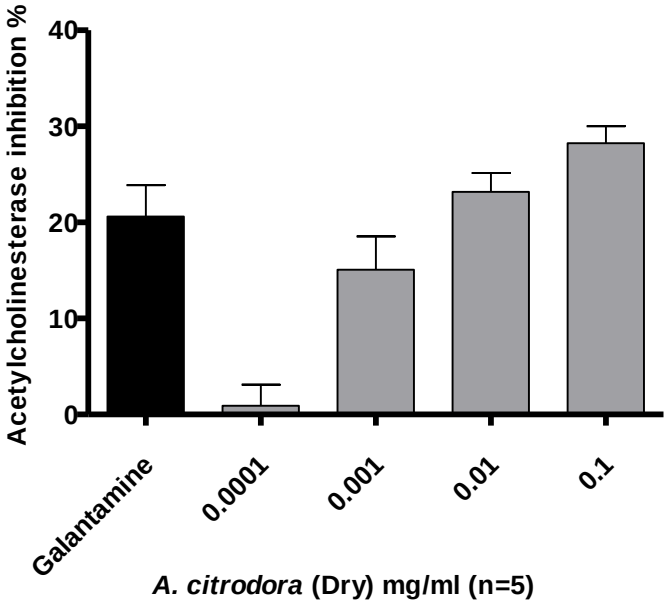

Fig 3.2

Percentage inhibition of AChE by *A. citrodora* dry essential oil compared to standard, galantamine (1.93e-4 mg/ml). Values are means ± SD, from at least three separate experiments. All concentrations of oil displayed significant activity Vs baseline, $p < 0.001$.

3.3.2 Anti-oxidant Properties

The 2,2-diphenylpicrylhydrazyl (DPPH) assay is widely used to evaluate the properties of plant constituents for scavenging free radicals. DPPH is a stable free radical and accepts an electron or hydrogen radical to become a stable diamagnetic molecule (Aazza et al., 2011). The method is based on the spectrophotometric measurement of the DPPH concentration change resulting from the reaction with an antioxidant. Essential oil of *A. citrodora* from dried & fresh leaves exhibited a comparable radical scavenging activity against DPPH radical in comparison to 0.1 % Butylated hydroxyanisole (BHA) as reference standard (Fig 3.3 and Fig 3.4).

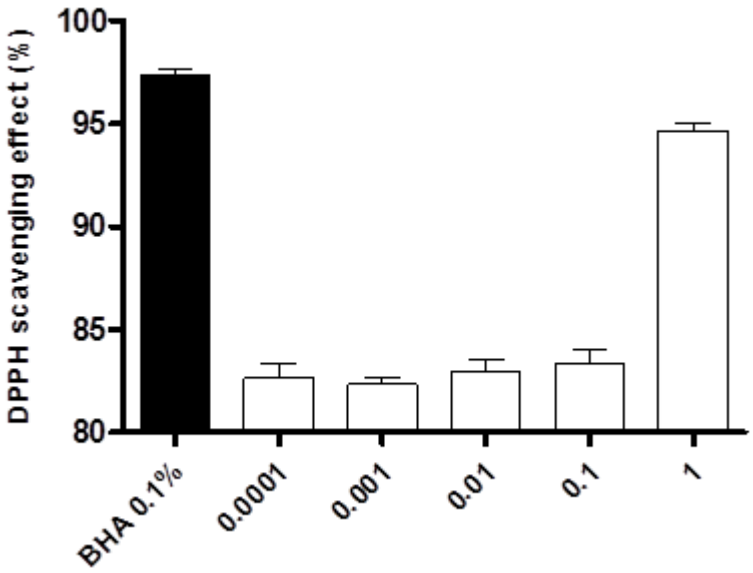

Fig 3.3

Antioxidant activity of *A. citrodora* fresh essential oil using DPPH Assay. Values are mean ± SEM, n=3, All concentrations of oil displayed significant activity Vs baseline, $p < 0.001$.

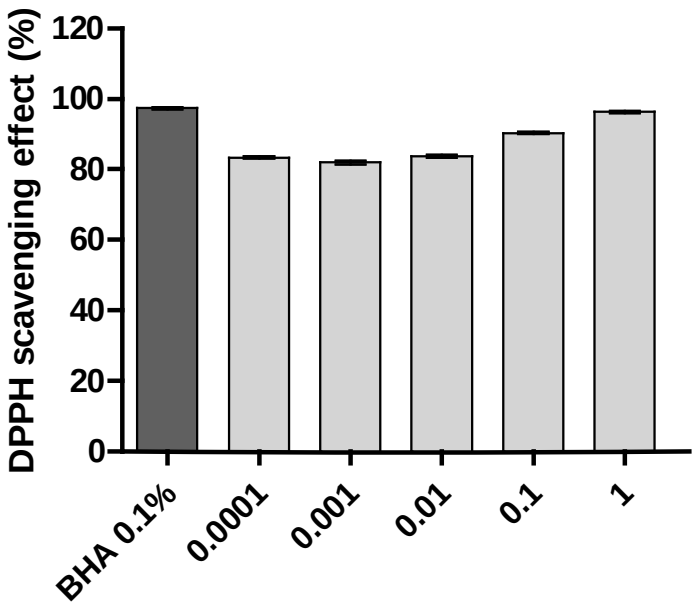

Fig 3.4

Antioxidant activity of *A. citrodora* dried essential oil using DPPH Assay. Values are mean ± SEM, n=3, All concentrations of oil displayed significant activity Vs baseline, $p < 0.001$.

3.3.3 Iron Chelation Properties

A robust antioxidant capacity was observed with the *A. citrodora* EO using the iron chelating test system. *A. citrodora* EOs derived from the fresh leaf displayed a significant dose-dependent iron-chelating property (between 0.001-1 mg/ml), while the dried leaf oil displayed a limited effect, only at 1 mg/ml and above, compared to 0.1 % EDTA as positive control.

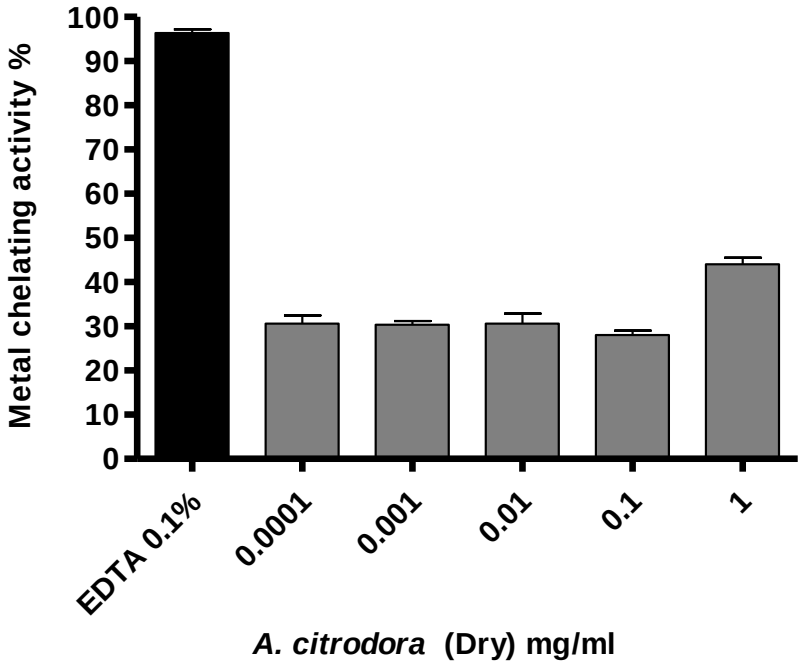

Fig 3.5

Antioxidant activity of *A. citrodora* (Dry) essential oils using Metal Iron chelating assay. Data are compared to standard, EDTA (0.1%). Values are means ± SD, from at least three separate experiments. All concentrations of oil displayed significant activity Vs baseline, $p < 0.001$.

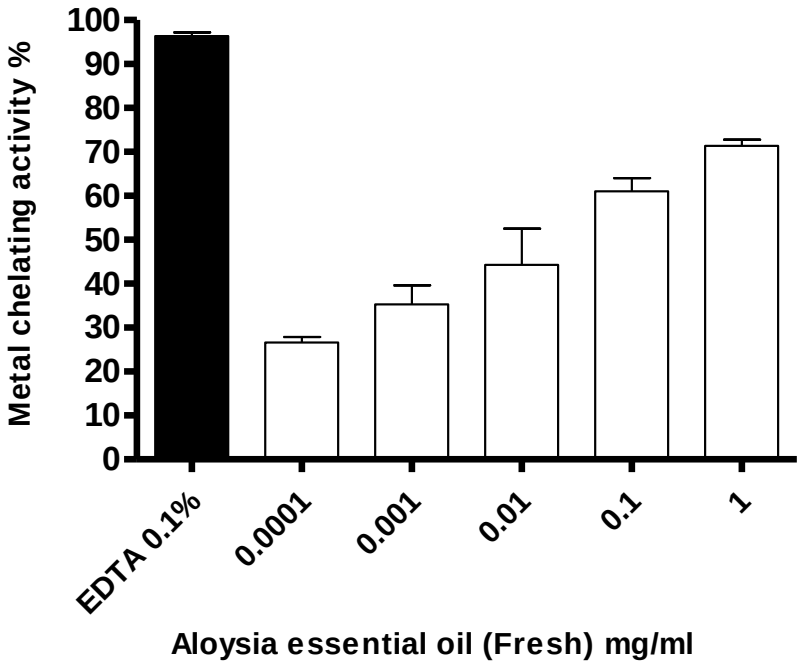

Fig 3.6

Antioxidant activity of *A. citrodora* (Fresh) essential oils using Metal Iron chelating assay. Data are compared to standard, EDTA (0.1%). Values are means ± SD, from at least three separate experiments. All concentrations of oil displayed significant activity Vs baseline, $p < 0.001$.

3.4 Discussion

The goal of this chapter was the biological evaluation of a traditionally used Jordanian medicinal plant, *A. citrodora* (which is accessible, abundant and has been subjected to limited neurological assessment) as a potential source of novel neuroactive compounds. Lemon verbena leaves were harvested in Amman area of Jordan and a portion was air-dried and a second portion used fresh, to obtain the EOs utilized in this present study.

The potential of the EOs of *A. citrodora* species in the treatment of early stages of AD was evaluated utilising the AChE inhibition assays. *A. citrodora* EOs derived from dried and fresh leaves displayed AChE inhibitory activity in our study compared with a standard galantamine, an activity that has not previously been reported for this plant species. The high content of monoterpenes may underpin this activity (Howes et al., 2003, Savelev et al., 2004) The anti-AChE activity of the oil could be attributed to Limonene, Caryophyllene oxide and/or 1,8-Cineole, which are major components found in the *A. citrodora* EO. Dried leaves oil showed a more clear AChE inhibitory activity than fresh oil, which could be related to higher respective levels of Limonene and Caryophyllene oxide (see Chapter 5). Recent studies have indicated that the constituents combined in a naturally occurring ratio are different than that of the whole natural oil. This has led to the suggestion that the bioactivity exhibited by the essential oil is probably due to synergetic activities of several components (Savelev et al., 2003, AH et al., 2008). For instance it is been reported that 1,8-cineole/α-pinene and 1,8-cineole/caryophyllene oxide combinations (both found in *A. citrodora*) have minor synergy (Savelev et al., 2003, AH et al., 2008).

In chapter 5, a docking model will be utilised in attempt to identify potential anti-cholinesterase components of the oils. Natural antioxidants that are present in medicinal plants are responsible for inhibiting or preventing the deleterious consequences of oxidative stress. These comprise free radical scavengers, including polyphenols, flavonoids and phenolic compounds. The *A. citrodora* oil exhibited a clear radical scavenging activity at all tested concentrations. This activity has been reported earlier in several studies for related plants (AH et al.,

2008, Ono et al., 2008, Quirantes-Piné et al., 2009) For example the aqueous extract of *Aloysia gratissima* (Verbenaceae) native to South America showed higher antioxidant activity than BHT, but lower than ferulic acid, (Maraschin, 2013), and the methanol extract of *Lippia schomburgkiana* (Verbenaceae) has been reported to display an EC_{50} value only three times lower than that of trolox in the DPPH test (da Silva et al., 2009)

Furthermore, *A. citrodora* infusion was evaluated by the DPPH test using Trolox as the reference compound and showed a high radical scavenging activity of superoxide, hydroxyl radical and hypochlorous acid (Valentão et al., 2002, Bilia et al., 2006, Bilia et al., 2008). Oxidative cellular damage is a multiphase process involving free-radical chain initiation and propagation steps. An important mechanism of anti-oxidative action is the chelation of transition metals, thus preventing catalysis of hydrogen peroxide decomposition via the Fenton-type reaction (Bush, 2003)**.** A line of treatment for neurodegenerative treatments currently under investigation is through selective low affinity binding of transition metals. (Allan Butterfield et al., 2002, Bush, 2003). Therefore, herein, the ability of *A. citriodora* essential oil to chelate iron (II) was investigated. As can be seen, the oil derived from fresh leaves was effectively capable of chelating iron (II) and did so in a concentration-dependent manner to approx. 70% of the level of EDTA. Oil derived from dry leaves was of capable of chelating iron (II) to a lesser extent, up to approx. 50% of that of EDTA. The anti-oxidant and iron-chelation properties displayed by *A. citrodora* in this chapter suggest that this may have potential for a neuroprotective capability which will be investigated in the next chapter, using *in vitro* cell culture models of oxidative stress- and β-amyloid-induced neurotoxicity.

Chapter 4

Pharmacological Profile of *Aloysia citrodora* Palau Essential Oil: Neuroprotective Properties

4.1 Introduction

Due to premature and slow death of specific neuronal populations, neurodegenerative diseases are accompanied by the loss of structural organization and functioning of the brain tissue. Despite the important differences in clinical manifestation and progressive cell loss of specific neuronal populations in a specific region, neurodegenerative diseases share some common features such as the appearance of aged brain, the extensive neurodegeneration, synaptic dysfunction, and the accumulation of intracellular or extracellular deposits of misfolded protein aggregates with a β-sheet conformation, such as β-amyloid (Aβ) in AD, α-synuclein in PD, mutated huntingtin in HD, resulting in respective behavioural deficits. (Farooqui, 2010).

In the previous chapter, *A. citrodora* EO was shown to display a range of anti-oxidant and metal-chelation properties which indicate that this natural product may have utilities in neuroprotection. A neuroprotectant is generally defined as an agent that prevents neuronal death by inhibiting one or more of the pathophysiological steps in the processes that follow injury to the nervous system, ischemia or application of neurotoxins. The definition includes interventions that slow or halt the progression of neuronal degeneration. The mechanisms involved in neurodegeneration are multifactorial, including a complex set of phenomena, including inflammation, glutamatergic neurotoxicity, increases in iron, nitric oxide and ROS, and depletion of endogenous antioxidants. Generally speaking, ROS can exert multiple damaging reactions to proteins, lipids, carbohydrates and nucleic

acids, disrupting cellular functions. The increased production of ROS is therefore a potential threat to cellular homeostasis and neuronal survival if production is not balanced by the capacity of endogenous antioxidant mechanisms (Jain, 2011).

Mouse catecholaminergic neuronal tumour, CAD cells (Cath.-a-differentiated) are a variant of a CNS catecholaminergic cell line established from a brain tumour in a transgenic mouse carrying wild-type SV40 T antigen under transcriptional control of rat tyrosine hydroxylase promoter. CAD has lost the immortalising oncogene and expresses neuron-specific proteins and synaptic vesicle proteins. CAD cells differentiate to form neuronal processes in serum free conditions (Qi et al., 1997). In this chapter, the preconditioning and neuroprotective properties of *A. citrodora* EO will be assessed using H_2O_2 and amyloid-induced toxicity in the CAD neuronal cell line grown in culture. Morphological differentiation can be induces in CAD by growing them in serum free media (fig 4.1 and 4.2).

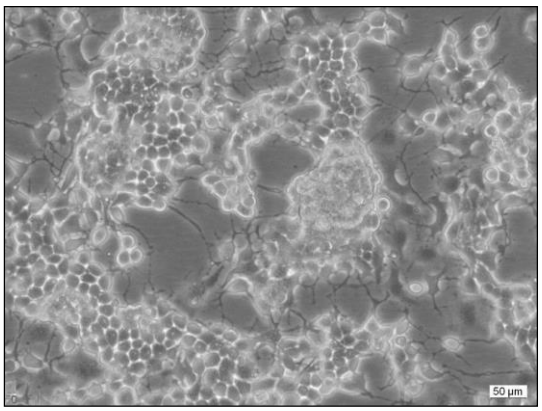

Fig 4.1 Undifferentiated CAD cell line in serum containing media
Phase contrast image

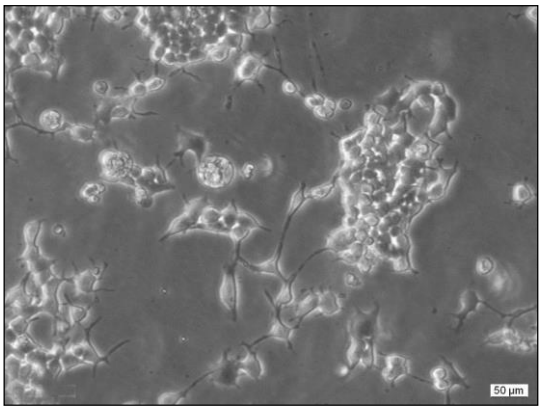

Fig 4.2 Differentiated CAD cell line in serum free showing long axons
Phase contrast image

4.2 Materials and Methods

4.2.1 CAD cell culture

(Cath.-a-differentiated) cultures and experiments were performed in CL1 facilities under sterile conditions. CAD cells were grown at 37°C and in 5% CO2 on 75 cm^2 tissue culture flasks (Sarstedt, Newton, NC) in Dulbecco's modified eagles' medium DMEM / F-12 Media - GlutaMAX™-I (GIBCO, Grand Island, NY), supplemented with 10% foetal bovine serum (FBS; Sigma, St. Louis, MO) Cells were passaged every 6–7 days at a 1:4 dilution. CAD differentiate to form neuronal processes in serum free conditions. To induce morphological differentiation, cells were switched to the same medium without serum supplementation after 12–24 h.

4.2.2 CAD cell line subculturing

Original medium from the T75 flask, were removed, rinsed once with 10 ml PBS, then 4 ml Accutase (Innovative Cell Techonologies, Cat#AT104) added to lift the cells. 4 ml complete medium were then added to neutralize. 8ml cell mixtures were added to a15 ml sterile centrifuge tube and centrifuged at 1000 rpm for 5 min. The superatant was removed and 5 ml complete medium added to resuspend the pellet. The cells were divided 1:3-4 into 75 cm^2 flasks, with 20 ml total medium in each flask.

4.2.3 Cryopreservation and storage of CAD Cell line

Sub-confluent cultures (70-80%) was dislodged by gentle pipetting; transferred to 15 ml falcon tube and centrifuged at 200xg for 5 minutes at 4 ºC. The pellet was resuspended in DMEM／F-12 Media - GlutaMAX™-I supplemented with 10% FBS and 10% DMSO. The cell suspension was immediately divided into and stored at –80 ºC for 24 hours and then transferred to liquid nitrogen.

4.2.4 Resuscitation of frozen CAD Cell Line

A cryogenic vial of cells from liquid nitrogen storage is collected wearing appropriate personal protective equipment. The vial was then quickly transferred to a 37°C water bath. It is important to thaw rapidly to minimise any damage to the cell membranes. The ampoule then was wiped out with a tissue soaked in 70%

alcohol prior to opening. The whole content of the ampoule is pipetted into 15 ml sterile falcon tube. Pre-warmed medium was added to reach a total volume of 10 ml, the tube then centrifuged at 1000 rpm for 5 min. supernatant was removed and the pellet was resuspended inDMEM/F-12 Media - GlutaMAX™-I supplemented with 10% FBS. The resuspended cells were grown at 37°C with 5% CO_2 in 75 cm^2 tissue culture flasks.

4.2.5 Treatment of cell cultures with H_2O_2

Hydrogen peroxide (H_2O_2)-induced insult with a series of increasing concentrations was performed to determine the dose-dependent effects on CAD cell survival. A stock solution of H_2O_2 (2500 µM) in PBS was freshly prepared. A series of concentrations were then prepared using Dulbecco's modified eagles' medium DMEM/F-12 Media - GlutaMAX™-I supplemented with 10% FBS to achieve final concentrations of 250 µM, 200 µM, 150 µM, 100 µM and 50 µM. Sub-confluent cultures (70-80%) was dislodged by gentle pipetting; transferred to a 15 ml falcon tube and centrifuged at 200xg for 5 minutes at 4 ºC. The pellet was resuspended in DMEM/F-12 Media GlutaMAX™-I supplemented with 10% FBS. The cell suspension was immediately plated in 24-well plates and incubated at 37°C and 5% CO_2. After 24 hours the media was replaced with the different H_20_2 concentrations prepared earlier and grown in culture for further 24 hours after which an MTT assay was performed (section 4.2.8).

The choice of essential oil concentrations was initially investigated by applying different concentrations of the oil (0.0001, 0.001, 0.01, 0.1mg/ml) for 24h to CAD cell cultures. Viability of neurons was assayed using a standard MTT assay (Freshney, Culture of Animal Cells 6th ed: 373, 2011). Survival of CAD cells was assessed by the MTT assay, after 24 hr pre-treatment with *A. citrodora* EO (0.001 and 0.01 mg/ml (w/v)) followed by 24 hr post-treatment with 250 µM H_2O_2 (i.e. *A. citrodora* containing media removed before addition of H_2O_2 - preconditioning method). A second set of experiments were performed when the *A. citrodora* containing media was not removed prior to exposure to the H_2O_2 - Neuroprotection method). N=12 well replicates from 3 independent cultures were carried out (* $p < 0.05$; ** $p < 0.01$; *** $p < 0.001$).

4.2.6 MTT cell proliferation assay

50 µl Phosphate Buffered Saline (PBS) (136.9 mM 2.68 mM KCl, 4.3 mM Na_2HP0_4, 1.4 mM KH_2P0_4, pH 7.4) containing 5 mg/ ml MTT was added to the cultures and incubated at 37°C and in 5% CO2 for 2.5 hours. Then MTT- containing medium was removed, the surface of the wells was rinsed with 300 µl PBS before the application of 250 µl isopropanol. After the purple crystals dissolved, the optical density of 100 µl sample was spectrophotometrically read at 595 nm (Thermo Labsystems Multiskan Ascent, V1.3).

4.2.7 Treatment of cell cultures with β-Amyloid

Human β-amyloid peptide, Ascent Scientific, UK, was dissolved in DMSO (dimethyl sulphoxide) at 1 mg/ml and stored at -80°C until use. Prior to use, the molar concentration of the peptide was calculated and diluted to 200 µM using sterile PBS. The peptide was then incubated for 72 hours at 37°C, 5% CO_2, without agitation. The peptide was then diluted to the required concentration using DMEM/F12 plus GlutaMAX® +10% FCS, inverted and gently added to neuronal cultures, with DMSO in DMEM/F12 plus GlutaMAX® +10% FCS as a control volume in control neuronal cultures.

4.2.8 CytoTox 96 non-radioactive assay (Promega, UK)

CytoTox 96 assay kit quantifies LDH (lactate dehydrogenase) levels as a measure of cell lysis (necrosis). Media was removed from cells and centrifuged at 13,000 rpm for two minutes. The supernatant containing the LDH was retained and the pellet resuspended in PBS, using the same volume removed from the cells, and placed back into the respective well of the 24 well plate. The 24 well plate was then frozen for two hours at -20°C to lyse all remaining cells. Cells were subsequently thawed and centrifuged at 13,000 rpm for two minutes; again the supernatant was retained as a measure of total remaining LDH. Dilutions; 1:10 and 1:20, were made of each supernatant using PBS as the diluent with DMEM/F12 plus 10% FCS used to calibrate the assay. 50 µl of substrate mix was added to 50 µl of each dilution prior to incubation for 30 minutes at room temperature in the dark. Neat, 1:10 and 1:20 dilutions were all completed in triplicate. Following this, 50 µl of stop solution was added to each well and the absorbance measured at 490 nm on a Multiskan

Ascent Plate Reader, Version 2.6. Cell lysis, via LDH release in the media supernatant, was calculated as a percentage of the sum of total LDH absorbance, combining the absorbance of positive control freeze-thawed cells and absorbance of media containing LDH.

4.2.9 Statistical analysis

All the experiments were performed in triplicate and statistical analysis of the data were performed using GraphPad Prism 5.0 program. A probability value Convention: (* $p < 0.05$; ** $p < 0.01$; *** $p < 0.001$).

4.3 Results

4.3.1 Treatment of CAD Cell Cultures with *Aloysia citrodora*

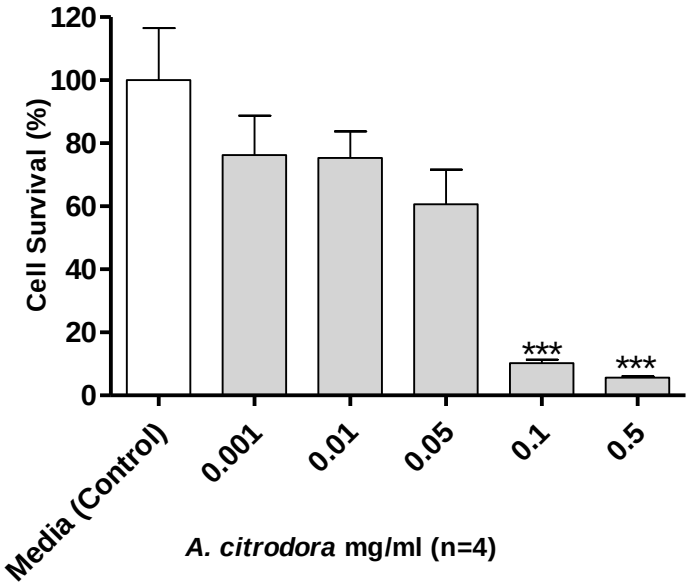

Fig 4.3

24 hours Treatment of CAD cell cultures with (Dry) *A. citrodora*. Concentrations 0.001, 0.01 and 0.05 mg/ml elicited no neurotoxic effect upon CAD cells. *** $p < 0.001$ compared to control.

4.3.2 Hydrogen peroxide insult: concentration-dependent effects of Hydrogen peroxide (24 hours)

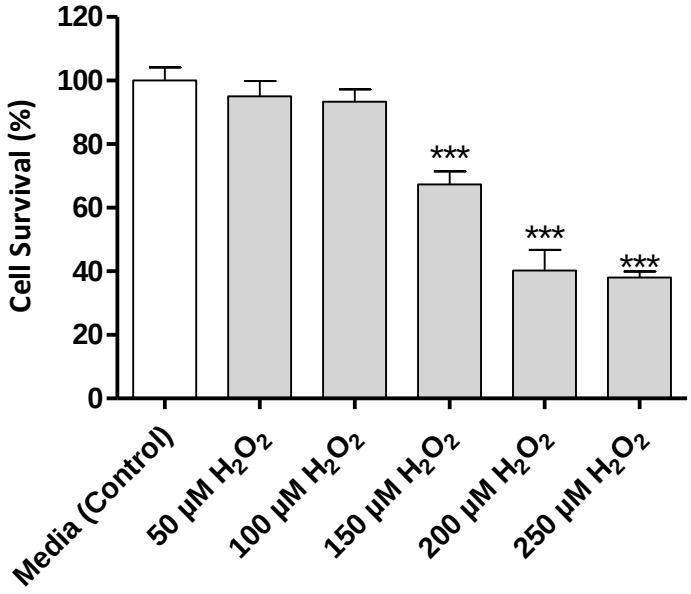

Fig 4.4

24 hours insult of CAD Cell Cultures with Hydrogen peroxide. 200 µM and 250 µM H_2O_2 elicited a significant neurotoxic effect up to 62% loss of cell viability. *** $p < 0.001$ compared to control.

4.3.3 Preconditioning of CAD cultures with *Aloysia citrodora* before 24 hours insult with 250 µM hydrogen peroxide

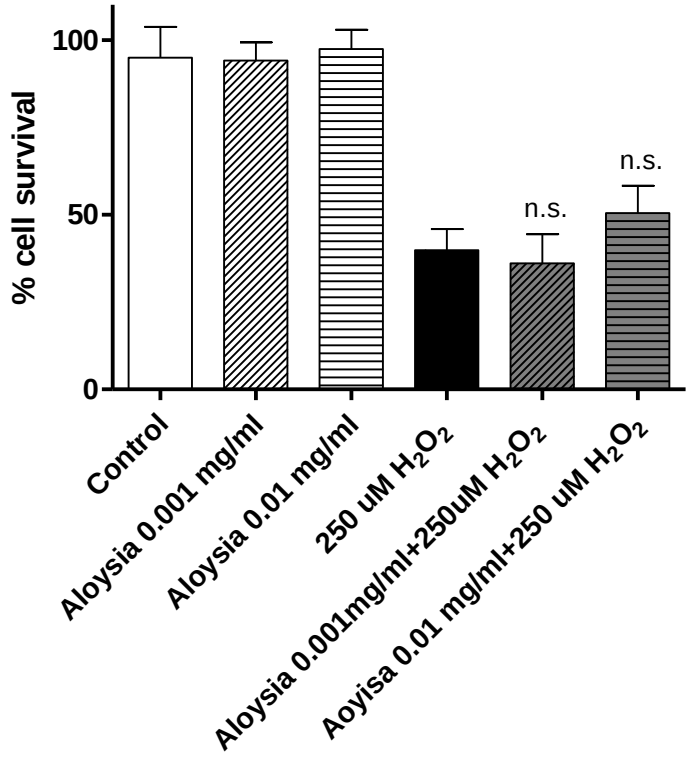

Fig 4.5

Preconditioning of CAD Cell Cultures with *A. citrodora* before 24 hours insult with 250 µM Hydrogen peroxide. No significant difference in comparison to 250 µM H_2O_2 treated cells.

4.3.4 Protection of CAD cells with *Aloysia citrodora* from 24 hours 250 µM hydrogen Peroxide insult

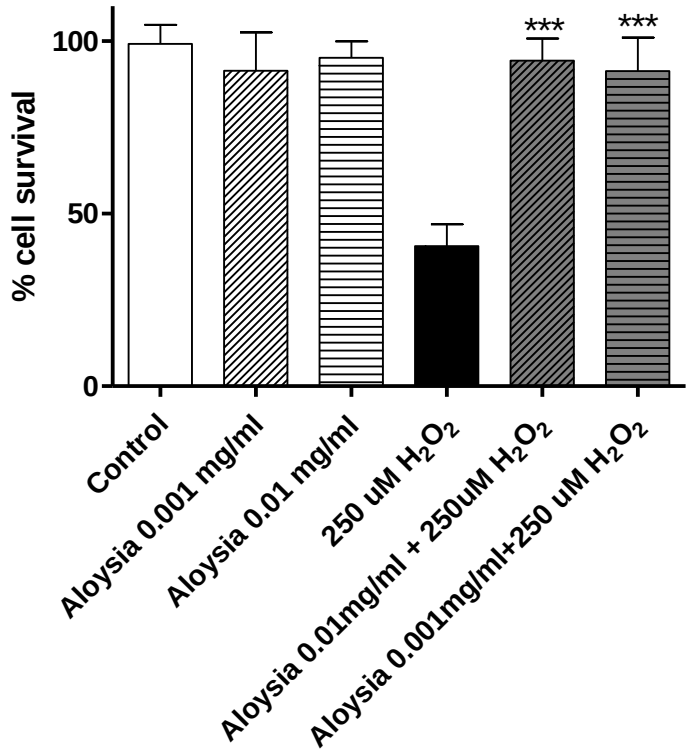

Fig 4.6

Protection of CAD neuronal cells with *A. citrodora* from 24 hours 250 µM Hydrogen peroxide insult. (*** $p < 0.001$ compared to 250 µM H_2O_2 treated cells).

4.3.5 CAD cell cultures insult with β-amyloid

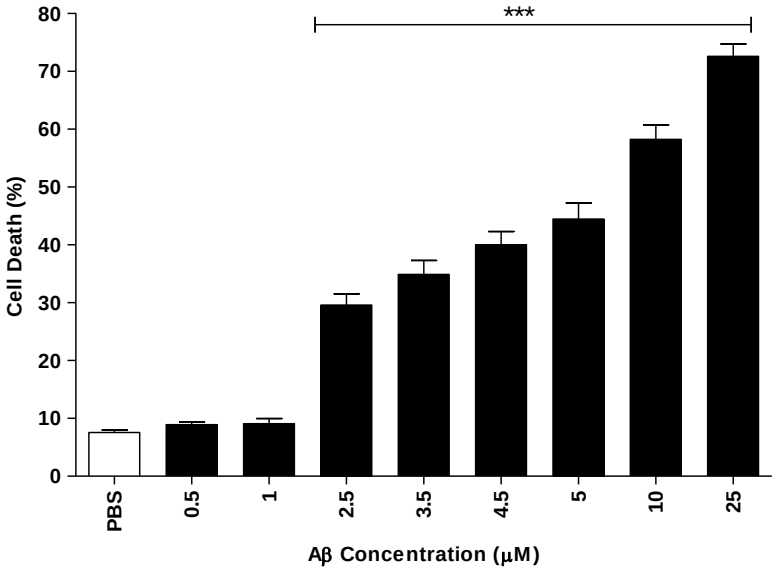

Fig 4.7

24 hours insult of CAD Cell Cultures with β-amyloid (*** $p < 0.001$ compared to PBS control)

4.3.6 Protection of CAD cells with *Aloysia citrodora* from 10 µMβ-amyloid insult

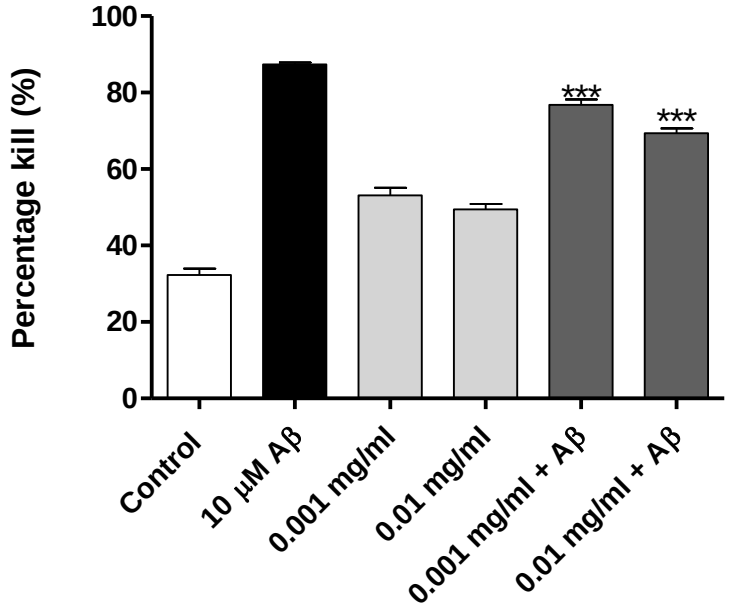

Fig 4.8

Protection of CAD cells with *A. citrodora* from 10 µM β-amyloid insult. N = 6 independent experiments. (*** $p < 0.001$ compared to 10 µM Aβ treated cells).

4.3.7 Protection of CAD cells with *Aloysia citrodora* from 15 µM β-amyloid insult

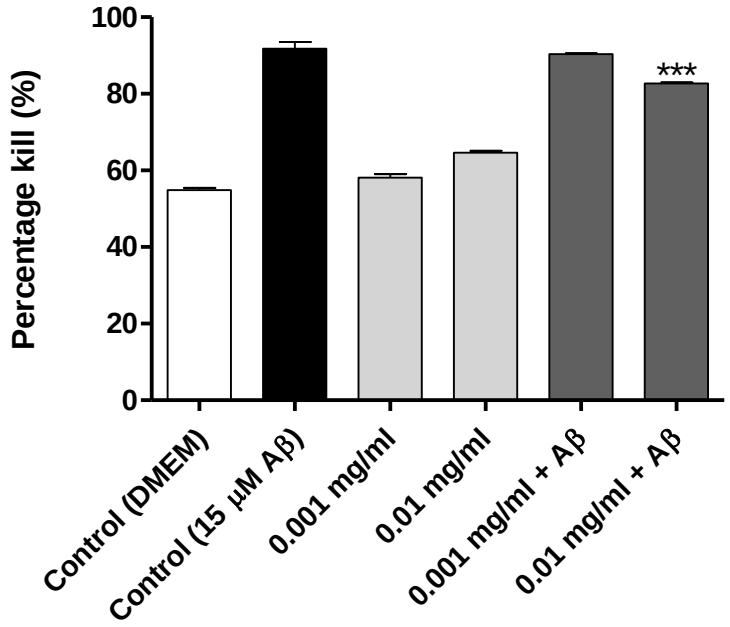

Fig 4.9

Protection of CAD cells with *A. citrodora* from 15 µM β-amyloid insult

N = 6 independent experiments. (*** $p < 0.001$)

4.4 Discussion

Oxidative stress resulting from increased formation of hydrogen peroxide and oxygen-derived free radicals, can damage biological molecules and initiate a cascade of events, including dysfunction of mitochondrial respiration, excitotoxicity, and a fatal rise in cytosolic calcium, and cause the cells to undergo necrosis or apoptosis (Van Houten et al., 2006). Among the various free radicals generated in the cell, hydroxyl radical and peroxynitrite are the most potent, and can damage cells via non-selective oxidation of proteins, lipids, fatty acids, and nucleic acid (Sayre et al., 2001, Barnham et al., 2004, Mariani et al., 2005). Proteins are initial targets of ROS, for instance, in AD, aberrant metal homeostasis may contribute to the formation of ROS and toxic Aβ oligomers, thus, facilitating the formation of amyloid plaques (Maynard et al., 2005). Also hydrogen peroxide accumulates during the incubation of β-amyloid or α-synuclein and hyperphosphorylated tau that show a close interrelationship (Geddes, 2005) and synergistic action (Wenning and Jellinger, 2005, Mamah et al., 2005).

In order to select an appropriate concentration of the essential oil to test for neuroprotection properties, 24 hr treatment of CAD cells with a range of concentrations (0.001, 0.01, 0.05, 0.1 and 0.5 mg/ml) was performed. Results are shown in Fig 4.3. Concentrations 0.001 and 0.01 mg/ml of *A. citrodora* did not elicit a neurotoxic effect, therefore were selected for neuroprotection tests. Interestingly, at concentrations 0.1 mg/ml and above, the oil elicited a neurotoxic effect itself, indicating the presence of a low affinity neurotoxin, possibly through $GABA_AR$ inhibition or glutamate receptor activation.

Hydrogen peroxide is a commonly used insult to elicit oxidative stress in cells. The effects of hydrogen peroxide upon CAD cells were investigated using a 24 hr incubation period. Results shown in Fig 4.4 show H_2O_2 significantly reduced cell survival in a dose-dependent manner relative to the control condition. The highest concentration of 250 µM H_20_2 was chosen to investigate the potential preconditioning and neuroprotective properties of A*. citrodora*. Utilising the preconditioning protocol (section 4.2.7), no protective effect was evident with either oil concentration tested versus 250 µM H_2O_2 (Fig 4.5). However, when cells were

pre-treated with oil and remained in the cultures when peroxide insults were applied, a clear neuroprotective effect was observed with both oil concentrations tested (Fig 4.6). This is consistent with the anti-oxidant and free radical chelating properties displayed by the oil as described in chapter 3.

This study provided new evidence that the *A. citrodora* EO essential oil (at the same concentrations shown to be neuroprotective against a H_2O_2 insult) displays significant neuroprotective properties versus β-amyloid-induced toxicity particularly at a concentration of 0.01 mg/ml. A further point to make is that the oil proves to afford higher protection against the lower concentration of 10 µM β-amyloid (Fig 4.9) than the higher concentration of 15 µM, which is unsurprising.

Therefore, in this present chapter, we demonstrated that the *A. citrodora* EO endows neuroprotective characteristics against the toxic effects of oxidative stress and β-amyloid in CAD neuronal cell culture. These results were consistent with the results reported in the previous chapters showing that *A. citrodora* EO has effective *in vitro* free-radical-scavenging effects and capability of chelating iron (II). *A. citrodora* share these properties with some of the best known neuroprotective plants such as Ginkgo biloba, Ginseng, and Curcuma. For instance Bastianetto et al., (2000) showed that Ginkgo biloba extract protects hippocampal primary cultured cells from H_2O_2 and β-amyloid induced toxicity. While Ginseng protected rat pheochromocytoma PC12 cells from H_2O_2 and β-amyloid induced toxicity in different experimental models of AD, (Chen et al., 2006). Also, Curcuminoids from Curcuma longa L. (Zingiberaceae) protected PC12 from β-amyloid and H_2O_2 insult (Kim et al., 2001).

This encouraging profile warrants further investigation by attempting to identify the *A. citrodora* EO constituents responsible for this activity, which will be discussed in Chapter 5.

Chapter 5

Pharmacological profile of *Aloysia citrodora* Palau essential Oil: Analysis and solid Phase Fractionation

5.1 Introduction

5.1.1 GC/MS analysis of *A. citrodora* EO

GC/MS has been widely used for the investigation of the chemical composition of essential oils. It has been effectively used for the identification of the main compounds in the isolated essential oils and for the distinction between different species of various spice plants (Daferera et al., 2000).

The chemical composition of *A. citrodora* phenolic compounds (flavonoids and phenolic acids) of the leaves of *A. citrodora* have been reviewed (Tomás-Barberán et al., 1987, Skaltsa and Shammas, 1988, Carnat et al., 1995, Nakamura et al., 1997, Carnat et al., 1999, Valentão et al., 1999, Argyropoulou et al., 2007). The chemical composition of *A. citrodora* extract has also been studied and reviewed (Montes et al., 1973, Kaiser and Lamparsky, 1976, Velasco-Negueruela et al., 1993, Bellakhdar et al., 1994, Zygadlo et al., 1994, Özek et al., 1996, Terblanché and Kornelius, 1996, Carnat et al., 1999, Pascual et al., 2001, Crabas et al., 2003, Kim and Lee, 2004, Sartoratto et al., 2004, Santos-Gomes et al., 2005, Argyropoulou et al., 2007). Genus Lippia shows rich genetic diversity, enabling it to synthesize a variety of essential oil constituents if grown in different parts of the world. However, the composition of the essential oil obtained from the same plant stock remains constant under the same environmental conditions (Catalan and de Lampasona, 2002, Santos-Gomes et al., 2005).

5.1.2 Solid phase extraction of *A. citrodora* EO

5.1.2.1 A brief history

Solid phase extraction (SPE) is a popular sample preparation method used for isolation, enrichment and/or clean-up of components of interest. SPE normally involves bringing an aqueous sample into contact with a solid phase or sorbent where the compound is selectively adsorbed on to the surface of the solid phase prior to elution (Dean, 2010). According to (Walton, 1970) the first literature reference for the use of Solid-phase extraction is to be found in the Bible even if the users were unaware of the science behind it. However the first modern use of SPE probably employed animal charcoal to remove pigments from chemical reaction mixtures. In such cases the charcoal was filtered out of the mixture and discarded along with the compounds it had absorbed, Our goal, however, is not to discard compounds of interest but to collect them preferably by concentrating them from a sample and removing those compounds we do not wish to analyse. In this sense SPE did not really become a scientific technique until the 1970s. Recently many developments in SPE technology have taken place including new formats (e.g. discs, pipette tips and 96-well plates), new sorbents (e.g. silica or polymer-based media and mixed-mode (Dean, 2010), and the development of automated and on-line systems (Mondello et al., 2002). Growth of SPE applications is directly attributable to the automation, high-throughput capability and the ease of use of SPE products.

5.1.2.2 Definition

Solid phase extraction is a physical extraction process that involves a liquid and a solid phase. The solid phase has a greater attraction for the isolate than the solvent in which the isolate is dissolved. As the sample solution passes through the sorbent bed, the isolate concentrates on this surface, while the other sample components pass through the bed (Camel, 2003). The selection of an appropriate SPE extraction sorbent depends on understanding the mechanism(s) of interaction between the sorbent and analyte of interest. That understanding in turn depends on knowledge of the hydrophobic, polar and ionogenic properties of both the solute and the sorbent. The most common retention mechanisms in SPE are based on

van der Waals forces, hydrogen bonding, dipole-dipole forces and cation-anion interactions (Żwir-Ferenc and Biziuk, 2006). Very selective extractions resulting in highly purified and concentrated isolates can be achieved by choosing sorbents with an attraction for the isolate but not for the other sample components. Generally SPE sorbents can be divided into three classes, i.e. normal phase, reversed phase and ion exchange. The most common sorbents are based on silica particles (irregular shaped particles with a particle diameter between 30 and 60 µm) to which functional groups are bonded to surface silanol groups to alter their retentive properties. A variety of different bonded silica are commercially available, offering a wide range of selective properties for extraction. In addition to silica some other common sorbents are based on florisil, alumina and macroreticular polymers.

Normal phase sorbents have polar functional groups e.g. unmodified silica cyano, amino and diol. The polar nature of these sorbents means that it is more likely that polar compounds, e.g. phenol, will be retained. In contrast, reversed phase sorbents have non-polar functional groups, e.g. octadecyl, octyl and methyl, and conversely are more likely to retain non-polar compounds, e.g. polycyclic aromatic hydrocarbons. Ion exchange sorbents have either cationic or anionic functional groups and when in the ionized form attract compounds of the opposite charge.

5.1.2.3 Basic Steps

Each of the steps shown can be controlled: the sorbent type can be selected; the sample can be manipulated to enhance retention of one chemical species over another; an elution liquid that has properties that are not just desirable to the compound of interest, but which may be convenient for your method of analysis or for subsequent sample handling can be selected; any number of wash steps can be used.

Pretreatment

Some samples require initial pretreatment to obtain the optimal extraction. This pretreatment can include homogenization of solid samples, adjustment of the

matrix to the proper ionic strength and pH, and removal of particulates via filtration or centrifugation. This step may also include addition of an internal standard.

Column Conditioning

Sorbent activation and functional group activation are achieved by passing a volume of an appropriate solvent or a mixture of solvent, through the column. Methanol or acetonitrile are commonly used for activating hydrophobic sorbents, while hexane or dichloromethane activate hydrophilic sorbents.

Sample Loading

To get a maximum purification efficiency, the sample flow needs to be controlled via vacuum or pressure. To achieve faster flow of viscous sample through a column, larger particle size can be used. The exchange capacity and selectivity are unaffected.

Retention

When the compound of interest distributes between the liquid sample and the solid surface, either by simple adsorption to the surface or through penetration of the outer layer of molecules on that surface, an equilibrium is set up. We can define that distribution by a coefficient, K, which indicates what fraction of the analyte has remained in solution and what fraction has adsorbed on or entered the solid phase. This distribution coefficient should be defined in terms of activities of the analyte in either phase. However, for convenience concentrations are used and therefore If this process occurs in a column packed with a sorbent into whose outer layer the compound distributes, then we are dealing with a system that is no longer a "batch" partition such as liquid-liquid extraction LLE. Instead the process more closely parallels distillation as the compound is entirely trapped on this solid surface and therefore, the distribution coefficient will be very large (Żwir-Ferenc and Biziuk, 2006).

Elution

When a liquid provides a more desirable environment for the analyte than the solid phase does, then the compound of interest is desorbed and can be collected in the

liquid as it exits the SPE device. This is called “elution”. It is characterized by a distribution coefficient, K value that is very small. One way to view the solid phase is as an intermediary between the sample and the elution solvent and this highlights a very important difference between LLE and SPE. An elution solvent may be used which is miscible with the sample in a solid-phase extraction, because the elution solvent and the sample never come into direct contact. Thus, our sample may be aqueous but our SPE elution solvent may be methanol, which is miscible in all proportions with water. Such a scheme is not possible in a LLE (Żwir-Ferenc and Biziuk, 2006).

The choice of solvent directly influences the retention of the compound on the sorbent and its subsequent elution, whereas the solvent polarity determines the solvent strength (or ability to elute the compound from the sorbent in a smaller volume than a weaker solvent). The solvent strengths for normal phase and reversed phase sorbents are shown in Table (5.1). Obviously this is the ideal. In some situations it may be that no individual solvent will perform its function adequately and so it is necessary to resort to mixed solvent systems. It should also be noted that for a normal phase solvent, both solvent polarity and solvent strength are coincident whereas this is not the case for a reversed phase sorbent. In practice, however, the solvents normally used for reversed phase sorbents are restricted to water, methanol, isopropyl alcohol and acetonitrile. For ion exchange sorbents, solvent strength is not the main effect (Dean, 2010).

Table 5.1

Solvent strengths for normal and reversed phase sorbents (Dean, 1998).

Solvent strength normal phase		**Solvent strength Reversed phase**
Weakest	Hexane	**Strongest**
	Iso-octane	
	Toluene	
	Chloroform	
	Dichloromethane	
	Tetrahydrofuran	
	Ethyl ether	
	Ethyl acetate	
	Acetone	
	Acetonitrile	
	Isopropyl alcohol	
	Methanol	
Strongest	Water	**Weakest**

Rinsing or Washing

During the retention step, many compounds in our complex sample may have been retained on the solid surface at the same time as our compound of interest. Likewise, at elution it is likely that some of these co-retained compounds will be eluted with our compound of interest. To minimize the interferences these undesirable compounds will create during the analysis stage, we may add one or more wash steps between retention and elution, to attempt to remove or rinse them out. Each wash step involves another distribution between the analyte and the co-retained species, the solid surface and the liquid that is passing over it. Each step can be controlled by careful selection of the sample loading, wash, and elution conditions.

5.1.2.4 Solid phase extraction objectives

Concentration

In order to be able to measure the quantity of a compound accurately it must be concentrated as much as possible. This will ensure the largest response from our detection system and will minimize errors in precision caused by background noise.

Clean-Up

Components of the sample that mask the analyte during the analysis (for example, when two or more compounds co-elute in a chromatographic experiment such as gas or liquid chromatography), sample preparation permits removal of such interferences before the analytical separation The cleaned-up extract gives clearly identifiable signals from the extracted components in the sample. Such a chromatogram is readily interpreted and the quantities of desired analytes present in that sample are easily measured.

Sample matrix removal/solvent exchange

Many analytical instruments (e.g. gas or liquid chromatographs, nuclear magnetic resonance or infrared spectrometers) require that the sample to be analyzed is in a specific environment. In such cases, you will need to remove the *sample ma*trix, and convert your sample into a form compatible with the instrument to be used. A significant advantage of SPE over LLE is that solvents that are miscible with the sample matrix, may be used to elute the analytes. The corresponding LLE commonly leaves the analytes in a water-immiscible solvent that must be dried down and the residue reconstituted in a suitable solvent before analysis may begin.

5.1.2.5 SPE and essential oils

Essential oils are characterized by a very complex mixture (Lawrence, 1997) whose components belong to different classes of compounds, including hydrocarbons, aldehydes, ketones, esters, alcohols, that range widely in concentration and variability among different plant species. They contain a variety of volatile molecules such as terpenes and terpenoids, phenol-derived aromatic components and aliphatic components (Bakkali et al., 2008). Several techniques can be used to extract essential oils from different parts of the aromatic plant, including water or steam distillation, solvent extraction, expression under pressure, supercritical fluid and subcritical water extractions (Edris, 2007).

5.1.2.6 SPE of *A. citrodora* EO

Many methods of essential oil fractionation have been reported in literature. Some of them are time and solvent consuming since they use large volumes of solvents (David 1987). Others are very attractive, but need a highly technological approach such as multidimensional gas chromatography (Mazza 1986).

This project approach is to fractionate the essential oil prior to analysis. The fractionation process will increase the concentration of the components and consequently ease the analysis. This Chapter reports a simple, inexpensive method that uses silica SPE to carry out a fractionation. Two different essential oils will be analysed, validated and fractionated.

5.1.3 Structure based Virtual Screening of *A. citrodora* EO constituents for anticholinesterase inhibitors

5.1.3.1 Introduction

The need for a rapid search for small molecules that may bind to targets of biological interest is of crucial importance in the drug discovery process. One way of achieving this is the in silico or virtual screening of large compound databases to identify a set of compounds that contain relatively many hits against the target, if a three-dimensional (3D) model of the target is available, then structure-based virtual screening can be done, utilizing a docking program. The docking program places a 3D structure in all available positions, conformations and orientations of each molecule from the screened data set into the target structure (the active site of an enzyme for instance). Each such docking mode is called a 'pose'. In order to identify the most energetically favourable pose, a good score for a molecule indicates potentially a good binding between the molecule and the target. All molecules in the data set are ranked according by their scores; top ranking molecules then can undergo further testing as they are predicted to be most active (Schneider et al., 2000). High-throughput virtual screening has become increasingly important in the context of drug discovery (Schneider and Böhm,

2002). Despite its many challenges the use of virtual screening has produced higher hit rates compared to random screening (Trosset et al., 2006).

5.1.3.2 Receptor modelling

To perform a structure-based virtual screening it is necessary to have the structure of the receptor of interest. Usually this structure is determined by experimental techniques such as X-ray crystallography. If the binding site and the function of the receptor is known or if the protein has been co-crystallized with a ligand, an analysis of the binding-site characteristics and interactions with the ligand can lead to important insights for the design or the docking of ligand molecules (Sotriffer and Klebe, 2002, Bitetti-Putzer et al., 2001).

5.1.3.3 Searching and pose prediction

Searching for the binding mode with highest score of any molecule is done by trying a number poses then keeping only energetically preferred poses. That means finding the correct orientation of the molecule in the active site, in addition, if the molecule is flexible the degrees of freedom include translational and rotational degrees of freedom of the ligand as a whole need to be searched.

5.1.3.4 Scoring

Many of the scoring functions fall into one of two main groups. One main group comprises knowledge-based scoring functions that are derived using statistics for the observed interatomic contact frequencies and/or distances in a large database of crystal structures of protein–ligand complexes (Gohlke et al., 2000).

The other group is scoring energy component methods based on physical interaction terms (Gohlke and Klebe, 2001). These methods are based on the assumption that the change in free energy upon binding of a ligand to its target can be decomposed into a sum of individual contributions. Although this is an approximations, these methods are very appealing as these simplifications result in functions that can be evaluated very rapidly, using regression-based methods, which assume often linear statistical relationship between the total free-energy change upon binding and a number of terms that characterize the binding event

such as hydrogen bonds and ion pairs, the amount of buried and contact surface, and molecular flexibility of the ligands. A training set of crystal structures of ligand-protein complexes and associated binding affinity data is used to optimize the coefficients of the regression equation. Many popular scoring functions have been derived this way including the one we are using in this study: GOLD score. GOLD is based on a genetic algorithm that mimics the process of evolution by applying genetic operators to a collection of poses for a given ligand called a population of chromosomes (GA). GOLD chromosomes contain conformational information of the flexible parts of the protein (OH of Ser, Thr and Tyr as well as lysine NH_3+) and of the ligand, as well as hydrogen bonds and lipophilic interactions. Chromosome decoding yields the corresponding 3D pose for the ligand, which is followed by a least-square (LS) fitting procedure (Bartolini et al., 2003), with the objective to maximize the overlap between ligand and receptor features. The energy of the resulting pose (fitness) consists of three terms: (1) hydrogen-bonding energy, (2) internal energy of the ligand, and (3) steric interaction energy. The population of chromosomes evolves through sequential application of genetic operations. Newly generated chromosomes are decoded, the fitness of the corresponding pose evaluated, and the chromosome is kept if it is fitter than the least-fit chromosome in the pool. After the application of a predefined number of genetic operations, the algorithm terminates, and the poses with the highest scores are saved (Jones et al., 1997).

5.1.3.5 Acetylcholinesterase (AChE)

AChE, one of the most essential enzymes in the family of serine hydrolases, catalyzes the hydrolysis of neurotransmitter acetylcholine, which plays a key role in memory and cognition. The physiological role of the AChE in neural transmission has been well known, however the role of AChE in neurodegenerative disease has been renewed owing to the evidences that support the role of this enzyme in accelerating the aggregation and deposition of the β-amyloid peptide (see chapter 2).

The binding pocket of AChE is a long and narrow region which consists of 2 separated ligand binding sites: the catalytic (central) site and the peripheral anionic

site (Raves et al., 1997, Kryger et al., 1999, Harel et al., 1996). The catalytic site is the binding site of classical AChE inhibitors, such as tacrine and huperzine A, which has been studied thoroughly. On the contrary, the function of the peripheral site has not been elucidated clearly as yet. Recent studies have demonstrated that the peripheral site might accelerate the aggregation and deposition of beta-amyloid peptide, which is considered as another cause of AD (McLaurin et al., 2000, Bartolini et al., 2003). Therefore, it is supposed that an ideal AChE inhibitor should bind to the catalytic and peripheral sites simultaneously, which could disrupt the interactions between the enzyme and the beta amyloid peptide, and hence slow down the progression of the disease (Munoz-Muriedas et al., 2004, Du and Carlier, 2004).

In order to further elucidate the mechanism of *A. citrodora* component on the enzyme and provide hints for a new derivative design, molecular docking and three-dimensional quantitative structure molecular docking studies were carried out, this virtual screening approach, was used to identify novel AChE inhibitors with high selectivity. The potential hit compounds obtained from this study can be further evaluated by *in vitro* and *in vivo* tests.

5.2 Materials and Methods

5.2.1 Plant Material

Fresh leaves of *A. citrodora* were collected from University of Jordan Faculty of Agriculture Botanic garden, spring 2011, when growth rate was maximal. The plant was authenticated by Professor Suleiman Al-Olimat from the Faculty of Pharmacy, University of Jordan, where the voucher specimen (herbarium number AC-V1) is kept. Leaves were dried carefully in the shade at room temperature and then homogenized to fine powder and stored in air within tight bottles.

5.2.2 Essential Oils Preparation

500g of dried leaves of *A. citrodora* were hydro-distilled with one Litre of water using a Clevenger-type apparatus (JSOW, India) for 3 hours. Essential oils obtained were dried with anhydrous sodium sulphate and stored at 4°C in amber glass vials until analysis. For all experiments, dilutions of pure Essential oils stock was performed fresh on the day of the assay.

5.2.3 Solid Phase Fractionation System

Agilent 971-FP Flash Purification System (Agilent, www.varianinc.com) was used for SPE of the essential oils. 100 µL of the essential oils was loaded onto a 4 g silica cartridge (SF10-4g) that is conditioned with pentane. The elution of the SPE cartridge was performed using a vacuum manifold at a velocity of 3 ml/sec using the following solvent sequence: Fraction I: pentane100%. Fraction II: pentane/ethyl ether 90:10. - Fraction III: ethyl ether 100%.

Fig 5.1

Agilent 971-FP Flash Purification System.

Fig 5.2

Agilent silica cartridge (SF10-4g)

Solid Phase Extraction System 971-FP Flash Purification System (Agilent - Dr Mike Carroll, University of Newcastle) was used for SPE of the *A. citrodora* EO. 971-FP is a high throughput, high recovery system for sample purification. It allows the setting up of multiple solvent systems for continuous availability without interrupting fractionation procedure and equipped with Low Pulse Pump which provides an even solvent flow. 100 µL of the essential oils was loaded on to a 4 g silica cartridge. The number of active sites available on the sorbent cannot be exceeded by the number of molecules of compound or otherwise breakthrough will occur. Therefore, 4 g silica cartridge (SF10-4g) was chosen for 100 µL of essential oil the silica cartridge had previously been conditioned with pentane. Wetting and conditioning the sorbent allows alkyl chains, on the surface of the silica, to be solvated to ensure good contact between the sample and the sorbent preventing poor recoveries. Silica sorbent is stable within a pH range of approximately 2 to 7.5 and is chemically stable to virtually all organic solvents. The elution of the SPE cartridge was performed using a vacuum manifold at a velocity of 3 ml/sec. The flow rate of the sample through the sorbent is important; excessively rapid flow will allow minimal time for the compound–sorbent interaction. This must be carefully balanced against the need to pass the entire sample through the cartridge.
The following solvent sequence was adopted: Fraction I: pentane - 100%. Fraction II: pentane/ethyl ether - 90:10. Fraction III: ethyl ether - 100%.

5.2.4 Gas Chromatography-Mass Spectrometry (GC-MS) Analysis

The GC–MS analyses were performed using Agilent 7890Agas chromatogram coupled to Agilent 5975C mass spectrometer (Agilent – Dr Melanie-Jayne Howes. Royal Botanic Gardens). Chromatography was performed on Column: DB-5MS, 30 m x 0.25 mm I.D., 0.25 µm (J. & W. Scientific, USA) using a temperature program of 40–300°C at a rate of 3°C min-1. The carrier gas was helium at a flow rate of 1 ml min-1 and the injection volume was 1 µL (split 1:10) at 220°C, via an autosampler. Detection was carried out by MS, fitted with electrospray ionization (EI) source operated at 70 eV, with a source temperature of 180°C; mass spectra were recorded in the 38–600m/z range. The *A. citrodora* oils were diluted to 1.0% (v/v) with diethyl ether (GLC pesticide residue grade, Fisher Scientific, UK) prior to analysis. Retention indices (RIs) were determined in relation to a series of *n*-

alkanes (C10–C16, Supelco, UK) and compounds were identified by comparing the RIs and mass spectra with published data. Percentage compositions of detected compounds were calculated by integrating all peaks in total ion chromatograms.

5.2.5 Virtual screening for Anticholinesterase Inhibitors

The crystal structure of human AChE (PDB:4EY7) was used in the study (Fig 5.3). A centre was established around the determined binding site. 15Å radius was chosen to form the search space. Default settings for small molecule-protein docking were used throughout the simulations. The structure of human AChE (PDB:4EY7) in complex with donepezil is depicted as a ribbon diagram in (Fig 5.4).

Molecular docking GOLD version 3.0.1 (Cambridge Crystallographic Data Centre, Cambridge, UK) was employed to investigate the binding mode. The default parameters of genetic algorithms (GA) were applied to search a reasonable binding conformation of the flexible ligands. The maximum number of GA runs was set to 10 for each compound. (ChemPLP) scoring function was used to evaluate the docking conformations. (ChemPLP) is the default scoring function in GOLD and on the whole was the best performing scoring function at both pose prediction and virtual screening. Docked conformations were saved in MOL2 format and then imported into Hermes for further analysis. The donepezil pose derived from GOLD was used as the reference compound for alignment. In order to consider the influence of crystallized water molecules on docking, donepezil was docked into the binding pocket with and without water molecules, separately docking conformations of donepezil superimposed with the X-ray crystal structure very well, which indicated that the co crystallized water had little impact on docking.

Eighty eight (88) AChE inhibitors in this study (including donepezil, galantamine, huperzine, rivastigmine and tacrine) were taken from (Lu et al., 2011), all of which were reported by the same laboratory which employed similar experimental conditions and procedures to obtain bioactivity data for the compounds. The *in vitro* bioactivities of the collected inhibitors were expressed as the concentration of the test compounds that inhibited the activity of AChE by 50% (IC_{50}) and listed in

Appendix I. The 3D chemical structures of these acetylcholinesterase inhibitors were sketched using ChemBioDraw Ultra (Ver12.0.2.1076 Cambridge Soft Corp., Cambridge, MA) then saved in .mol file formats. These were considered the training set. All chemical constituents of *A. citrodora* EO (Appendix II) were sketched using ChemBioDraw Ultra (Ver12.0.2.1076 Cambridge Soft Corp., Cambridge, MA) and saved in .mol file format as well. Each compound was tested for 10 genetic algorithm runs, producing 10 different poses for each compound, with the top 5 conformations saved for analysis. The optimal docking protocol and scoring function (CHEMPLP) was chosen and the output options created sub directories for each ligand conformation docked in order of best fit.

Fig 5.3

Structure of human AChE depicted as a ribbon diagram. The two independent molecules in the asymmetric unit of the crystal are green and blue (PDB:4EY7).

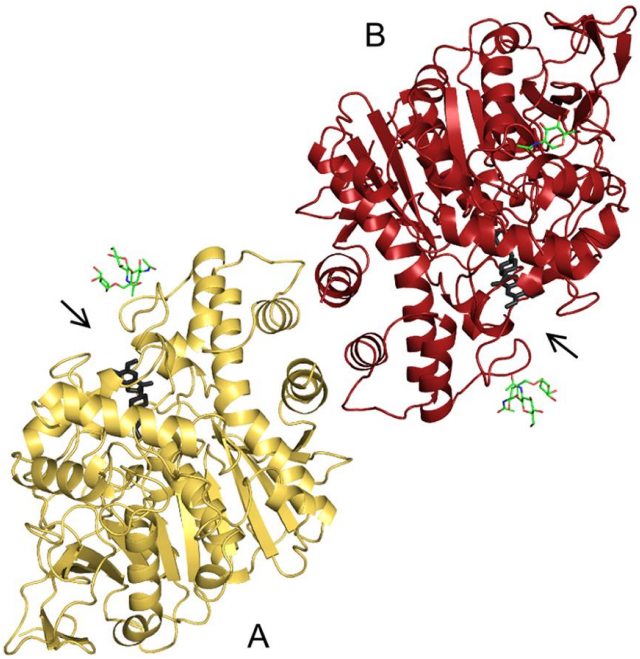

Fig 5.4

The structure of AChE in complex with donepezil (PDB:4EY7) is depicted as a ribbon diagram. The two independent molecules A and B in the asymmetric unit of the crystal are coloured yellow and red respectively. Bound donepezil is shown in stick representation and coloured black. Protein Glycosylation is shown as sticks. Arrows depict the entrance of the active site gorge in the physiological dimer (Cheung et al., 2012).

5.3 Results

5.3.1 GC/MS Analysis of *A. citrodora* EO

The chemical compositions of the EOs from *A. citrodora* collected from Jordan are summarized in (Table 5.2) Eighty three compounds were identified. The chemical composition of the essential oil in the order of retention time is listed in Appendix II.

Table 5.2 (GC/MS) analysis of *A. citrodora* fresh and dry essential oil: Percentage composition of top main constituents.

Compound	Chemical structure	Fresh	Dry
Limonene	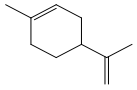	13.6%	20.1%
Caryophyllene oxide	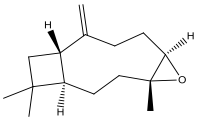	2.2%	8.4%
Curcumene	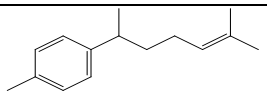	3.5%	6.3%
Spathulenol	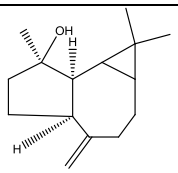	3.1%	5.0%
1,8-Cineole	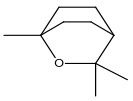	9.2%	9.4%
Geranial	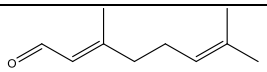	20.1%	6.3%
Neral	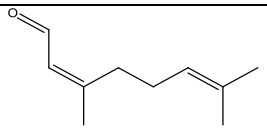	15.1%	3.7%
α-Terpineol	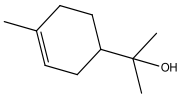	3.6%	3.6%
6-Methyl-5-hepten- 2-one	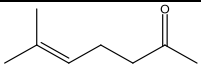	1.5%	3.4%

5.3.2 Solid Phase Extraction of *A. citrodora* EO Constituents

Solid phase extraction was performed using the following conditions:

Sample: *A. citrodra* essential oil

Sorbent: 4 g silica cartridge (SF10-4g)

Conditioning: The cartridge was conditioned with 5 ml pentane

Loading: 100 µL of *A. citrodra* essential oil was loaded onto the cartridge.

Elution:

Flow rate of 1 ml/sec.

- Fraction I: pentane100%.
- Fraction II: pentane/ethyl ether 90:10.
- Fraction III: ethyl ether 100%.

Percent composition of *A. citrodora EO* and its fractionation are shown in Appendix III. Fraction I contained only hydrocarbons; fraction II carbonyl compounds, ethers, esters and tertiary alcohols; Fraction III primary alcohols, acids and diols. The recoveries were satisfactory for almost all analytes. Table 5.3 shows an example of the eluted compounds in each fraction.

Table 5.3 Examples of the compounds found in each SPE fractions

Fraction I	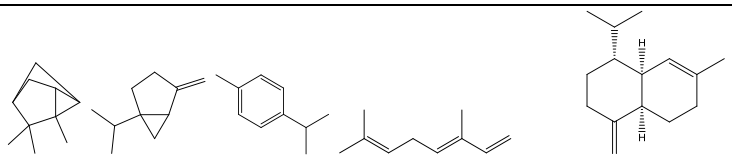
Fraction II	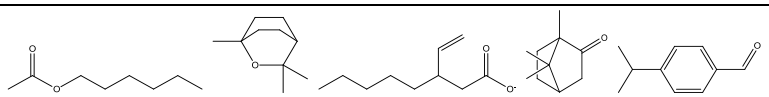
Fraction III	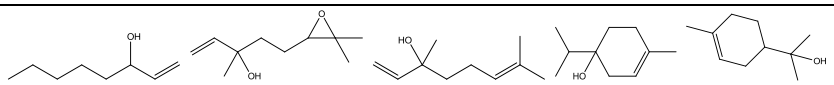

5.3.3 Structure based virtual screening of *A. citrodora* EO constituents for anticholinesterase inhibitors

The top scoring hits from *A. citrodora* EO constituents were imported to Hermes software to view crystal structures with docked ligands (Fig 5.8 to 5.14). The scores of these top hits had values comparable to those possessed by optimal conformations of huperzine, rivastigmine, donepezil and galantamine in the active site.

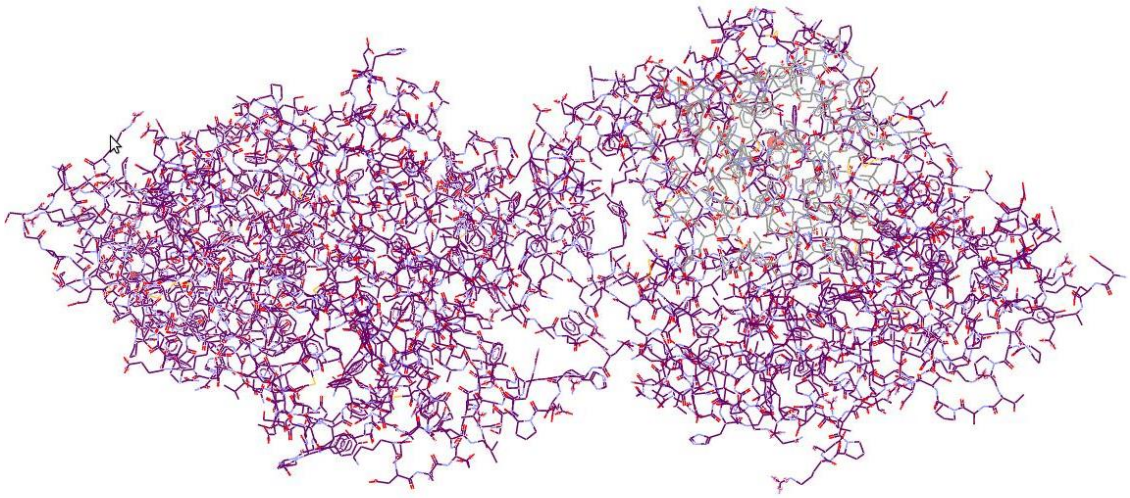

Fig 5.5

Structure of human AChE. 15Å radius from centre of the binding site from AChE (PDB:4EY7) with docked donepezil was defined as the search space shown in Blue, done by GOLD Molecular docking version 3.0.1.

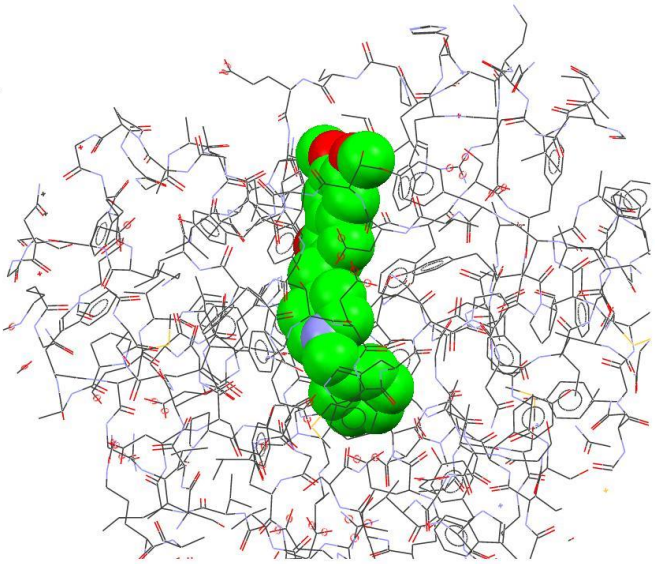

Fig 5.6

A magnification of the defined 15Å radius search space with donepezil docked: A space fill model. GOLD Molecular docking version 3.0.1

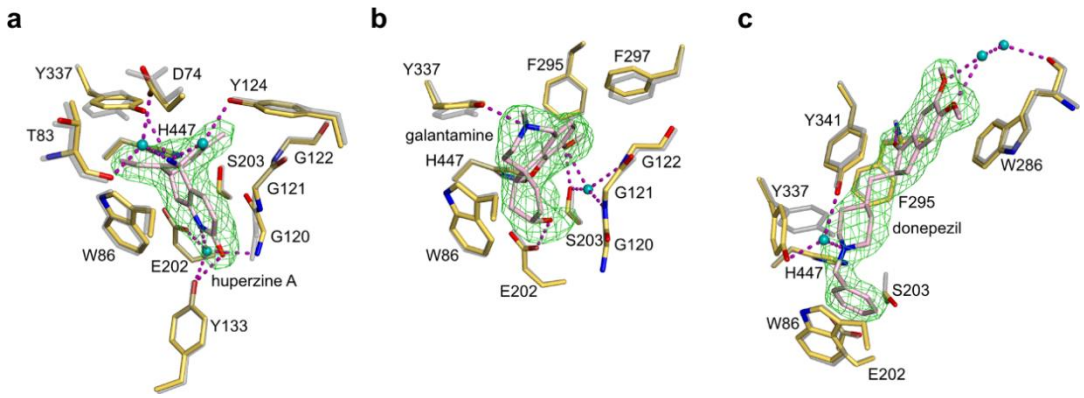

Figure 5.7

Close up views of the AChE active site with bound a) huperzine A, b) galantamine, and c) donepezil. Carbons are in pink in the ligands and light yellow in residues of the complex (Cheung et al., 2012).

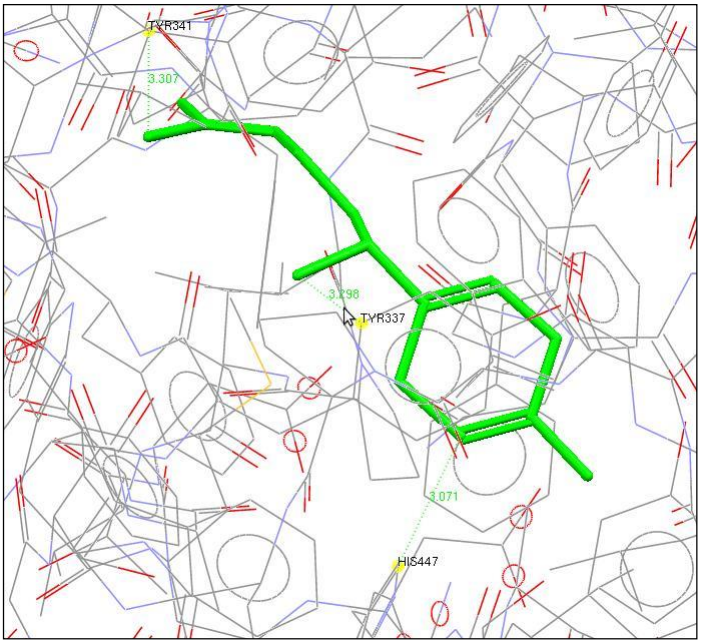

Fig 5.8

1st Ranked Hit: Close up views of the rhAChE active site with bound **β-Curcumene**, (carbon atoms in green) showing Ligand-Protein interactions points (yellow) at TYR 341, TYR337, HIS 447, β-Curcumene have the highest hit score of PLP 75.64

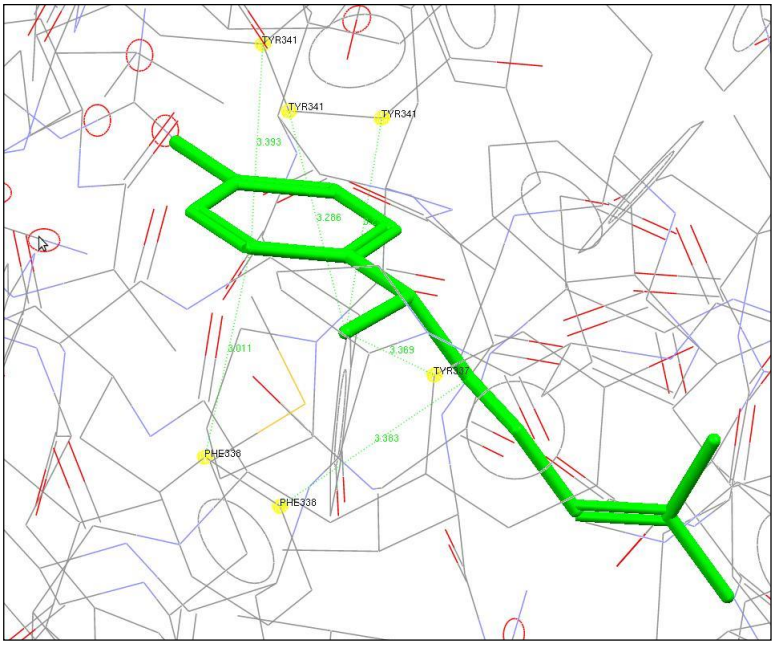

Fig 5.9

2nd Ranked Hit: Close up views of the rhAChE active site with bound **Curcumene**, (carbon atoms in green) showing Ligand-Protein interactions points (yellow) at TYR 341, TYR 337, PHE 338.

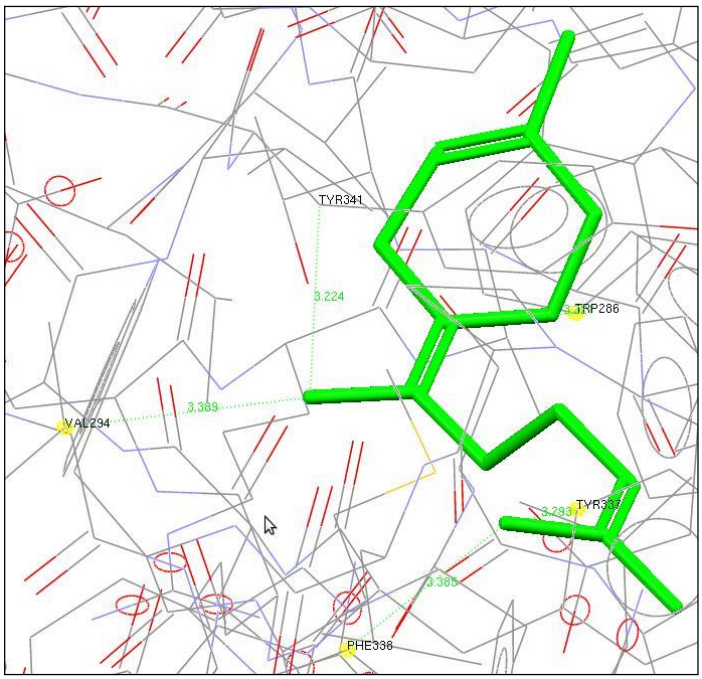

Fig 5.10

3rd Ranked Hit: Close up views of the rhAChE active site with bound **Bisabolene** (carbon atoms in green) showing Ligand-Protein interactions points (yellow) at TYR 341, TYR 337, TRP 286, PHE 338 and VAL 294.

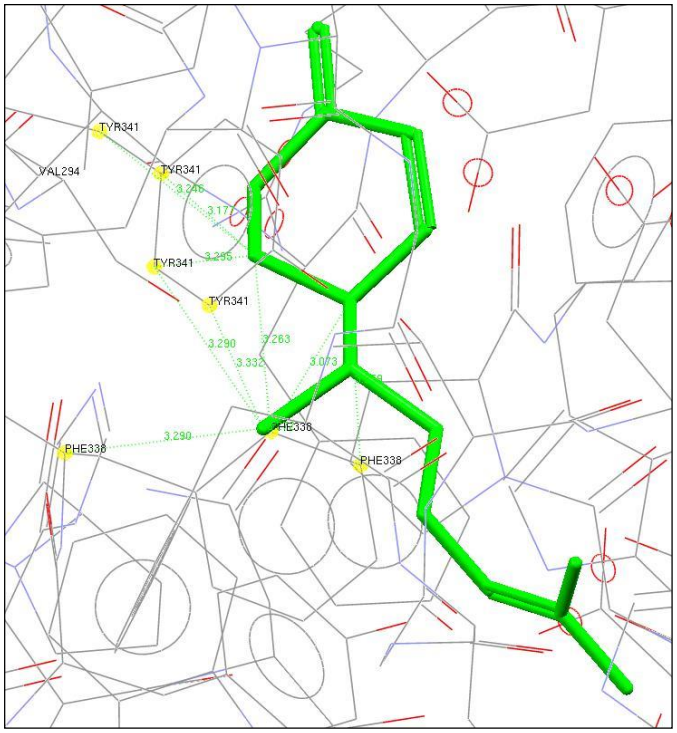

Fig 5.11

4th Ranked Hit: Close up views of the rhAChE active site with bound **β-Sesquiphellandrene** (carbon atoms in green) showing Ligand-Protein interactions points (yellow) at TYR 341, PHE 338, VAL 294.

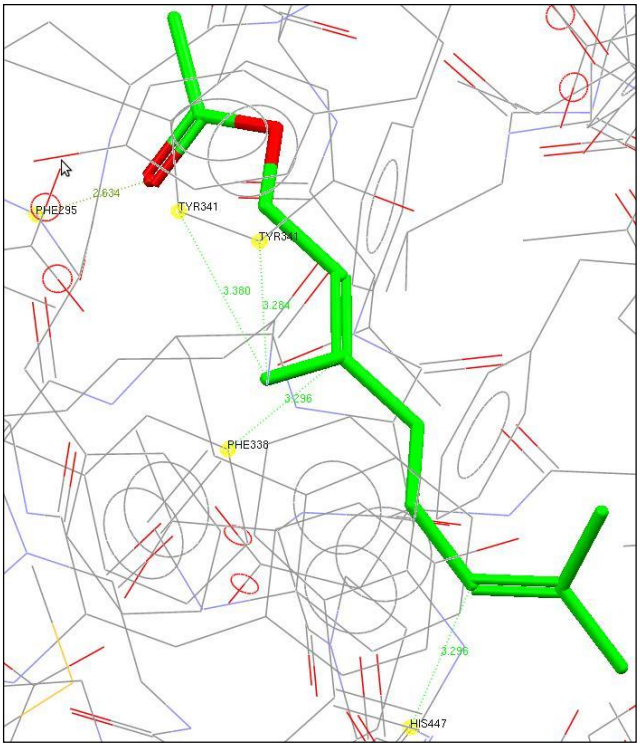

Fig 5.12

5th Ranked Hit: Close up views of the rhAChE active site with bound **Geranyl Acetate** (Carbon atoms shown in green, Oxygen atoms in red) showing Ligand-Protein interactions points (yellow) at TYR 341, PHE 338, PHE 295, HIS 447.

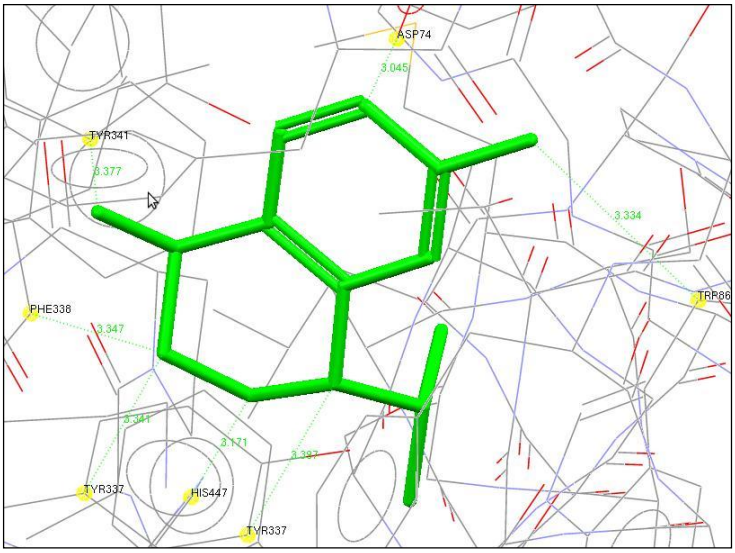

Fig 5.13

6th Ranked Hit: Close up views of the rhAChE active site with bound **trans-Calamenene**, (Carbon atoms in green) showing Ligand-Protein interactions points (yellow) at TYR 341, TYR337, PHE338, HIS 447, TRP86, and ASP74.

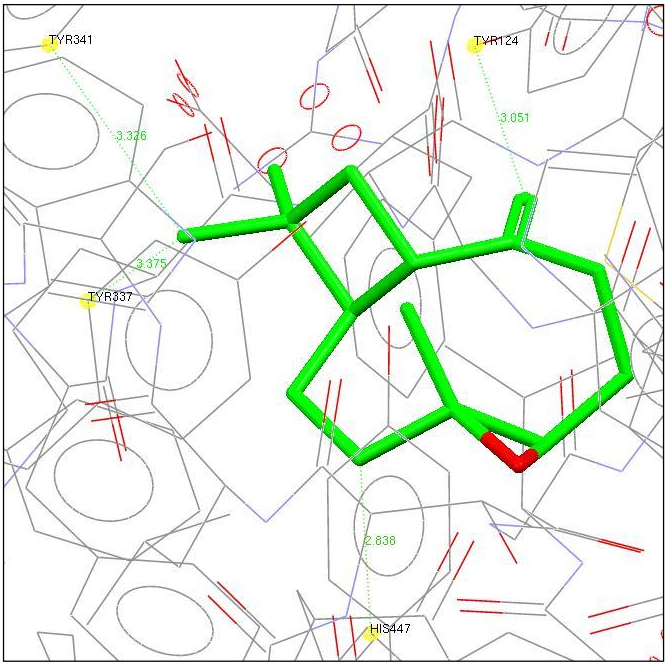

Fig 5.14

7nd Ranked Hit: Close up views of the rhAChE active site with bound **Caryophyllene oxide (**Carbon atoms shown in green, Oxygen atoms in red) showing Ligand-Protein interactions points (yellow) at TYR 341, TYR337, TYR124 HIS 447.

5.4 Discussion

5.4.1 Gas Chromatography-Mass Spectrometry (GC-MS) analysis

The chemical composition of the essential oil from leaves of *A. citrodora* of Jordanian origin is listed in appendix II, Eighty three (83) chemicals were identified. The essential oil was characterized by the presence of terpenoids, monoterpenes and sesquiterpenes, and 6-methyl-5-hepten-2-one, the main constituents were Limonene (12.14%) Caryophyllene oxide (10.44 %), Curcumene (9.17 %), Spathulenol (7.16 %), 1,8-Cineole (7.94%), all of which constitute 47% of the total oil (Table 5.1), followed by Geranial (4.03 %) and Neral (2.55%), α-Terpineol (3.27%) and 6-Methyl-5-hepten- 2-one (2.37%) (Table 5.2). These results are in agreement with the literature (Montes et al., 1973, Kaiser and Lamparsky, 1976, Velasco-Negueruela et al., 1993, Bellakhdar et al., 1994, Zygadlo et al., 1994, Özek et al., 1996, Terblanché and Kornelius, 1996, Carnat et al., 1999, Pascual et al., 2001, Crabas et al., 2003, Kim and Lee, 2004, Sartoratto et al., 2004, Santos-Gomes et al., 2005, Argyropoulou et al., 2007) The oil was devoid of compounds from the phenylpropanoid pathway (Crabas et al., 2003, Santos-Gomes et al., 2005).

Limonene is the component most abundant in essential oils of the genus Lippia, followed by p-cymene, a-pinene, camphor, b-caryophyllene, linalool and thymol in a decreasing order (Pascual et al., 2001, Terblanché and Kornelius, 1996) and *21* (Kim and Lee, 2004, Zygadlo et al., 1994). In our study, α-pinene, β-caryophyllene and linalool, p-cymene, and thymol were also identified at low levels. *A. citrodora* is characterized by high contents of monoterpenes and sesquiterpenes. Terpenoids comprise a very large group of natural products and comprise two or more branched 5 carbon units, formed from mevalonic acid. Skeletons consisting of multiplets of 2, 3, 4 or 6 of these linked together in many different ways are found in a variety of mostly cyclic compounds including monoterpenes (10 carbons in the skeleton), sesquiterpenes (15 carbons), diterpenes (20 carbons) and triterpenoids (30 carbons), respectively. These compounds tend to be lipophilic, so they are able to cross the blood-brain barrier. Also, monoterpenes, and some of the

sesquiterpenes, are volatile, and are responsible for the strong odours and flavours of many herbs, spices and traditional medicines.

It should be emphasized that a variety of geographical and ecological factors can lead to qualitative and quantitative differences in the essential oil produced. A number of other factors can influence its composition, such as the developmental stage of the plant, its physiology, the age of leaves and the growing conditions (Bellakhdar et al., 1994, Zygadlo et al., 1994, Santos-Gomes et al., 2005). The composition of the oil is also affected by the isolation method and the conditions of analysis (Crabas et al., 2003, Kim and Lee, 2004, Sartoratto et al., 2004, Santos-Gomes et al., 2005).

5.4.2 Solid Phase Extraction

Although SPE is a well-established sample preparation technique with broad applications base, only a small number of studies have utilized SPE for the fractionation of essential oils. (Antonelli and Fabbri, 1999) used SPE for the fractionation of tarragon (*Artemisia dracunculus*) and rose (*Rosa damascena*) essential oils, (500 mg / 3 mL silica cartridge that had previously been conditioned with 3 mL of pentane) using the following solvent sequence: Fraction A: 3 mL of pentane; Fraction B: 6 mL of pentane/ethyl ether 90:10; Fraction C: 3 mL of ethyl ether. Essential oil components were pre-separated into three fractions with 90 % mean recovery of the analytes. Fraction A contained hydrocarbons; B, contained esters, ethers, oxides, carbonyl compounds and tertiary alcohols; and C, which contained other alcohols, acids and diols. (Dawidowicz and Dybowski, 2010) used a SPE column packed with octadecyl silica sorbent to separate oxygenated compounds with low molecular mass from the rest of the essential oil components using 68% methanol. Oxygenated compounds of low molecular mass occurring in essential oils of *Salvia officinalis*, *Artemisia absinthium*, *Artemisia vulgaris*, and *Thuja occidentalis* completely eluted from the SPE column using this method. The average recovery of these compounds in methanolic fraction was almost 100%, whereas the average recovery of the remaining essential oil compounds were all above 90% and satisfactory for preliminary separation of essential oils for analytical and preparative purposes.

The solid Phase Extraction System 971-FP Flash Purification System (Agilent) was used for SPE of the *A. citrodora* EO. The system allows the establishment of multiple solvent systems for continuous availability without interrupting the fractionation procedure and is equipped with Low Pulse Pump which provides an even solvent flow. 4 g silica cartridge (SF10-4g) was chosen for 100 µl of essential oil for normal phase SPE where the sorption of the functional groups of the compound from a non-polar solvent to the polar surface of the stationary phase. The mechanism of sorption involves polar interactions such as hydrogen bonding, dipole–dipole interactions, π–π interactions and induced dipole–dipole interactions.

To achieve retention, the interaction between the solute and the stationary phase must dominate. Fraction I contained all hydrocarbons; fraction II carbonyl compounds, ethers, esters and tertiary alcohols; Fraction II primary alcohols, acids and diols. The recoveries were satisfactory for almost all the analytes. This method was successful in fractionating the essential oil into three distinct fractions in one simple step easily, quickly and using small amounts of organic solvents.

To test whether the SPE developed for *A. citrodora* EO is also useful for the fractionation of essential oils from other plants containing the same or similar main components. The same protocol was applied for the fractionation of the Lavender (*Lavandula angustifolia* Mill.) EO. The method was equally successful in fractionating lavender essential oil into three fractions with more than 90% recovery (Appendix VI) opening the way for the possibility of using this method for other essential oils and for utilizing SPE for comparing between different essential oils specific fractions.

SPE will allow fractions of the essential oil with close chemical moieties to be tested in *vivo* and *in vitro* for beneficial properties in neurodegenerative diseases, and results can be compared with whole essential oil, to uncover what part of the oil hold the active components and if there are any synergistic, anti-synergistic or masking effects among different essential oil constituents. This will make it easier to characterize the molecules responsible for any beneficial activity.

5.4.3 Virtual Screening for Anticholinesterase Inhibitors

Acetylcholinesterase (EC 3.1.1.7) belongs to carboxyl esterase family of enzymes. It is a serine protease that hydrolyses the neurotransmitter ACh with high catalytic activity (Lewis et al., 2002). AChE can be found mainly at neuromuscular junctions and cholinergic brain synapses, where its activity serves to terminate synaptic transmission. X-ray structures of AChE co-crystallized with various ligands provide insights into the essential structural elements essential to its catalytic mechanism. The active site of AChE comprises of 2 sub sites: the anionic site and the esteratic sub site (Greenblatt et al., 1999). The anionic sub site accommodates the positive quaternary amine of ACh, however, the cationic moieties of different substrates are not bound by a negatively-charged amino acid in the enzymatic anionic site, but rather by interaction with 14 aromatic residues that line the gorge leading to the active site (Inestrosa et al., 2008). Crystal structure analysis showed that the active site of AChE enzyme spans a gorge about 20 Å in length which is lined by 14 aromatics residues, and is conserved across different species. The function of the AChE enzyme is mainly controlled by tryptophan residues (Gupta et al., 2011).

Many essential oils and their monoterpene constituents have been investigated for their effects on AChE, For example, the essential oils from *Melissa officinalis* and *Rosmarinus officinalis* have been reported to inhibit erythrocyte AChE *in vitro* (Perry et al., 1996). However these monoterpene AChE inhibitors were weak compared with the anti-AChE alkaloid like physostigmine (Perry et al., 2000). Of the essential oil constituents from different medicinal plants 1,8-cineole and camphor have shown activity against human erythrocyte AChE (Adewusi et al., 2010). γ-terpinene, and α-pinene; geraniol and linalool were also found to be weak inhibitors of human erythrocyte AChE (Miyazawa et al., 1997, Perry et al., 2000). Other monoterpenes that are reported to inhibit AChE include citral, bornyl acetate, geraniol and limonene, which are inhibitors of electric eel AChE as well (Ryan and Byrne, 1988).

Monoterpenes consist of a hydrocarbon skeleton which may contribute to their anti-AChE activity. The hydrophobic active site of AChE is reported to be susceptible to hydrophobic interactions (Hansch and Deutsch, 1966). Monoterpenes may be

cyclic (e.g. 1,8-cineole and α-pinene) or acyclic (e.g. geraniol and linalool), a feature that may also influence anti-AChE activity. This structural diversity of the active anti-AChE terpenoids some of which bear no obvious resemblance to ACh complicates the prediction of potential structure activity relationships.

Most crystallographic studies of AChE involve the electric ray (*Torpedo californica*) homologues. Although there are 100 AChE structures deposited in the Protein Data Bank, only five human AChE structures of the catalytic core have been solved to date. Donepezil binds to rhAChE in a significantly different conformation than it does to Torpedo californica AChE (tAChE) thus exemplifying how the human enzyme is more accurate for the study of drug binding (Cheung et al., 2012).

This study was able to use a recombinant human form of the enzyme at a resolution of 2.15 Å representing a good platform for structure-based ligand modelling and docking. Top 7 scoring hits showed high similarities in the protein residues with which they interact both amongst themselves, and known inhibitors like Huperzine A and Donepezil (Table 5.4). The most common interactions were with TYR 341 + 337, PHE 338 and HIS 447 respectively. The majority of these interactions are manifested in hydrogen bonding, hydrophobic and π-π interactions.

Hydrogen bonds, and strong hydrophobic interactions formed between the inhibitors and the nearby AChE side chains serve dual roles: 1) to inhibit the catalytic activity of AChE by competing with ACh binding site and 2) to prevent amyloid fibrillogenesis by blocking the Ab recognition zone at the peripheral site. Potential clinical relevance of these compounds requires further investigation. Considering the relatively weak anti-AChE activity of terpenoids reported to date, it is unlikely that they may be used therapeutically for cognitive disorders. However, analogues of active terpenoid compounds may be developed to enhance efficacy. And these findings indicate that plants may yield novel AChE inhibitors, other than alkaloids, which may have advantages in relation to efficacy and adverse-effect profile.

Table 5.4

Ligand-Protein interactions between top hits compounds and AChE active site

	TYR 133	TYR 337	TYR 341	TYR 124	TRP 86	TRP 286	PHE 338	PHE 295	HIS 447	VAL 294	ASP 74
Huperzine A	X	X									
Donepezil		X	X		X	X					
β-Curcumene		X	X						X		
Curcumene		X	X				X				
Bisabolene		X	X			X	X			X	
trans-Calamenene		X	X		X		X		X		X
Caryophyllene oxide		X	X	X					X		
β-Sesquiphellandrene			X				X			X	
Geranyl Acetate			X				X	X	X		

In light of the knowledge gained from the observations of the interactions between AChE and potential inhibitors, it can be seen that the combination of molecular docking, and virtual screening efforts is a promising strategy for discovering more effective inhibitory compounds from essential oils that will impact future experimental studies on these constituents.

Chapter 6

General Discussion and Future Directions

6.1 General Discussion

Medicinal plant products have a long history of use for treating neurological symptoms. Yet the study of the mechanisms of action for neuroactive natural medicinal products is in its infancy. With new advances in scientific techniques we are able to take a closer look at the therapeutic actions of the complex biologically active molecules that have arisen as a result of natural selection, over perhaps 300 million years. This thesis brings together contemporary perspectives and research methods to try to understand the mechanisms underlying the neuroactive actions of plant based natural products and to validate their use in neurotherapies.

Interest in medicinal plant research and the aroma-therapeutic effects of EOs in humans has increased in recent years, especially for the treatment of pathologies with profound social impact such as AD. Several plant species are used in medical herbalism for their effects on anxiety, restlessness, excitability and depression. These include lemon balm *(Melissa officinalis*), lavender (*Lavandula angustifolia*), chamomile (*Matricaria chamomilla*), bergamot (*Monarda* species), neroli (*Citrus aurantium*) and valerian (*Valeriana officinalis*) (Perry et al., 2006, Elliott et al., 2007). Several recent clinical trials have concurred with the value of aromatherapy in people with dementia (Perry et al., 2006, Kennedy et al., 2011). The safety of these EO based approaches has also been established in clinical populations. Despite this, however, the central mechanisms by which the EOs exert their effects are largely unknown.

A. citrodora (Verbenaceae) is an aromatic plant that is cultivated in some parts of Jordan, mainly for its food and medicinal purposes. Some plant material described as *M. officinalis* (known in Arabic as ‘melissa’) was identified as *A. citrodora* (also

known locally as melissa); both species have similar traditional uses and produce a yellow to light green EO with special aroma similar to that of lemon (Abuhamdah et al., 2005). *M. officinalis* has been of particular interest on account of its sedative; cognitive-enhancing, and anxiolytic-like effects, all relevant pathophysiological actions seen in AD (Viola et al., 1995, Akhondzadeh et al., 2003, Kennedy et al., 2003, Kennedy et al., 2004, Abu-Hamdah et al., 2005, Perry and Perry, 2006, Elliott et al., 2007, Kennedy and Wightman, 2011). Limited data are available which explore the effects of *A. citrodora* oils pertinent to AD, in comparison with *M. officinalis.* Detailed pharmacological research is required to verify their effectiveness. The goal of this present study was the phytochemical and biological evaluation of a traditionally used Jordanian medicinal plant, *A. citrodora* (which is accessible, abundant and has been subjected to limited neurological assessment) as a potential source of novel neuroactives in order to address the primary hypothesis cited in Chapter 1.

The first step in the *A. citrodora* EO pharmacological screen was the investigation of the binding activity of the EOs to the well-known ligand-gated ion channel receptor molecular targets in a series of dose–response competition binding experiments. Based on [^{35}S] TBPS, [^{3}H] flunitrazepam and [^{3}H] MK-801 binding assays, no significant inhibitory effect was observed for *A. citrodora* EOs derived from fresh or dried leaves, spanning a wide concentration range. In contrast, *A. citrodora* essential oil inhibited [^{3}H] nicotine binding to well washed rat forebrain membranes, with mean apparent IC_{50} of 0.0018 mg/ml. This pharmacological profile is in marked contrast to our previous published findings with the essential oils derived from the European Melissa EO (*M. officinalis*) which displayed no apparent binding affinity for neuronal nicotinic receptors, but showed a clear binding affinity for the channel site of the $GABA_AR$, previously proposed to be due to the presence of the component, ocimine (Mahita et al., 2014). Neuronal nicotinic acetylcholine receptors represent novel targets for CNS therapeutics, and may have substantial roles in mediating antinociception and modulating cognitive performance. Furthermore, there is growing evidence that nicotinic agonists are neuroprotective both *in vitro* and *in vivo* via α4β2 and α7 neuronal nicotinic receptor subtypes (Chapter 1). Additional studies are required to confirm the pharmacological identity (agonist or antagonist) of the *A. citriodora* essential oil.

Many medicinal plants have been the basis for the successful development of cholinesterase inhibitors, used successfully in dementia therapeutics. The next step of this thesis was the screening of *A. citrodora* EO for anti-cholinesterase properties. Both EOs from dried and fresh leaves elicited an effective acetylcholinesterase inhibitory activity. Dried leaves oil showed a more clear AChE inhibitory activity than fresh oil, which may be related to higher respective levels of limonene and caryophyllene oxide. The need for a rapid search for small molecules that may bind to targets of biological interest is of crucial importance in the drug discovery process. One way of achieving this is *in silico* or virtual screening of large compound databases to identify a set of compounds that contains relatively many hits against the target. If a three-dimensional (3D) model of the target is available, then structure-based virtual screening can be performed, utilising a docking program. Herein, a recombinant human form of the anticholinesterase enzyme was used for the first time as a platform for structure-based ligand modelling and docking. The seven top scoring hits in the *A. citrodora* EO show complementarities with the protein residues with which they interact common to themselves, and known prototypical AChE inhibitors. The majority of these interactions are manifested in hydrogen bonding, hydrophobic and π-π interactions. Furthermore, bisabolene and trans-calamenene displayed the most interactions and are the only ones which interact with key tryptophan residues, as seen with the protype, donepezil. Although some of the hits are already reported to have anti AChE activity such as curcumene (Fujiwara et al., 2010), caryophyllene oxide (Savelev et al., 2003, Costa et al., 2012) and β-sesquiphellandrene (Bonesi et al., 2010) the remaining hits, such as bisabolene and trans-calamenene have not been reported to date and could present novel AChE inhibitors. Although the potential clinical relevance of these virtual screening results requires further investigation, these findings indicate that plant essential oils may yield further novel AChE inhibitors, other than alkaloids, which may have advantages in relation to efficacy and adverse-effect profile.

A. citrodora EO, both dried and fresh, also exhibited potent radical scavenging activity and iron (II) chelating properties, which may, in addition to the nicotinic receptor activity, may underlie the neuroprotective characteristics displayed. Hydrogen peroxide accumulates during the incubation of β-amyloid and both show

a close synergistic action in neurodegenerative diseases. The ability of fresh *A. citrodora* EO to significantly ameliorate both hydrogen peroxide and Aβ-induced neurotoxicity offers scope for this oil to be utilised *in vivo*.

The next question posed by this thesis: what are the bioactive constituents which underpin these useful pharmacological properties? Using state-of-the art GC/MS analysis at Kew Gardens Research laboratory, the chemical composition of the essential oil derived from the leaves of *A. citrodora* was determined; More than eighty components, comprising of mainly mono-and sesquiterpenoids, were detected in the EOs obtained from Jordanian *A. citrodora* dried or fresh leaves (Table 5.2). The essential oil was characterized by the presence of terpenoids, monoterpenes and sesquiterpenes, and 6-methyl-5-hepten-2-one, the main constituents being limonene, caryophyllene oxide, curcumene, spathulenol, 1,8-cineole constituting 47% of the total oil. Other major constituents include geranial, neral, α-terpineol and 6-methyl-5-hepten- 2-one. Irrespective of whether derived from dried or fresh leaves, limonene, geranial, neral and 1,8-cineole were the dominating monoterpenoids. The qualitative composition of the EOs from fresh and dried *A. citrodora* leaves was similar, although quantitative differences were observed; notably, the EO from fresh leaves contained a higher percentage composition of geranial and neral (isomeric monoterpenoids collectively known as citral) compared to the EO from dried leaves; whilst dried leaves EO contained a higher percentage of limonene, compared to the fresh leaves EO. The fraction of monoterpene was enriched, mainly due to an increase in the contribution of limonene with the dried leaf oil. Importantly, all other components remained more or less unchanged both qualitatively and quantitatively. The monoterpenoids limonene, geranial, neral and 1,8-cineole have previously been reported as some of the main constituents of EOs from *A. citrodora* (including EOs documented from species described as synonyms for *A. citrodora*) (Montes et al., 1973, Özek et al., 1996, Terblanché & Kornelius, 1996, Carnat et al., 1999, Pascual et al., 2001). It is essential to characterise the chemical composition of EOs investigated pharmacologically, as oil composition from a particular species may vary considerably due to various factors, including genetic and environment influences. Indeed, *A. citrodora* oil composition is reported to differ due to plant growth stage and harvest time, whether wild or cultivated and geographical origin

(Zygadlo et al., 1994, Sartoratto et al., 2004, Argyropoulou et al., 2007, Gil et al., 2007, Santos-Gomes et al., 2005, Di Leo Lira et al., 2008, Zoubiri & Baaliouamer, 2011).

We were interested to compare the chemical composition of *A. citrodora and M. officinalis*, to provide scientific evidence for similarity between these two plant species and acceptance or otherwise, for using them as alternatives for each other in traditional medicine market across the world. This further addresses the primary hypothesis posed in Chapter 1. The EOs shared common components, but there were clear differences in the quantity of these particular chemicals. The main components detected in *M. officinalis* were the monoterpenoids, neral and geranial while in lemon verbena, these were limonene, neral, geranial, and 1,8-cineole. Both have the sesquiterpenoid, caryophyllene oxide whereas *A. citrodora* also have curcumene and spathulenol (Table 6.1). There were chemical differences in the quantity and constituents of the EOs obtained from two plants species, which may furthermore explain the different pharmacological profiles (Table 6.2).

Table 6.1

Comparison of A. *citrodora* and *M. officinalis* primary constituents

Aloysia citrodora	***Melissa officinalis***
Neral 15.1% Geranial 20.1% Limonene 13.6% 1,8-cineole 9.2%	Neral 24.2% Geranial 33.5%
Caryophyllene oxide 2.2% Curcumene 3.5% Spathulenol 3.1%	Caryophyllene oxide 12.2%

Table 6.2

Comparison between *A. citrodora* and *M. officinalis* essential oil pharmacological profile

	Aloysia citrodora	***Melissa officinalis***
Radioligand receptor binding	Conc. dependent inhibition of [^{3}H] nicotine binding to neuronal nicotinic receptor.	Conc. dependent inhibition of [^{35}S] TBPS binding to $GABA_AR$
Anti-AChE activity	Conc. dependent inhibition.	No apparent inhibition.
DPPH radical scavenging	Radical-scavenging activity.	Radical-scavenging activity.
Ferrous ion chelating	Metal chelating activity.	No apparent activity.

The GC/MS analysis of *A. citrodora* EO showed that it contains a variety of volatile molecules such as terpenes and terpenoids, phenol-derived aromatic components and aliphatic compounds, all of which belong to different classes of hydrocarbons, aldehydes, ketones, esters, and alcohols. Thus, to fractionate the essential oil prior to analysis was the logical next step, as the fractionation process will increase the concentration of the components and consequently ease the subsequent analysis. Furthermore, fractions can be compared with the original whole essential oil, to uncover which part of the oil holds the active components and if there are any synergistic, anti-synergistic or masking effects among different essential oil constituents. Many methods of essential oil fractionation have been reported in literature. Some of them are time consuming and use large volumes of solvents others need a highly technological approach such as LC-GC or multidimensional gas

chromatography. This thesis reports a simple, inexpensive method that uses silica SPE to carry out a fractionation of different essential oils. This method was successful in fractionating essential oils into three distinct fractions in one simple step easily, quickly and using small amounts of organic solvents. This protocol successfully separated the oils into hydrocarbons; carbonyl compounds, ethers, esters and tertiary alcohols; primary alcohols, acids and diols. The putative AChE actives identified by the computer modelling were fractionated in two separate fractions, the hydrocarbons: β-curcumene, curcumene, bisabolene, trans-calamenene, and β-sesquiphellandrene, while geranyl acetate and caryophyllene oxide were fractionated together. In light of these results, it can be seen that the combination of SPE fractionation linked with molecular docking, and virtual screening efforts offers a promising strategy for discovering further neuroactive chemotypes from essential oils that will direct future experimental studies on essential oil products.

Overall, this thesis reports that although the two “Melissa” plants are used traditionally for similar therapeutic uses, they display distinct chemical compositions, pharmacological properties and neuroprotective abilities. We propose that the combination of positive activities (Figure 6.1) provide a strong case for the use of *A. citrodora* essential oil as a therapeutic agent for a range of neurodegenerative diseases.

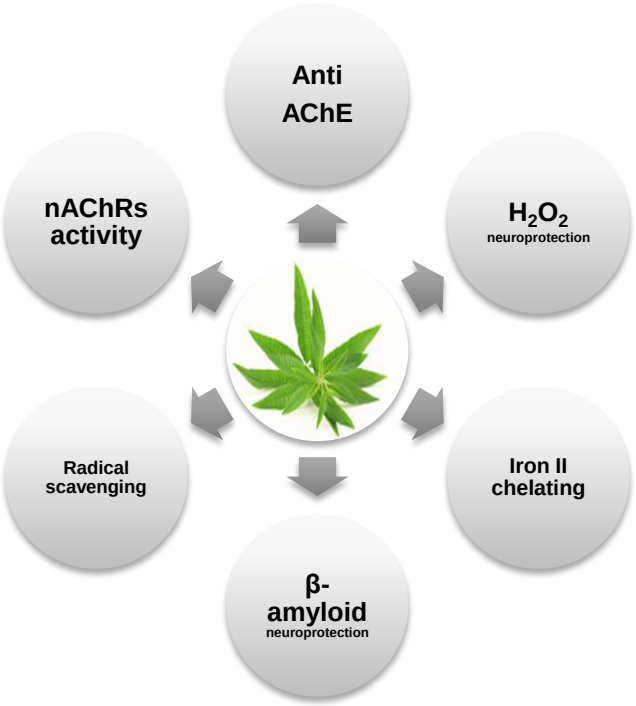

Fig 6.1

Summary of useful *A. citrodora* properties pertinent to neurodegenerative disease

6.2 Future Directions

This project demonstrated that the *A. citrodora* EO displays a wide range of useful pharmacological properties which are worthy of further study *in vivo*. Utilising a range of our all-in-one behavioural tests (Ennaceur et al., 2010), it can be assessed whether the EO has positive effects on a range of behavioural aspects pertinent to neurodegenerative diseases (both motor, affective and cognitive). The new SPE protocol developed in this study can be used for the fractionation of other plant essential oils which would make further testing and analysis easier and more effective; in fact, this could be used as a standard protocol for essential oils in general. It would be important to screen *A. citrodora* EO fractions produced by the SPE method using the same tests performed for the whole crude oil to compare and contrast the results, and address the issues of pharmacological synergy and interference. Structure based virtual screening can be performed using the anticholinesterase inhibitor model developed in this study for other medicinal plant products in order to expand the panel of putative novel AChE inhibitors. The seven hits require urgent validation to confirm the utility of this methodology. Furthermore, more complex targets could be studied in a similar fashion (voltage-gated sodium channel, nAChR, $GABA_AR$ channel etc). This will naturally be more demanding due to the lack of high-quality, high-resolution structural information for these targets.

Collectively, the results accumulated in this thesis provide a better understanding of the pharmacology of the *A. citrodora* EO and its constituents relating to its potential use in treating neurodegenerative diseases.

References

AAZZA, S., LYOUSSI, B. & MIGUEL, M. G. 2011. Antioxidant and Antiacetylcholinesterase Activities of Some Commercial Essential Oils and Their Major Compounds. *Molecules,* 16**,** 7672-7690.

ABU-HAMDAH, S., AFIFI, F. U., SHEHADEH, M. & KHALID, S. 2005. Simple quality-control procedures for selected medicinal plants commonly used in Jordan. *Pharmaceutical biology,* 43**,** 1-7.

ABUHAMDAH, S., ABUHAMDAH, R., AL-OLIMAT, S. & CHAZOT, P. 2013. Phytochemical Investigations and Antibacterial Activity of Selected Medicinal Plants from Jordan. *European Journal of Medicinal Plants,* 3.

ADEWUSI, E. A., MOODLEY, N. & STEENKAMP, V. 2010. Medicinal plants with cholinesterase inhibitory activity: a review.

AH, H. M., EL-BELTAGI, H. S. & NASR, N. 2008. Assessment of Volatile Components, Free Radical-Scavenging Capacity and Anti-Microbial Activity of Lemon Verbena Leaves. *Research Journal of Phytochemistry,* 2**,** 84-92.

AKHONDZADEH, S., NOROOZIAN, M., MOHAMMADI, M., OHADINIA, S., JAMSHIDI, A. & KHANI, M. 2003a. Melissa officinalis extract in the treatment of patients with mild to moderate Alzheimer's disease: a double blind, randomised, placebo controlled trial. *Journal of Neurology, Neurosurgery & Psychiatry,* 74**,** 863-866.

AKHONDZADEH, S., NOROOZIAN, M., MOHAMMADI, M., OHADINIA, S., JAMSHIDI, A. H. & KHANI, M. 2003b. Melissa officinalis extract in the treatment of patients with mild to moderate Alzheimer's disease: a double blind, randomised, placebo controlled trial. *J Neurol Neurosurg Psychiatry,* 74**,** 863-6.

ALHEBSHI, A. H., GOTOH, M. & SUZUKI, I. 2013. Thymoquinone protects cultured rat primary neurons against amyloid β-induced neurotoxicity. *Biochemical and Biophysical Research Communications,* 433**,** 362-367.

ALLAN BUTTERFIELD, D., CASTEGNA, A., LAUDERBACK, C. M. & DRAKE, J. 2002. Evidence that amyloid beta-peptide-induced lipid peroxidation and its sequelae in Alzheimer's disease brain contribute to neuronal death. *Neurobiology of aging,* 23**,** 655-664.

ANDERSEN, J. K. 2004. Oxidative stress in neurodegeneration: cause or consequence? *Nature Medicine*, 10 Suppl, S18-25.

ANTONELLI, A. & FABBRI, C. 1999. Essential oils: SPE fractionation. *Chromatographia,* 49**,** 125-130.

ARGYROPOULOU, C., DAFERERA, D., TARANTILIS, P. A., FASSEAS, C. & POLISSIOU, M. 2007. Chemical composition of the essential oil from leaves of Lippia citriodora (Verbenaceae) at two developmental stages. *Biochemical Systematics and Ecology,* 35**,** 831-837.

BAKKALI, F., AVERBECK, S., AVERBECK, D. & IDAOMAR, M. 2008. Biological effects of essential oils–a review. *Food and chemical toxicology,* 46**,** 446-475.

BARNHAM, K. J., MASTERS, C. L. & BUSH, A. I. 2004. Neurodegenerative diseases and oxidative stress. *Nature Reviews Drug Discovery,* 3**,** 205-214.

BARTOLINI, M., BERTUCCI, C., CAVRINI, V. & ANDRISANO, V. 2003. β-Amyloid aggregation induced by human acetylcholinesterase: inhibition studies. *Biochemical pharmacology,* 65**,** 407-416.

BASTIANETTO, S., RAMASSAMY, C., DORE, S., CHRISTEN, Y., POIRIER, J. & QUIRION, R. 2000. The Ginkgo biloba extract (EGb 761) protects hippocampal neurons against cell death induced by beta-amyloid. *European Journal of Neuroscience,* 12**,** 1882-90.

BAUR, R. & SIGEL, E. 2003. On high-and low-affinity agonist sites in GABAA receptors. *Journal of neurochemistry,* 87**,** 325-332.

BEAL, F., LANG, A. E. & LUDOLPH, A. C. 2005. *Neurodegenerative Diseases: Neurobiology, Pathogenesis and Therapeutics*, Cambridge University Press.

BEHRENS, A. 2003. Physiological and pathological functions of the prion protein homologue Dpl. *British medical bulletin,* 66**,** 35-42.

BELLAKHDAR, J., IDRISSI, A. I., CANIGUERAL, S., IGLESIAS, J. & VILA, R. 1994. Composition of lemon verbena (Aloysia triphylla (L'Herit.) Britton) oil of Moroccan origin. *Journal of Essential Oil Research,* 6**,** 523-526.

BEYER, K. 2007. Mechanistic aspects of Parkinson's disease: α-synuclein and the biomembrane. *Cell biochemistry and biophysics,* 47**,** 285-299.

BILIA, A., GIOMI, M., INNOCENTI, M., GALLORI, S. & VINCIERI, F. 2008. HPLC–DAD–ESI–MS analysis of the constituents of aqueous preparations of verbena and lemon verbena and evaluation of the antioxidant activity. *Journal of pharmaceutical and biomedical analysis,* 46**,** 463-470.

BILIA, A., GIOMI, M., INNOCENTI, M. & VINCIERI, F. 2006. Yields in phenylpropanoids and antioxidant properties of different aqueous extracts of lemon verbena (Lippia citriodora K.). *Planta Medica,* 72**,** P_244.

BIRKS, J. 2006. Cholinesterase inhibitors for Alzheimer's disease. *Cochrane Database Syst Rev***,** Cd005593.

BITETTI-PUTZER, R., JOSEPH-MCCARTHY, D., HOGLE, J. M. & KARPLUS, M. 2001. Functional group placement in protein binding sites: a comparison of GRID and MCSS. *Journal of computer-aided molecular design,* 15**,** 935-960.

BLISS, T. V. & COLLINGRIDGE, G. L. 1993. A synaptic model of memory: long-term potentiation in the hippocampus. *Nature,* 361**,** 31-9.

BOHME, I., RABE, H. & LUDDENS, H. 2004. Four amino acids in the alpha subunits determine the gamma-aminobutyric acid sensitivities of GABAA receptor subtypes. *Journal of Biological Chemistry,* 279**,** 35193-200.

BOLOGNIN, S., MESSORI, L. & ZATTA, P. 2009. Metal ion physiopathology in neurodegenerative disorders. *NeuroMolecular Medicine,* 11**,** 223-38.

BON, S., VIGNY, M. & MASSOULIE, J. 1979. Asymmetric and globular forms of acetylcholinesterase in mammals and birds. P*roceedings of the National Academy of Sciences Proc Natl U S A,* 76**,** 2546-50.

BOND, M., ROGERS, G., PETERS, J., ANDERSON, R., HOYLE, M., MINERS, A., MOXHAM, T., DAVIS, S., THOKALA, P. & WAILOO, A. 2012. The effectiveness and cost-effectiveness of donepezil, galantamine, rivastigmine and memantine for the treatment of Alzheimer's disease (review of Technology Appraisal No. 111): a systematic review and economic model.

BONESI, M., MENICHINI, F., TUNDIS, R., LOIZZO, M. R., CONFORTI, F., PASSALACQUA, N. G., STATTI, G. A. & MENICHINI, F. 2010. Acetylcholinesterase and butyrylcholinesterase inhibitory activity of Pinus species essential oils and their constituents. *Journal of Enzyme Inhibition and Medicinal Chemistry,* 25**,** 622-628.

BONILLA, E. 2000. Huntington disease. A review]. *Investigación clínica,* 41**,** 117.

BRAHMACHARI, G. & SCIENTIFIC, W. 2012. *Bioactive Natural Products: Opportunities and Challenges in Medicinal Chemistry*, World Scientific Publishing Company.

BRINI, M., CALÌ, T., OTTOLINI, D. & CARAFOLI, E. 2014. Neuronal calcium signaling: function and dysfunction. *Cellular and Molecular Life Sciences***,** 1-28.

BURKE, R. E. 2004. Recent advances in research on Parkinson disease: synuclein and parkin. *The neurologist,* 10**,** 75-81.

BUSH, A. I. 2003. The metallobiology of Alzheimer's disease. *TRENDS in Neurosciences,* 26**,** 207-214.

BUSTOS, S. G., MALDONADO, H. & MOLINA, V. A. 2009. Disruptive effect of midazolam on fear memory reconsolidation: decisive influence of reactivation time span and memory age. *Neuropsychopharmacology,* 34**,** 446-57.

CACCAMO, D., CURRO, M., CONDELLO, S., FERLAZZO, N. & IENTILE, R. 2010. Critical role of transglutaminase and other stress proteins during neurodegenerative processes. *Amino Acids,* 38**,** 653-8.

CAMEL, V. 2003. Solid phase extraction of trace elements. *Spectrochimica Acta Part B: Atomic Spectroscopy,* 58**,** 1177-1233.

CAO, N. & YAO, Z.-X. 2013. Oligodendrocyte N-Methyl-d-aspartate Receptor Signaling: Insights into Its Functions. *Molecular Neurobiology,* 47**,** 845-856.

CARNAT, A., CARNAT, A.-P., CHAVIGNON, O., HEITZ, A., WYLDE, R. & LAMAISON, J.-L. 1995. Luteolin 7-diglucuronide, the major flavonoid compound from Aloysia triphylla and Verbena officinalis. *Planta medica,* 61**,** 490.

CARNAT, A., CARNAT, A., FRAISSE, D. & LAMAISON, J. 1999. The aromatic and polyphenolic composition of lemon verbena tea. *Fitoterapia,* 70**,** 44-49.

CATALAN, C. A. & DE LAMPASONA, M. E. 2002. 5 The chemistry of the genus Lippia (Verbenaceae). *Oregano: The genera Origanum and Lippia***,** 127-149.

CHAN, H. C., CHANG, R. C., KOON-CHING IP, A., CHIU, K., YUEN, W. H., ZEE, S. Y. & SO, K. F. 2007. Neuroprotective effects of Lycium barbarum Lynn on protecting retinal ganglion cells in an ocular hypertension model of glaucoma. *Experimental Neurology,* 203**,** 269-73.

CHAZOT, P. L., FOTHERBY, A. & STEPHENSON, F. A. 1993. Evidence for the involvement of a carboxyl group in the vicinity of the MK801 and magnesium ion binding site of the N-methyl-D-aspartate receptor. *Biochemical Pharmacology,* 45**,** 605-10.

CHEN, F., ECKMAN, E. A. & ECKMAN, C. B. 2006. Reductions in levels of the Alzheimer's amyloid beta peptide after oral administration of ginsenosides. *FASEB Journal,* 20**,** 1269-71.

CHEN, L., WEI, Y., WANG, X. & HE, R. 2009. D-Ribosylated Tau forms globular aggregates with high cytotoxicity. *Cellular* and *Molecular Life Sciences,* 66**,** 2559-71.

CHEN, L., WEI, Y., WANG, X. & HE, R. 2010. Ribosylation rapidly induces alpha-synuclein to form highly cytotoxic molten globules of advanced glycation end products. *PLoS One,* 5**,** e9052.

CHEUNG, J., RUDOLPH, M. J., BURSHTEYN, F., CASSIDY, M. S., GARY, E. N., LOVE, J., FRANKLIN, M. C. & HEIGHT, J. J. 2012. Structures of human acetylcholinesterase in complex with pharmacologically important ligands. *Journal of Medicinal Chemistry,* 55**,** 10282-10286.

CHIES, C., BRANCO, C., SCOLA, G., AGOSTINI, F., GOWER, A. & SALVADOR, M. 2013. Antioxidant Effect of Lippia alba (Miller) N. E. Brown. *Antioxidants,* 2**,** 194-205.

CORSI, M., FINA, P. & TRIST, D. G. 1996. Co-agonism in drug-receptor interaction: illustrated by the NMDA receptors. Trends *in Pharmacological Sciences,* 17**,** 220-2.

COSTA, P., GONÇALVES, S., GROSSO, C., ANDRADE, P. B., VALENTÃO, P., BERNARDO-GIL, M. G. & ROMANO, A. 2012. Chemical profiling and biological screening of Thymus lotocephalus extracts obtained by supercritical fluid extraction and hydrodistillation. *Industrial Crops and Products,* 36**,** 246-256.

COUNTS, S. E., NADEEM, M., WUU, J., GINSBERG, S. D., SARAGOVI, H. U. & MUFSON, E. J. 2004. Reduction of cortical TrkA but not p75(NTR) protein in early-stage Alzheimer's disease. *Annals of Neurology,* 56**,** 520-31.

CRABAS, N., MARONGIU, B., PIRAS, A., PIVETTA, T. & PORCEDDA, S. 2003. Extraction, separation and isolation of volatiles and dyes from Calendula officinalis L. and Aloysia triphylla (L'Her.) Britton by supercritical CO2. *Journal of Essential Oil Research,* 15**,** 272-277.

CRAFT, J. M., WATTERSON, D. M. & VAN ELDIK, L. J. 2005. Neuroinflammation: a potential therapeutic target. *Expert Opinion on Therapeutic Targets,* 9, 887-900.

CREWS, L., TSIGELNY, I., HASHIMOTO, M. & MASLIAH, E. 2009. Role of synucleins in Alzheimer's disease. *Neurotoxicity Research,* 16**,** 306-17.

CUI, K., LUO, X., XU, K. & VEN MURTHY, M. R. 2004. Role of oxidative stress in neurodegeneration: recent developments in assay methods for oxidative stress and nutraceutical antioxidants. *Progress in Neuro-Psychopharmacology & Biological Psychiatry,* 28**,** 771-99.

CUNY, G. D. 2012. Foreword: neurodegenerative diseases: challenges and opportunities. *Future Medicinal Chemistry,* 4**,** 1647-9.

DA SILVA, N. A., DA SILVA, J., ANDRADE, E., CARREIRA, L., SOUSA, P. & MAIA, J. 2009. Essential oil composition and antioxidant capacity of Lippia schomburgkiana. *Natural product communications,* 4**,** 1281.

DAFERERA, D. J., ZIOGAS, B. N. & POLISSIOU, M. G. 2000. GC-MS analysis of essential oils from some Greek aromatic plants and their fungitoxicity on Penicillium digitatum. *Journal of Agricultural and Food Chemistry,* 48**,** 2576-2581.

DAWIDOWICZ, A. L. & DYBOWSKI, M. P. 2010. SPE isolation of low-molecular oxygen compounds from essential oils. *Journal of separation science,* 33**,** 3213-3220.

DEAN, J. R. 1998. *Extraction methods for environmental analysis*, John Wiley Chichester.

DEAN, J. R. 2010. *Extraction techniques in analytical sciences*, Wiley. com.

DEARMOND, S. J. & PRUSINER, S. B. 2003. Perspectives on prion biology, prion disease pathogenesis, and pharmacologic approaches to treatment. *Clinics in laboratory medicine,* 23**,** 1-41.

DECKER, M. W., MAJCHRZAK, M. J. & ARNERIC, S. P. 1993. Effects of lobeline, a nicotinic receptor agonist, on learning and memory. *Pharmacol Biochem Behav,* 45**,** 571-6.

DEKOSKY, S. T., WILLIAMSON, J. D., FITZPATRICK, A. L., KRONMAL, R. A., IVES, D. G., SAXTON, J. A., LOPEZ, O. L., BURKE, G., CARLSON, M. C. & FRIED, L. P. 2008. Ginkgo biloba for prevention of dementia. *JAMA: the journal of the American Medical Association,* 300**,** 2253-2262.

DELLACASSA, E. & BANDONI, A. L. 2003. Aloysia citriodora P alau. *Revista de Fitoterapia,* 3**,** 19-25.

DENG, W., AIMONE, J. B. & GAGE, F. H. 2010. New neurons and new memories: how does adult hippocampal neurogenesis affect learning and memory? *Nature Reviews Neuroscience,* 11**,** 339-350.

DHEEN, S. T., KAUR, C. & LING, E. A. 2007. Microglial activation and its implications in the brain diseases. *Current Medicinal Chemistry,* 14**,** 1189-97.

DONG, X.-X., WANG, Y. & QIN, Z.-H. 2009. Molecular mechanisms of excitotoxicity and their relevance to pathogenesis of neurodegenerative diseases. *Acta Pharmacologica Sinica,* 30**,** 379-387.

DU, D.-M. & CARLIER, P. R. 2004. Development of bivalent acetylcholinesterase inhibitors as potential therapeutic drugs for Alzheimer's disease. *Current pharmaceutical design,* 10**,** 3141-3156.

DUSCHARZKY, C., POSSETTO, M. L., TALARICO, L. B., GARCÍA, C. C., MICHIS, F., ALMEIDA, N. V., LAMPASONA, M. D., SCHUFF, C. & DAMONTE, E. B. 2005. Short communication-Evaluation of chemical and antiviral properties of essential oils from South American plants. *Antiviral Chemistry and Chemotherapy-Institutional Subscription,* 16**,** 247-252.

DWYER, B. E., TAKEDA, A., ZHU, X., PERRY, G. & SMITH, M. A. 2005. Ferric cycle activity and Alzheimer disease. *Curr Neurovasc Res,* 2**,** 261-7.

EDRIS, A. E. 2007. Pharmaceutical and therapeutic potentials of essential oils and their individual volatile constituents: a review. *Phytotherapy Research,* 21**,** 308-323.

ELLIOTT, M., ABUHAMDAH, S., HOWES, M., LEES, G., BALLARD, C. & HOLMES, C. 2007. The essential oils from Melissa officinalis L. and Lavandula angustifolia Mill. as potential treatment for agitation in people with severe dementia. *The International Journal of Essential Oil Therapeutics,* 1**,** 143-52.

ELLMAN, G. L., COURTNEY, K. D., ANDRES JR, V. & FEATHERSTONE, R. M. 1961. A new and rapid colorimetric determination of acetylcholinesterase activity. *Biochemical Pharmacology,* 7**,** 88-95.

EMERIT, J., EDEAS, M. & BRICAIRE, F. 2004. Neurodegenerative diseases and oxidative stress. *Biomedicine* & *Pharmacotherapy,* 58**,** 39-46.

ENNA, S. J. 1978. The GABA Receptor Assay: Focus on Human Studies. *In:* FONNUM, F. (ed.) *Amino Acids as Chemical Transmitters.* Springer US.

FACHERIS, M., BERETTA, S. & FERRARESE, C. 2004. Peripheral markers of oxidative stress and excitotoxicity in neurodegenerative disorders: tools for diagnosis and therapy? *Journal of Alzheimers Disease,* 6**,** 177-84.

FAROOQUI, A. A. 2010. Neurochemical Aspects of Neurodegenerative Diseases. *Neurochemical Aspects of Neurotraumatic and Neurodegenerative Diseases.* Springer.

FAROOQUI, A. A. & HORROCKS, L. A. 2007. *Glycerophospholipids in the brain: phospholipases A2 in neurological disorders*, Springer.

FONNUM, F. 1984. Glutamate: A Neurotransmitter in Mammalian Brain. *Journal of Neurochemistry,* 42**,** 1-11.

FOSTER, A. C. & FAGG, G. E. 1987. Neurobiology. Taking apart NMDA receptors. *Nature,* 329**,** 395.

FUJIWARA, M., YAGI, N. & MIYAZAWA, M. 2010. Acetylcholinesterase Inhibitory Activity of Volatile Oil from Peltophorum dasyrachis Kurz ex Bakar (Yellow Batai) and Bisabolane-Type Sesquiterpenoids. *Journal of Agricultural and Food Chemistry,* 58**,** 2824-2829.

GEDDES, J. W. 2005. α-Synuclein: a potent inducer of tau pathology. *Experimental neurology,* 192**,** 244-250.

GHIANI, C. A., TULIGI, G., MACIOCCO, E., SERRA, M., SANNA, E. & BIGGIO, G. 1996. Biochemical evaluations of the effects of loreclezole and propofol on the $GABA_A$ receptor in rat brain. *Biochemical Pharmacology,* 51**,** 1527-34.

GHOSAL, S., LAL, J., SRIVASTAVA, R., BHATTACHARYA, S. K., UPADHYAY, S. N., JAISWAL, A. K. & CHATTOPADHYAY, U. 1989. Immunomodulatory and CNS effects of sitoindosides IX and X, two new glycowithanolides from Withania somnifera. *Phytotherapy Research,* 3**,** 201-206.

GIL, J. M. & REGO, A. C. 2008. Mechanisms of neurodegeneration in Huntington's disease. *European Journal of Neuroscience,* 27**,** 2803-2820.

GOHLKE, H., HENDLICH, M. & KLEBE, G. 2000. Knowledge-based scoring function to predict protein-ligand interactions. *Journal of molecular biology,* 295**,** 337-356.

GOHLKE, H. & KLEBE, G. 2001. Statistical potentials and scoring functions applied to protein–ligand binding. *Current opinion in structural biology,* 11**,** 231-235.

GRASSO, T. 2007. *Lippia citriodora* [Online]. Available: <http://it.wikipedia.org/wiki/File:Lippia_citriodora_0023.JPG> [Accessed 20/12 2013].

GREENBLATT, H., KRYGER, G., LEWIS, T., SILMAN, I. & SUSSMAN, J. 1999. Structure of acetylcholinesterase complexed with (−)-galanthamine at 2.3 Å resolution. *FEBS Letters,* 463**,** 321-326.

GUPTA, S., FALLARERO, A., JÄRVINEN, P., KARLSSON, D., JOHNSON, M. S., VUORELA, P. M. & MOHAN, C. G. 2011. Discovery of dual binding site acetylcholinesterase inhibitors identified by pharmacophore modeling and sequential virtual screening techniques. *Bioorganic & medicinal chemistry letters,* 21**,** 1105-1112.

HAASS, C. & SELKOE, D. J. 2007. Soluble protein oligomers in neurodegeneration: lessons from the Alzheimer's amyloid β-peptide. *Nature reviews Molecular cell biology,* 8**,** 101-112.

HAGEN, T. M. 2003. Oxidative stress, redox imbalance, and the aging process. *Antioxidants* & *Redox Signaling,* 5**,** 503-6.

HANSCH, C. & DEUTSCH, E. W. 1966. The use of substituent constants in the study of structure-activity relationships in cholinesterase inhibitors. *Biochimica et Biophysica Acta (BBA)-Biophysics including Photosynthesis,* 126**,** 117-128.

HARDIMAN, O. & DOHERTY, C. P. 2011. *Neurodegenerative Disorders: A Clinical Guide*, Springer.

HAREL, M., QUINN, D. M., NAIR, H. K., SILMAN, I. & SUSSMAN, J. L. 1996. The X-ray structure of a transition state analog complex reveals the molecular origins of the catalytic power and substrate specificity of acetylcholinesterase. *Journal of the American Chemical Society,* 118**,** 2340-2346.

HARTLEY, D. M., ZHAO, C., SPEIER, A. C., WOODARD, G. A., LI, S., LI, Z. & WALZ, T. 2008. Transglutaminase induces protofibril-like amyloid beta-protein assemblies that are protease-resistant and inhibit long-term potentiation. *Journal of Biological Chemistry,* 283**,** 16790-800.

HASHIMOTO, M., ROCKENSTEIN, E., CREWS, L. & MASLIAH, E. 2003. Role of protein aggregation in mitochondrial dysfunction and neurodegeneration in Alzheimer's and Parkinson's diseases. *NeuroMolecular Medicine,* 4**,** 21-36.

HATFIELD, T., SPANIS, C. & MCGAUGH, J. L. 1999. Response of amygdalar norepinephrine to footshock and GABAergic drugs using in vivo microdialysis and HPLC. *Brain Res,* 835**,** 340-5.

HELLSTROM-LINDAHL, E., COURT, J., KEVERNE, J., SVEDBERG, M., LEE, M., MARUTLE, A., THOMAS, A., PERRY, E., BEDNAR, I. & NORDBERG, A. 2004. Nicotine reduces A beta in the brain and cerebral vessels of APPsw mice. *European Journal* of *Neuroscience,* 19**,** 2703-10.

HEO, J. H., LEE, S. T., CHU, K., OH, M. J., PARK, H. J., SHIM, J. Y. & KIM, M. 2008. An open-label trial of Korean red ginseng as an adjuvant treatment for cognitive impairment in patients with Alzheimer's disease. *Eur J Neurol,* 15**,** 865-8.

HEO, J. H., LEE, S. T., OH, M. J., PARK, H. J., SHIM, J. Y., CHU, K. & KIM, M. 2011. Improvement of cognitive deficit in Alzheimer's disease patients by long term treatment with korean red ginseng. *Journal of Ginseng Research,* 35**,** 457-61.

HERL, L., THOMAS, A. V., LILL, C. M., BANKS, M., DENG, A., JONES, P. B., SPOELGEN, R., HYMAN, B. T. & BEREZOVSKA, O. 2009. Mutations in amyloid precursor protein affect its interactions with presenilin/γ-secretase. *Molecular and Cellular Neuroscience,* 41**,** 166-174.

HO, Y. S., SO, K. F. & CHANG, R. C. 2010. Anti-aging herbal medicine--how and why can they be used in aging-associated neurodegenerative diseases? *Ageing Res Rev,* 9**,** 354-62.

HOLLMANN, M. & HEINEMANN, S. 1994. Cloned glutamate receptors. *Annual Review of Neuroscience,* 17**,** 31-108.

HOUGHTON, P., HOWES, M.-J., LEE, C. & STEVENTON, G. 2007. Uses and abuses of in vitro tests in ethnopharmacology: visualizing an elephant. *Journal of Ethnopharmacology,* 110**,** 391-400.

HOWES, M. J. R., PERRY, N. S. & HOUGHTON, P. J. 2003. Plants with traditional uses and activities, relevant to the management of Alzheimer's disease and other cognitive disorders. *Phytotherapy Research,* 17**,** 1-18.

HUANG, L., ABUHAMDAH, S., HOWES, M. J. R., DIXON, C. L., ELLIOT, M. S., BALLARD, C., HOLMES, C., BURNS, A., PERRY, E. K. & FRANCIS, P. T. 2008. Pharmacological profile of essential oils derived from Lavandula angustifolia and Melissa officinalis with anti-

agitation properties: focus on ligand-gated channels. *Journal of Pharmacy and Pharmacology,* 60**,** 1515-1522.

IKONOMIDOU, C., STEFOVSKA, V. & TURSKI, L. 2000. Neuronal death enhanced by N-methyl-D-aspartate antagonists. *Proceedings of the National Academy of Sciences USA,* 97**,** 12885-90.

IM, W. B., PREGENZER, J. F. & THOMSEN, D. R. 1994. Effects of GABA and various allosteric ligands on TBPS binding to cloned rat $GABA_A$ receptor subtypes. *British Journal of Pharmacology,* 112**,** 1025-30.

INESTROSA, N. C., DINAMARCA, M. C. & ALVAREZ, A. 2008. Amyloid–cholinesterase interactions. *FEBS Journal,* 275**,** 625-632.

JAIN, K. K. 2011. *The handbook of neuroprotection*, Springer.

JELLINGER, K. A. 2009. Recent advances in our understanding of neurodegeneration. *Journal of neural transmission,* 116**,** 1111-1162.

JENNER, P. 2003. Oxidative stress in Parkinson's disease. *Annals of Neurology,* 53 Suppl 3**,** S26-36; discussion S36-8.

JONES, G., WILLETT, P., GLEN, R. C., LEACH, A. R. & TAYLOR, R. 1997. Development and validation of a genetic algorithm for flexible docking. *Journal of molecular biology,* 267**,** 727-748.

JONNALA, R. R., TERRY, A. V., JR. & BUCCAFUSCO, J. J. 2002. Nicotine increases the expression of high affinity nerve growth factor receptors in both in vitro and in vivo. *Life Sciences ,* 70**,** 1543-54.

JURANEK, I. & BEZEK, S. 2005. Controversy of free radical hypothesis: reactive oxygen species–cause or consequence of tissue injury. *General Physiology and Biophysics,* 24**,** 263-78.

KABASHI, E., VALDMANIS, P. N., DION, P. & ROULEAU, G. A. 2007. Oxidized/misfolded superoxide dismutase-1: the cause of all amyotrophic lateral sclerosis? *Annals of Neurology,* 62**,** 553-9.

KAISER, R. & LAMPARSKY, D. 1976. Natural occurrence of photocitrals and some of their derivatives (Constituents of verbena oil, 1st communication). *Helvetica Chimica Acta,* 59**,** 1797-1802.

KAWAMATA, J., SUZUKI, S. & SHIMOHAMA, S. 2011. Enhancement of nicotinic receptors alleviates cytotoxicity in neurological disease models. *Therapeutic Advances in Chronic Disease,* 2**,** 197-208.

KENNEDY, D., WAKE, G., SAVELEV, S., TILDESLEY, N., PERRY, E. K., WESNES, K. A. & SCHOLEY, A. B. 2003a. Modulation of mood and cognitive performance following acute administration of single doses of Melissa officinalis (Lemon balm) with human CNS nicotinic and muscarinic receptor-binding properties. *Neuropsychopharmacology,* 28**,** 1871-1881.

KENNEDY, D. O., DODD, F. L., ROBERTSON, B. C., OKELLO, E. J., REAY, J. L., SCHOLEY, A. B. & HASKELL, C. F. 2011. Monoterpenoid extract of sage (Salvia lavandulaefolia) with cholinesterase inhibiting properties improves cognitive performance and mood in healthy adults. *Journal of Psychopharmacology,* 25**,** 1088-1100.

KENNEDY, D. O., LITTLE, W. & SCHOLEY, A. B. 2004. Attenuation of laboratory-induced stress in humans after acute administration of Melissa officinalis (Lemon Balm). *Psychosomatic medicine,* 66**,** 607-613.

KENNEDY, D. O., PACE, S., HASKELL, C., OKELLO, E. J., MILNE, A. & SCHOLEY, A. B. 2005. Effects of cholinesterase inhibiting sage (Salvia officinalis) on mood, anxiety and performance on a psychological stressor battery. *Neuropsychopharmacology,* 31**,** 845-852.

KENNEDY, D. O., WAKE, G., SAVELEV, S., TILDESLEY, N. T., PERRY, E. K., WESNES, K. A. & SCHOLEY, A. B. 2003b. Modulation of mood and cognitive performance following acute administration of single doses of Melissa officinalis (Lemon balm) with human

CNS nicotinic and muscarinic receptor-binding properties. *Neuropsychopharmacology,* 28**,** 1871-81.

KENNEDY, D. O. & WIGHTMAN, E. L. 2011. Herbal extracts and phytochemicals: plant secondary metabolites and the enhancement of human brain function. *Advances in Nutrition: An International Review Journal,* 2**,** 32-50.

KIM, D. S., KIM, J. Y. & HAN, Y. S. 2007. Alzheimer's disease drug discovery from herbs: neuroprotectivity from beta-amyloid (1-42) insult. *Journal of Alternative and Complementary Medicine,* 13**,** 333-40.

KIM, D. S., PARK, S. Y. & KIM, J. K. 2001. Curcuminoids from Curcuma longa L. (Zingiberaceae) that protect PC12 rat pheochromocytoma and normal human umbilical vein endothelial cells from betaA(1-42) insult. *Neuroscience Letters,* 303**,** 57-61.

KIM, H., PARK, B. S., LEE, K. G., CHOI, C. Y., JANG, S. S., KIM, Y. H. & LEE, S. E. 2005. Effects of naturally occurring compounds on fibril formation and oxidative stress of beta-amyloid. *Journal of Agricultural and Food Chemistry,* 53**,** 8537-41.

KIM, N. S. & LEE, D. S. 2004. Headspace solid-phase microextraction for characterization of fragrances of lemon verbena (Aloysia triphylla) by gas chromatography-mass spectrometry. *Journal of separation science,* 27**,** 96-100.

KLEIJNEN, J. & KNIPSCHILD, P. 1992. Ginkgo biloba. *The Lancet,* 340**,** 1136-1139.

KLEPPNER, S. R. & TOBIN, A. J. 2001. GABA signalling: therapeutic targets for epilepsy, Parkinson's disease and Huntington's disease. *Expert Opinion* on *Therapeutic Targets ,* 5**,** 219-39.

KONG, Q., CHANG, L.-C., TAKAHASHI, K., LIU, Q., SCHULTE, D. A., LAI, L., IBABAO, B., LIN, Y., STOUFFER, N. & MUKHOPADHYAY, C. D. 2014. Small-molecule activator of glutamate transporter EAAT2 translation provides neuroprotection. *The Journal of clinical investigation,* 124**,** 1255-1267.

KRYGER, G., SILMAN, I. & SUSSMAN, J. L. 1999. Structure of acetylcholinesterase complexed with E2020 (Aricep): implications for the design of new anti-Alzheimer drugs. *Structure,* 7**,** 297-307.

KUTZING, M. K., LUO, V. & FIRESTEIN, B. L. 2012. Protection from glutamate-induced excitotoxicity by memantine. *Annals of biomedical engineering,* 40**,** 1170-1181.

LAI, S.-W., YU, M.-S., YUEN, W.-H. & CHANG, R. C.-C. 2006. Novel neuroprotective effects of the aqueous extracts from Verbena officinalis. *Neuropharmacology,* 50**,** 641-650.

LAMAISON, J., PETITJEAN FREYTET, C. & CARNAT, A. 1993. Le verbascoside, compose phenolique majeur des feuilles de frene (Fraxinus excelsior) et de verveine (Aloysia triphylla). *Plantes médicinales et phytothérapie,* 26.

LAWRENCE, B. M. 1997. Progress in essential oils. *Perfumer & flavorist,* 22.

LE BOURG, E. 2001. Oxidative stress, aging and longevity in Drosophila melanogaster. *FEBS Lett,* 498**,** 183-6.

LEWIS, W. G., GREEN, L. G., GRYNSZPAN, F., RADIĆ, Z., CARLIER, P. R., TAYLOR, P., FINN, M. & SHARPLESS, K. B. 2002. Click chemistry in situ: acetylcholinesterase as a reaction vessel for the selective assembly of a femtomolar inhibitor from an array of building blocks. *Angewandte Chemie,* 114**,** 1095-1099.

LI, N., LIU, B., DLUZEN, D. E. & JIN, Y. 2007. Protective effects of ginsenoside Rg2 against glutamate-induced neurotoxicity in PC12 cells. *Ethnopharmacology,* 111**,** 458-63.

LIMPERT, A. S. & COSFORD, N. D. 2013. Translational enhancers of EAAT2: therapeutic implications for neurodegenerative disease. *Proc Natl Acad Sci USA,* 110**,** 9415-9420.

LIPTON, S. A. 2006. Paradigm shift in neuroprotection by NMDA receptor blockade: Memantine and beyond. *Nature Review Drug Discovery,* 5**,** 160-170.

LIPTON, S. A., GU, Z. & NAKAMURA, T. 2007. Inflammatory mediators leading to protein misfolding and uncompetitive/fast off-rate drug therapy for neurodegenerative disorders. *International Review of Neurobiology,* 82**,** 1-27.

LLOYD, K., DEMONTIS, G., BROEKKAMP, C., THURET, F. & WORMS, P. 1982. Neurochemical and neuropharmacological indications for the involvement of GABA and glycine receptors in neuropsychiatric disorders. *Advances in biochemical psychopharmacology,* 37**,** 137-148.

LOIZZO, M. R., MENICHINI, F., CONFORTI, F., TUNDIS, R., BONESI, M., SAAB, A. M., STATTI, G. A., CINDIO, B. D., HOUGHTON, P. J., MENICHINI, F. & FREGA, N. G. 2009. Chemical analysis, antioxidant, antiinflammatory and anticholinesterase activities of Origanum ehrenbergii Boiss and Origanum syriacum L. essential oils. *Food Chemistry,* 117**,** 174-180.

LOPEZ, A. A., ROJAS, H. N. & JIMENEZ, M. C. 1979. Plant extracts with cytostatic properties growing in Cuba. I]. *Revista cubana de medicina tropical,* 31**,** 97.

LÓPEZ, V., MARTÍN, S., GÓMEZ-SERRANILLOS, M. P., CARRETERO, M. E., JÄGER, A. K. & CALVO, M. I. 2010. Neuroprotective and neurochemical properties of mint extracts. *Phytotherapy Research,* 24**,** 869-874.

LOWRY, O. H., ROSEBROUGH, N. J., FARR, A. L. & RANDALL, R. J. 1951. Protein measurement with the Folin phenol reagent. *Journal of Biological Chemistry,* 193**,** 265-75.

LU, S. H., WU, J. W., LIU, H. L., ZHAO, J. H., LIU, K. T., CHUANG, C. K., LIN, H. Y., TSAI, W. B. & HO, Y. 2011. The discovery of potential acetylcholinesterase inhibitors: a combination of pharmacophore modeling, virtual screening, and molecular docking studies. *Journal* of *Biomedical Science,* 18**,** 8.

LUFT, T., PEREIRA, G. S., CAMMAROTA, M. & IZQUIERDO, I. 2004. Different time course for the memory facilitating effect of bicuculline in hippocampus, entorhinal cortex, and posterior parietal cortex of rats. *Neurobiology of Learning and Memory,* 82**,** 52-6.

LUO, Q., CAI, Y., YAN, J., SUN, M. & CORKE, H. 2004. Hypoglycemic and hypolipidemic effects and antioxidant activity of fruit extracts from Lycium barbarum. *Life Sci,* 76**,** 137-49.

MAELICKE, A. & ALBUQUERQUE, E. X. 2000. Allosteric modulation of nicotinic acetylcholine receptors as a treatment strategy for Alzheimer's disease. *European* Journal of *Pharmacology,* 393**,** 165-70.

MAHADIK, P. S., SENTHILKUMAR, G., POWAR, A. S., DEVPRAKASH, D., MANI, T. T. & GAVALI, S. A. 2012. Chemical and Biological Properties of Benzodiazepines-An overview. *Research Journal of Pharmacy and Technology,* 5**,** 181-189.

MAHITA, M., ABUHAMDAH, R., HOWES, M.-J., ENNACEUR, A., ABUHAMDAH, S. & CHAZOT, P. 2014. Identification of a Novel GABA A Receptor Channel Ligand Derived from Melissa officinalis and Lavandula angustifolia Essential Oils. *European Journal of Medicinal Plants,* 4.

MAKKAR, S. R., ZHANG, S. Q. & CRANNEY, J. 2010. Behavioral and neural analysis of GABA in the acquisition, consolidation, reconsolidation, and extinction of fear memory. *Neuropsychopharmacology,* 35**,** 1625-1652.

MAMAH, C. E., LESNICK, T. G., LINCOLN, S. J., STRAIN, K. J., DE ANDRADE, M., BOWER, J. H., AHLSKOG, J. E., ROCCA, W. A., FARRER, M. J. & MARAGANORE, D. M. 2005. Interaction of α-synuclein and tau genotypes in Parkinson's disease. *Annals of neurology,* 57**,** 439-443.

MAN, S. C., CHAN, K. W., LU, J. H., DURAIRAJAN, S. S., LIU, L. F. & LI, M. 2012. Systematic review on the efficacy and safety of herbal medicines for vascular dementia. *Evidence-Based Complementary and Alternative Medicine,* 2012**,** 426215.

MARASCHIN, M. 2013. Phytochemical profile, toxicity and antioxidant activity of Aloysia gratissima (Verbenaceae). *Quim. Nova,* 36**,** 69-73.

MARIANI, E., POLIDORI, M., CHERUBINI, A. & MECOCCI, P. 2005a. Oxidative stress in brain aging, neurodegenerative and vascular diseases: an overview. *Journal of Chromatography B,* 827**,** 65-75.

MARIANI, E., POLIDORI, M. C., CHERUBINI, A. & MECOCCI, P. 2005b. Oxidative stress in brain aging, neurodegenerative and vascular diseases: an overview. *Chromatography B Analytical Technologies in Biomedical Life Sciences,* 827**,** 65-75.

MARÍN, O. 2012. Interneuron dysfunction in psychiatric disorders. *Nature Reviews Neuroscience,* 13**,** 107-120.

MARUZZELLA, J. C. & LIGUORI, L. 1958. The in vitro antifungal activity of essential oils. *Journal of the American Pharmaceutical Association,* 47**,** 250-254.

MARUZZELLA, J. C. & SICURELLA, N. A. 1960. Antibacterial activity of essential oil vapors. *Journal of the American Pharmaceutical Association,* 49**,** 692-694.

MASSOTTI, M., SCHLICHTING, J. L., ANTONACCI, M. D., GIUSTI, P., MEMO, M., COSTA, E. & GUIDOTTI, A. 1991. gamma-Aminobutyric acidA receptor heterogeneity in rat central nervous system: studies with clonazepam and other benzodiazepine ligands. *Journal of Pharmacology and Experimental Therapeutics,* 256**,** 1154-60.

MAYNARD, C. J., BUSH, A. I., MASTERS, C. L., CAPPAI, R. & LI, Q. X. 2005. Metals and amyloid-β in Alzheimer's disease. *International journal of experimental pathology,* 86**,** 147-159.

MCLAURIN, J., YANG, D.-S., YIP, C. & FRASER, P. 2000. Review: modulating factors in amyloid-β fibril formation. *Journal of structural biology,* 130**,** 259-270.

MIGLIORE, L., FONTANA, I., COLOGNATO, R., COPPEDE, F., SICILIANO, G. & MURRI, L. 2005. Searching for the role and the most suitable biomarkers of oxidative stress in Alzheimer's disease and in other neurodegenerative diseases. *Neurobiology of Aging,* 26**,** 587-95.

MISRA, R. 1998. Modern drug development from traditional medicinal plants using radioligand receptor-binding assays. *Medicinal Research Reviews,* 18**,** 383-402.

MIYAZAWA, M., WATANABE, H. & KAMEOKA, H. 1997. Inhibition of acetylcholinesterase activity by monoterpenoids with ap-menthane skeleton. *Journal of agricultural and food chemistry,* 45**,** 677-679.

MONDELLO, L., LEWIS, A. C., BARTLE, K. D. & WILEY, J. 2002. *Multidimensional chromatography*, Wiley Chichester.

MONTES, M., VALENZUELA, L., WILKOMIRSKY, T. & ARRIVE, M. 1973. SUR LA COMPOSITION DE L'ESSENCE D'ALOYSIA TRIPHYLLA („CEDRON"). *Planta medica,* 23**,** 119-124.

MORTON, J. F. 1981. *Atlas of medicinal plants of Middle America: Bahamas to Yucatan*, Charles C. Thomas.

MOSS, M., COOK, J., WESNES, K. & DUCKETT, P. 2003. Aromas of rosemary and lavender essential oils differentially affect cognition and mood in healthy adults. *International Journal of Neuroscience,* 113**,** 15-38.

MUNOZ-MURIEDAS, J., LOPEZ, J., OROZCO, M. & LUQUE, F. J. 2004. Molecular modelling approaches to the design of acetylcholinesterase inhibitors: new challenges for the treatment of Alzheimer's disease. *Current pharmaceutical design,* 10**,** 3131-3140.

NAKAMURA, T., OKUYAMA, E., TSUKADA, A., YAMAZAKI, M., SATAKE, M., NISHIBE, S., DEYAMA, T., MORIYA, A., MARUNO, M. & NISHIMURA, H. 1997. Acteoside as the analgesic principle of Cedron (Lippia triphylla), a Peruvian medicinal plant. *Chemical and pharmaceutical bulletin,* 45**,** 499-504.

NELSON, R. J. & TRAINOR, B. C. 2007. Neural mechanisms of aggression. *Nature Reviews Neuroscience,* 8**,** 536-546.

NEWMAN, D. J., CRAGG, G. M. & SNADER, K. M. 2003. Natural products as sources of new drugs over the period 1981-2002. *J Nat Prod,* 66**,** 1022-37.

ODDO, S., CACCAMO, A., GREEN, K. N., LIANG, K., TRAN, L., CHEN, Y., LESLIE, F. M. & LAFERLA, F. M. 2005. Chronic nicotine administration exacerbates tau pathology in a transgenic model of Alzheimer's disease. *Proceedings of the National Academy of Sciences USA,* 102**,** 3046-3051.

OINONEN, P. P., JOKELA, J. K., HATAKKA, A. I. & VUORELA, P. M. 2006. Linarin, a selective acetylcholinesterase inhibitor from Mentha arvensis. *Fitoterapia,* 77**,** 429-34.

OKEN, B. S., STORZBACH, D. M. & KAYE, J. A. 1998. The efficacy of Ginkgo biloba on cognitive function in Alzheimer disease. *Archives of Neurology,* 55**,** 1409.

ONO, M., ODA, E., TANAKA, T., IIDA, Y., YAMASAKI, T., MASUOKA, C., IKEDA, T. & NOHARA, T. 2008. DPPH radical-scavenging effect on some constituents from the aerial parts of Lippia triphylla. *Journal of natural medicines,* 62**,** 101-106.

ÖZEK, T., KIRIMER, N., BASER, K. & TÜMEN, G. 1996. Composition of the essential oil of Aloysia triphylla (L'Herit.) Britton grown in Turkey. *Journal of Essential Oil Research,* 8**,** 581-583.

PASCUAL, M., SLOWING, K., CARRETERO, E., SÁNCHEZ MATA, D. & VILLAR, A. 2001. Lippia: traditional uses, chemistry and pharmacology: a review. *Journal of ethnopharmacology,* 76**,** 201-214.

PERRY, E. K., PICKERING, A. T., WANG, W. W., HOUGHTON, P. & PERRY, N. S. 1998. Medicinal plants and Alzheimer's disease: Integrating ethnobotanical and contemporary scientific evidence. *The Journal of Alternative and Complementary Medicine,* 4**,** 419-428.

PERRY, E. K., PICKERING, A. T., WANG, W. W., HOUGHTON, P. J. & PERRY, N. S. 1999. Medicinal Plants and Alzheimer's Disease: from Ethnobotany to Phytotherapy**. *Journal of pharmacy and pharmacology,* 51**,** 527-534.

PERRY, N., COURT, G., BIDET, N., COURT, J. & PERRY, E. 1996. EUROPEAN HERBS WITH CHOLINERGIC ACTIVITIES: POTENTIAL IN DEMENTIA THERAPY. *International Journal of Geriatric Psychiatry,* 11**,** 1063-1069.

PERRY, N. & PERRY, E. 2006. Aromatherapy in the management of psychiatric disorders. *CNS drugs,* 20**,** 257-280.

PERRY, N. S., HOUGHTON, P. J., JENNER, P., KEITH, A. & PERRY, E. K. 2002. Salvia lavandulaefolia essential oil inhibits cholinesterase in vivo. *Phytomedicine,* 9**,** 48-51.

PERRY, N. S., HOUGHTON, P. J., THEOBALD, A., JENNER, P. & PERRY, E. K. 2000. In-vitro Inhibition of Human Erythrocyte Acetylcholinesterase by Salvia lavandulaefolia Essential Oil and Constituent Terpenes. *Journal of Pharmacy and Pharmacology,* 52**,** 895-902.

PIECZENIK, S. R. & NEUSTADT, J. 2007. Mitochondrial dysfunction and molecular pathways of disease. *Experimental and Molecular Pathology,* 83**,** 84-92.

POLYA, G. 2003. *Biochemical Targets of Plant Bioactive Compounds: A Pharmacological Reference Guide to Sites of Action and Biological Effects*, Taylor & Francis.

PRZEDBORSKI, S., VILA, M. & JACKSON-LEWIS, V. 2003. Series Introduction: Neurodegeneration: What is it and where are we? *The Journal of Clinical Investigation,* 111**,** 3-10.

QI, Y., WANG, J. K., MCMILLIAN, M. & CHIKARAISHI, D. M. 1997. Characterization of a CNS cell line, CAD, in which morphological differentiation is initiated by serum deprivation. *The Journal of neuroscience,* 17**,** 1217-1225.

QUIRANTES-PINÉ, R., FUNES, L., MICOL, V., SEGURA-CARRETERO, A. & FERNÁNDEZ-GUTIÉRREZ, A. 2009. High-performance liquid chromatography with diode array detection coupled to electrospray time-of-flight and ion-trap tandem mass spectrometry to identify phenolic compounds from a lemon verbena extract. *Journal of Chromatography A,* 1216**,** 5391-5397.

RAO, A. V. & BALACHANDRAN, B. 2002. Role of oxidative stress and antioxidants in neurodegenerative diseases. *Nutr Neurosci,* 5**,** 291-309.

RAVES, M. L., HAREL, M., PANG, Y.-P., SILMAN, I., KOZIKOWSKI, A. P. & SUSSMAN, J. L. 1997. Structure of acetylcholinesterase complexed with the nootropic alkaloid,(-)-huperzine A. *Nature structural biology,* 4**,** 57-63.

REICHLING, J., SCHNITZLER, P., SUSCHKE, U. & SALLER, R. 2009. Essential oils of aromatic plants with antibacterial, antifungal, antiviral, and cytotoxic properties–an overview. *Forschende Komplementärmedizin/Research in Complementary Medicine,* 16**,** 79-90.

REZAI, N., DUGGAN, C., CAIRNS, D., LEES, G. & CHAZOT, P. L. 2003. Modulation of [3H] TBOB binding to the rodent GABAA receptor by simple disaccharides. *Biochem Pharmacol,* 65**,** 619-23.

RICHTER, L., DE GRAAF, C., SIEGHART, W., VARAGIC, Z., MÖRZINGER, M., DE ESCH, I. J. P., ECKER, G. F. & ERNST, M. 2012. Diazepam-bound GABAA receptor models identify new benzodiazepine binding-site ligands. *Nature Chemical Biology,* 8**,** 455-464.

ROBERT CRICHTON, R. W. 2013. Alzheimer's Disease. *Metal-based Neurodegeneration.* John Wiley and Sons Ltd.

RUBIO, A., PEREZ, M. & AVILA, J. 2006. Acetylcholine receptors and tau phosphorylation. *Current Molecular Medicine,* 6**,** 423-8.

RYAN, M. & BYRNE, O. 1988. Plant-insect coevolution and inhibition of acetylcholinesterase. *Journal of chemical ecology,* 14**,** 1965-1975.

SALOMON, A. R., MARCINOWSKI, K. J., FRIEDLAND, R. P. & ZAGORSKI, M. G. 1996. Nicotine inhibits amyloid formation by the beta-peptide. *Biochemistry,* 35**,** 13568-78.

SANTOS-GOMES, P. C., FERNANDES-FERREIRA, M. & VICENTE, A. M. 2005. Composition of the essential oils from flowers and leaves of Vervain [Aloysia triphylla (L'Herit.) Britton] grown in Portugal. *Journal of Essential Oil Research,* 17**,** 73-78.

SARTORATTO, A., MACHADO, A. L. M., DELARMELINA, C., FIGUEIRA, G. M., DUARTE, M. C. T. & REHDER, V. L. G. 2004. Composition and antimicrobial activity of essential oils from aromatic plants used in Brazil. *Brazilian Journal of Microbiology,* 35**,** 275-280.

SAVELEV, S., OKELLO, E., PERRY, N., WILKINS, R. & PERRY, E. 2003. Synergistic and antagonistic interactions of anticholinesterase terpenoids in Salvia lavandulaefolia essential oil. *Pharmacology Biochemistry and Behavior,* 75**,** 661-668.

SAVELEV, S. U., OKELLO, E. J. & PERRY, E. K. 2004. Butyryl-and acetyl-cholinesterase inhibitory activities in essential oils of Salvia species and their constituents. *Phytotherapy Research,* 18**,** 315-324.

SAYRE, L. M., PERRY, G., HARRIS, P. L., LIU, Y., SCHUBERT, K. A. & SMITH, M. A. 2000. In situ oxidative catalysis by neurofibrillary tangles and senile plaques in Alzheimer's disease: a central role for bound transition metals. *Journal of Neurochemistry,* 74**,** 270-9.

SAYRE, L. M., SMITH, M. A. & PERRY, G. 2001. Chemistry and biochemistry of oxidative stress in neurodegenerative disease. *Current medicinal chemistry,* 8**,** 721-738.

SCHLIEBS, R., LIEBMANN, A., BHATTACHARYA, S. K., KUMAR, A., GHOSAL, S. & BIGL, V. 1997. Systemic administration of defined extracts from Withania somnifera (Indian Ginseng) and Shilajit differentially affects cholinergic but not glutamatergic and GABAergic markers in rat brain. *Neurochemistry International,* 30**,** 181-90.

SCHNEIDER, G. & BÖHM, H.-J. 2002. Virtual screening and fast automated docking methods. *Drug Discovery Today,* 7**,** 64-70.

SCHNEIDER, G., CLÉMENT-CHOMIENNE, O., HILFIGER, L., SCHNEIDER, P., KIRSCH, S., BÖHM, H. J. & NEIDHART, W. 2000. Virtual screening for bioactive molecules by evolutionary de novo design. *Angewandte Chemie International Edition,* 39**,** 4130-4133.

SCOTT, L. J. & GOA, K. L. 2000. Galantamine: a review of its use in Alzheimer's disease. *Drugs,* 60**,** 1095-122.

SESTI, F., LIU, S. & CAI, S. Q. 2010. Oxidation of potassium channels by ROS: a general mechanism of aging and neurodegeneration? *Trends Cell Biol,* 20**,** 45-51.

SHARPLES, C. G. & WONNACOTT, S. 2001. Neuronal nicotinic receptors. *Tocris reviews,* 19**,** 1-12.

SHIBATA, N. & KOBAYASHI, M. 2008. [The role for oxidative stress in neurodegenerative diseases]. *Brain Nerve,* 60**,** 157-70.

SIEDO, S. J. & BOTANY, T. U. O. T. A. A. 2007. *Systematics of Aloysia (Verbenaceae)*, The University of Texas at Austin.

SKALTSA, H. & SHAMMAS, G. 1988. Flavonoids from Lippia citriodora. *Planta medica,* 54**,** 465.

SMITH, M. A., ZHU, X., TABATON, M., LIU, G., MCKEEL, D. W., JR., COHEN, M. L., WANG, X., SIEDLAK, S. L., DWYER, B. E., HAYASHI, T., NAKAMURA, M., NUNOMURA, A. & PERRY, G. 2010. Increased iron and free radical generation in preclinical Alzheimer disease and mild cognitive impairment. Journal of *Alzheimer's Disease,* 19**,** 363-72.

SOBOLEVSKY, A. I., ROSCONI, M. P. & GOUAUX, E. 2009. X-ray structure, symmetry and mechanism of an AMPA-subtype glutamate receptor. *Nature,* 462**,** 745-756.

SOHAL, R. S. 2002. Oxidative stress hypothesis of aging. *Free Radic Biol Med,* 33**,** 573-4.

SOTRIFFER, C. & KLEBE, G. 2002. Identification and mapping of small-molecule binding sites in proteins: computational tools for structure-based drug design. *Il Farmaco,* 57**,** 243-251.

STOESSL, A. J. 2012. Neuroimaging in the early diagnosis of neurodegenerative disease. *Transl Neurodegener,* 1**,** 5.

SUNDARAM, R. & GOWTHAM, L. 2012. *Microglia and regulation of inflammation-mediated neurodegeneration: Prevention and treatment by phytochemicals and metabolic nutrients*. *International Journal of Green Pharmacy*, 6.

TANOVIC, A. & ALFARO, V. 2006. [Glutamate-related excitotoxicity neuroprotection with memantine, an uncompetitive antagonist of NMDA-glutamate receptor, in Alzheimer's disease and vascular dementia]. *Revue neurologique,* 42**,** 607-16.

TERBLANCHÉ, F. & KORNELIUS, G. 1996. Essential oil constituents of the genus Lippia (Verbenaceae)—a literature review. *Journal of essential oil research,* 8**,** 471-485.

THIES, W. & BLEILER, L. 2013. 2013 Alzheimer's disease facts and figures. *Alzheimer's & Dementia,* 9**,** 208-45.

TOMAS-BARBERAN, F. A., HARBORNE, J. B. & SELF, R. 1987. Twelve 6-oxygenated flavone sulphates from Lippia nodiflora and L. canescens. *Phytochemistry,* 26**,** 2281-2284.

TRAORE-KEITA, F., GASQUET, M., DI GIORGIO, C., OLLIVIER, E., DELMAS, F., KEITA, A., DOUMBO, O., BALANSARD, G. & TIMON-DAVID, P. 2000. Antimalarial activity of four plants used in traditional medicine in Mali. *Phytotherapy Research,* 14**,** 45-47.

TROSSET, J. Y., DALVIT, C., KNAPP, S., FASOLINI, M., VERONESI, M., MANTEGANI, S., GIANELLINI, L. M., CATANA, C., SUNDSTRÖM, M. & STOUTEN, P. F. 2006. Inhibition of protein–protein interactions: The discovery of druglike β-catenin inhibitors by combining virtual and biophysical screening. *Proteins: Structure, Function, and Bioinformatics,* 64**,** 60-67.

TUCKER, A. O., A.J. REDFORD, J. SCHER, AND M.D. TRICE. 2010. *Dried Botanical ID* [Online]. Delaware State University, Identification Technology Program. Available: <http://idtools.org/id/dried_botanical> [Accessed 20/12 2013].

VALENTÃO, P., ANDRADE, P. B., AREIAS, F., FERRERES, F. & SEABRA, R. M. 1999. Analysis of vervain flavonoids by HPLC/diode array detector method. Its application to quality control. *Journal of agricultural and food chemistry,* 47**,** 4579-4582.

VALENTÃO, P., FERNANDES, E., CARVALHO, F., ANDRADE, P. B., SEABRA, R. M. & BASTOS, M. D. L. 2002. Studies on the antioxidant activity of Lippia citriodora infusion: scavenging effect on superoxide radical, hydroxyl radical and hypochlorous acid. *Biological and Pharmaceutical Bulletin,* 25**,** 1324-1327.

VAN HOUTEN, B., WOSHNER, V. & SANTOS, J. H. 2006. Role of mitochondrial DNA in toxic responses to oxidative stress. *DNA repair,* 5**,** 145-152.

VELASCO-NEGUERUELA, A., PÉREZ-ALONSO, M. J., GUZMÁN, C. A., ZYGADLO, J. A., ARIZA-ESPINAR, L., SANZ, J. & GARCÍA-VALLEJO, M. C. 1993. Volatile constitutents of four Lippia species from Córdoba (Argentina). *Journal of Essential Oil Research,* 5**,** 513-524.

VENTRIGLIA, M., ZANARDINI, R., BONOMINI, C., ZANETTI, O., VOLPE, D., PASQUALETTI, P., GENNARELLI, M. & BOCCHIO-CHIAVETTO, L. 2013. Serum Brain-Derived Neurotrophic Factor Levels in Different Neurological Diseases. *BioMed research international,* 2013.

VICENTE MIRANDA, H. & OUTEIRO, T. F. 2010. The sour side of neurodegenerative disorders: the effects of protein glycation. *Journal of Pathology,* 221**,** 13-25.

VIOLA, H., WASOWSKI, C., DE STEIN, M. L., WOLFMAN, C., SILVEIRA, R., DAJAS, F., MEDINA, J. & PALADINI, A. 1995. Apigenin, a component of Matricaria recutita flowers, is a central benzodiazepine receptors-ligand with anxiolytic effects. *Planta medica,* 61**,** 213-216.

WAKE, G., COURT, J., PICKERING, A., LEWIS, R., WILKINS, R. & PERRY, E. 2000. CNS acetylcholine receptor activity in European medicinal plants traditionally used to improve failing memory. *Journal of Ethnopharmacol,* 69**,** 105-14.

WALTON, W. R. I. U. H. F. 1970. W. Riemann III und H. F. Walton: Ion Exchange in Analytical Chemistry. Pergamon Press, Oxford 1970. 295 Seiten. Preis: 30 s. *Berichte der Bunsengesellschaft für physikalische Chemie,* 74**,** 1292-1292.

WANG, H., BEDFORD, F. K., BRANDON, N. J., MOSS, S. J. & OLSEN, R. W. 1999. GABA(A)-receptor-associated protein links GABA(A) receptors and the cytoskeleton. *Nature,* 397**,** 69-72.

WENNING, G. K. & JELLINGER, K. A. 2005. The role of [alpha]-synuclein and tau in neurodegenerative movement disorders. *Current opinion in neurology,* 18**,** 357-362.

WHITEHOUSE, P. J. & KALARIA, R. N. 1995. Nicotinic receptors and neurodegenerative dementing diseases: basic research and clinical implications. *Alzheimer Disease and Associated Disorders,* 9 Suppl 2**,** 3-5.

WILDE, G. J., PRINGLE, A. K., WRIGHT, P. & IANNOTTI, F. 1997. Differential vulnerability of the CA1 and CA3 subfields of the hippocampus to superoxide and hydroxyl radicals in vitro. *Journal of Neurochemistry,* 69**,** 883-6.

WILHELMUS, M. M., GRUNBERG, S. C., BOL, J. G., VAN DAM, A. M., HOOZEMANS, J. J., ROZEMULLER, A. J. & DRUKARCH, B. 2009. Transglutaminases and transglutaminase-catalyzed cross-links colocalize with the pathological lesions in Alzheimer's disease brain. *Brain Pathology,* 19**,** 612-22.

WISHART, T. M., PARSON, S. H. & GILLINGWATER, T. H. 2006. Synaptic vulnerability in neurodegenerative disease. *Journal of Neuropathology and Experimental* Neurology*,* 65**,** 733-9.

WONG, A. C., SMITH, M. & BOON, H. S. 1998. HErbal remedies in psychiatric practice. *Archives of General Psychiatry,* 55**,** 1033-1044.

WU, H., GUO, H. & ZHAO, R. 2006. Effect of Lycium barbarum polysaccharide on the improvement of antioxidant ability and DNA damage in NIDDM rats. *Yakugaku Zasshi,* 126**,** 365-71.

XIAO, B., TU, J. C., PETRALIA, R. S., YUAN, J. P., DOAN, A., BREDER, C. D., RUGGIERO, A., LANAHAN, A. A., WENTHOLD, R. J. & WORLEY, P. F. 1998. Homer regulates the association of group 1 metabotropic glutamate receptors with multivalent complexes of homer-related, synaptic proteins. *Neuron,* 21**,** 707-716.

YAMAGUCHI, F., ARIGA, T., YOSHIMURA, Y. & NAKAZAWA, H. 2000. Antioxidative and Anti-Glycation Activity of Garcinol from Garcinia indica Fruit Rind. *Journal of Agricultural and Food Chemistry,* 48**,** 180-185.

YARBROUGH, G. G., TAYLOR, D. P., ROWLANDS, R. T., CRAWFORD, M. S. & LASURE, L. L. 1993. Screening microbial metabolites for new drugs--theoretical and practical issues. *J Antibiot (Tokyo),* 46**,** 535-44.

YUNG-CHI, C. & PRUSOFF, W. H. 1973. Relationship between the inhibition constant and the concentration of inhibitor which causes 50 per cent inhibition of an enzymatic reaction. *Biochemical pharmacology,* 22**,** 3099-3108.

ZAMORANO-PONCE, E., MORALES, C., RAMOS, D., SEPÚLVEDA, C., CARES, S., RIVERA, P., FERNÁNDEZ, J. & CARBALLO, M. 2006. Anti-genotoxic effect of Aloysia triphylla infusion against acrylamide-induced DNA damage as shown by the comet assay technique. *Mutation Research/Genetic Toxicology and Environmental Mutagenesis,* 603**,** 145-150.

ZANARDI, A., LEO, G., BIAGINI, G. & ZOLI, M. 2002. Nicotine and neurodegeneration in ageing. *Toxicology Letters,* 127**,** 207-15.

ZATTA, P. 2003. *Metal Ions and Neurodegenerative Disorders*, World Scientific.

ZECCA, L., YOUDIM, M. B., RIEDERER, P., CONNOR, J. R. & CRICHTON, R. R. 2004a. Iron, brain ageing and neurodegenerative disorders. *Nature Review Neuroscience,* 5**,** 863-73.

ZECCA, L., YOUDIM, M. B. H., RIEDERER, P., CONNOR, J. R. & CRICHTON, R. R. 2004b. Iron, brain ageing and neurodegenerative disorders. *Nature Review Neuroscience,* 5**,** 863-873.

ZHOU, C., HUANG, Y. & PRZEDBORSKI, S. 2008. Oxidative stress in Parkinson's disease: a mechanism of pathogenic and therapeutic significance. *Ann N Y Acad Sci,* 1147**,** 93-104.

ZLOKOVIC, B. V. 2008. The blood-brain barrier in health and chronic neurodegenerative disorders. *Neuron,* 57**,** 178-201.

ŻWIR-FERENC, A. & BIZIUK, M. 2006. Solid phase extraction technique–trends, opportunities and applications. *Polish Journal of Environmental* Studies*,* 15**,** 677-690.

ZYGADLO, J., LAMARQUE, A., MAESTRI, D., GUZMÁN, C., LUCINI, E., GROSSO, N. & ARIZA-ESPINAR, L. 1994. Volatile Constituents of Aloysia triphylla (L'Herit.) Britton. *Journal of Essential Oil Research,* 6**,** 407-409.

Appendix I

Virtual Screening for Anticholinesterase Inhibitors Training Set

no.	Structure			IC50 (mM)	pIC50
	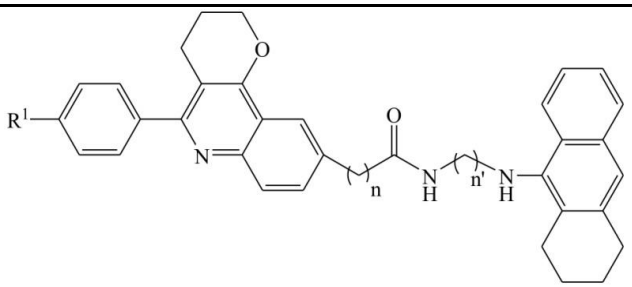				
	n	n'	R1		
1	0	10	Cl	0.05	7.30
2	2	6	H	0.0111	7.95
3	2	8	H	0.014	7.85
	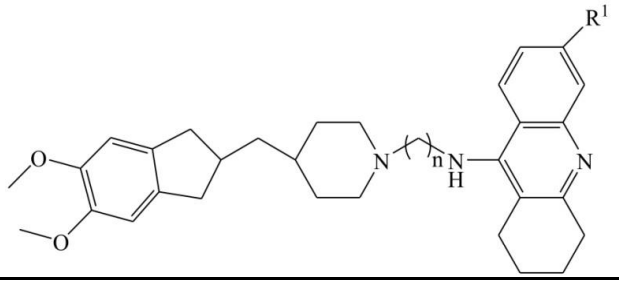				
	n		R1		
4	2		H	0.00513	9.71
5	3		H	0.00216	9.33
6	2		Cl	0.0026	9.41
7	3		Cl	0.00106	9.03
	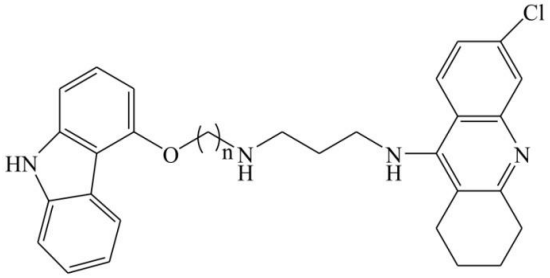				
		n			
8		4		0.00165	8.78
9		5		0.00154	8.81
10		6		0.00257	8.59
	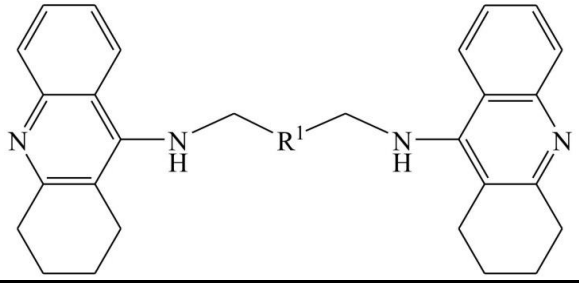				
		R1			
11				0.424	6.37

12	$(CH_2)_2CO(CH_2)_2$	0.00183	8.74

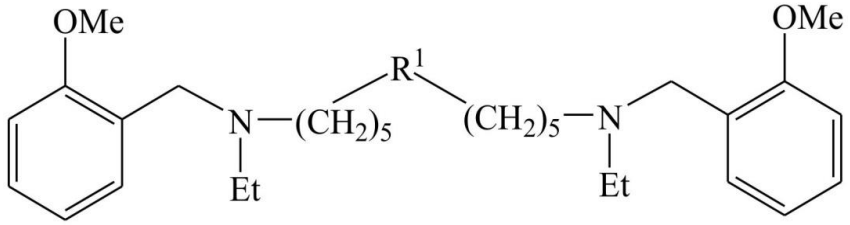

	R1		
13	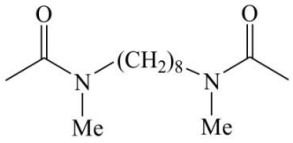	0.0161	7.79
14	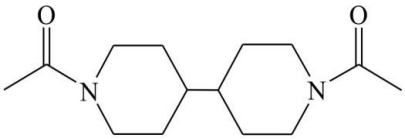	0.00332	8.48
15	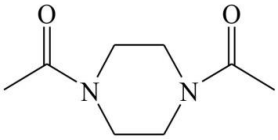	0.0257	7.59
16	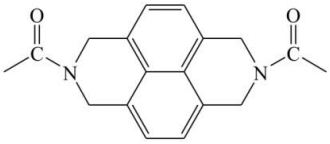	0.00483	8.32
17	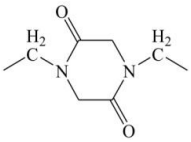	0.0159	7.80
18	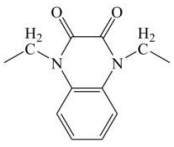	0.00141	8.85
19	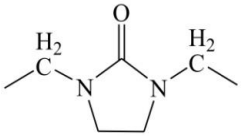	0.0724	7.14
20	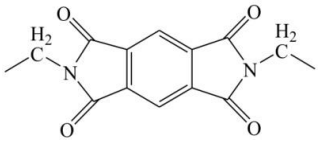	0.0077	8.11

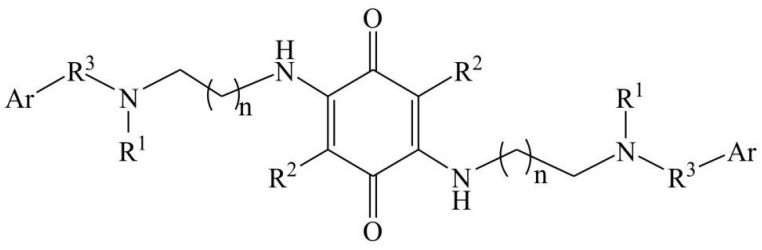

n	Ar	R1	R2	R3

21	5	2-$MeOC_6H_4$	Et	H	CH_2	0.00155	8.81
22	5	2-$MeOC_6H_4$	Et	Br	CH_2	0.00266	8.58
23	2	2-$MeOC_6H_4$	Et	H	CH_2	0.00225	8.65
24	3	2-$MeOC_6H_4$	Et	H	CH_2	0.0136	7.87
25	4	2-$MeOC_6H_4$	Et	H	CH_2	0.00236	8.63
26	5	2-$MeOC_6H_4$	Et	H	$(CH_2)_2$	0.0173	7.76
27	5	2-$MeOC_6H_4$	Me	H	CH_2	0.0778	7.11
28	5	C_6H_5	Et	H	CH_2	0.0733	7.13
29	5	4-$MeOC_6H_4$	Et	H	CH_2	0.0511	7.29
30	5	3-$MeOC_6H4$	Et	H	CH_2	0.0138	7.86
31	5	2-MeC_6H_4	Et	H	CH_2	0.0719	7.14
32	5	2-thienyl	Et	H	CH_2	0.0604	7.22
33	5	2-pyridyl	Et	H	CH_2	0.125	6.90
34	5	3-pyridyl	Et	H	CH_2	0.133	6.88
35	5	4-pyridyl	Et	H	CH_2	0.192	6.72

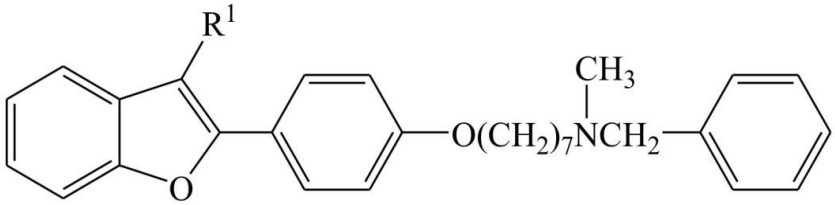

	R1		
36	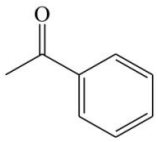	0.0407	7.39
37	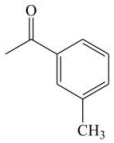	0.127	6.90
38	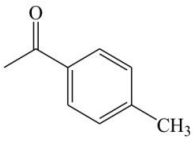	0.0105	7.98
39	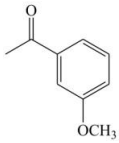	0.127	6.90
40	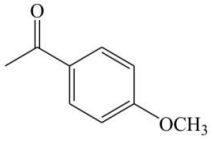	0.281	6.55

41	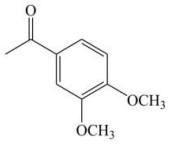	0.177	6.75

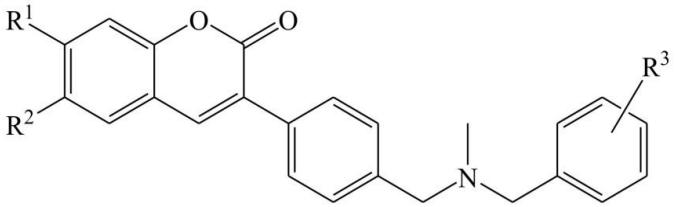

	R1	R2	R3		
42	OCH_3	OCH_3	*o* -NO_2	0.987	6.01
43	OCH_3	OCH_3	*m* -NO_2	0.368	6.43
44	OCH_3	OCH_3	*p* -NO_2	24.6	4.61
45	OCH_3	OCH_3	*o* -CH_3	0.366	6.44
46	OCH_3	OCH_3	*m* -CH_3	0.122	6.91
47	OCH_3	OCH_3	*o* -OCH_3	0.0621	7.21
48	OCH_3	OCH_3	*m* -OCH_3	0.714	6.15
49	OCH_3	OCH_3	*p* -OCH_3	2.26	5.65
50	H	NH_2	H	0.281	6.55

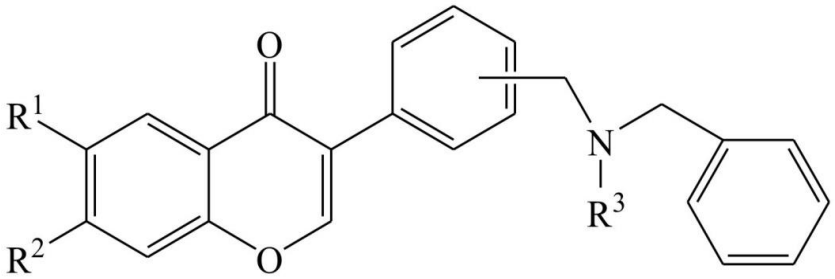

	chain	R1	R2	R3		
51	para	OCH_3	OCH_3	CH_3	1.23	5.91
52	meta	OCH_3	OCH_3	CH_3	2.02	5.69
53	meta	OCH_3	OCH_3	C_2H_5	1.59	5.80

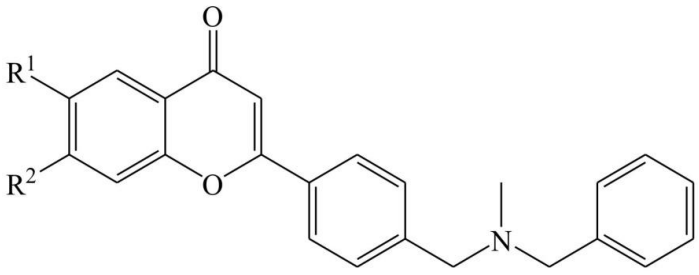

	R1	R2		
54	OCH3	H	18.1	4.74
55	H	OCH_3	80.5	4.09

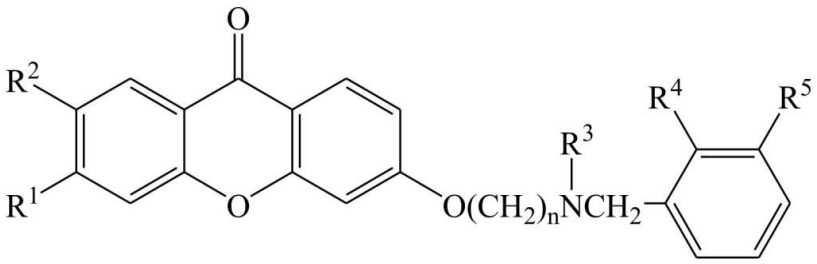

	n	R1	R2	R3	R4	R5		
56	5	H	H	Me	H	H	7.78	5.11
57	7	H	H	Me	H	H	2.82	5.55
58	8	H	H	Me	H	H	10.3	4.99
59	7	OCH_3	OCH_3	Me	H	H	2.32	5.63
60	7	H	H	Me	H	OCH_3	40	4.40
61	7	H	H	Et	OCH_3	H	3.15	5.50

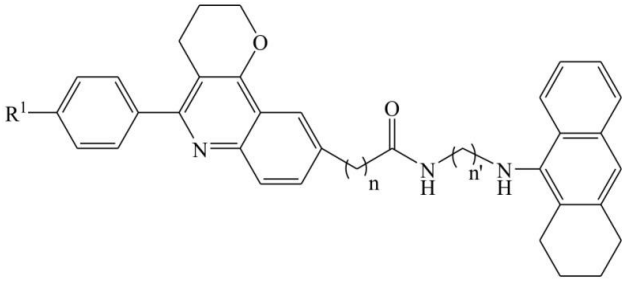

	n	n'	R1		
62	0	7	Cl	0.183	7.74

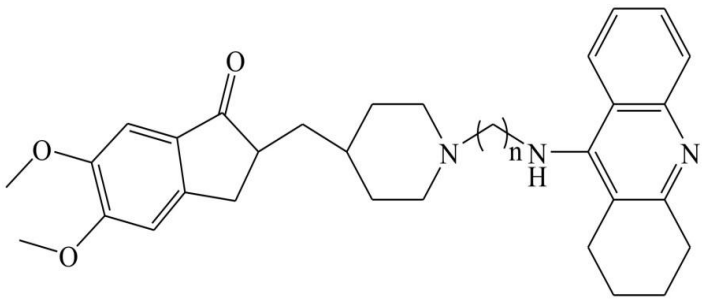

	n		
63	2	0.00404	8.39
64	3	0.00088	9.06

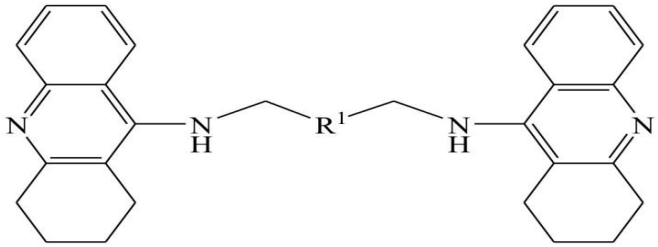

	R1		
65	$(CH_2)_5$	0.00081	9.09
66	$CH_2NHCOCONHCH_2$	0.00665	8.18

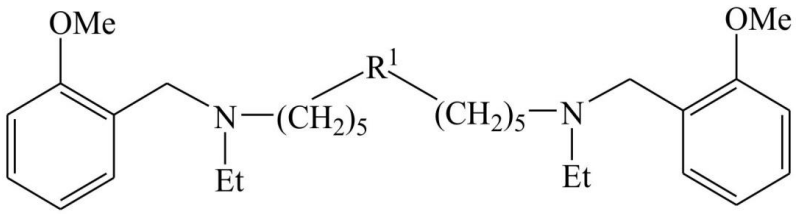

	R1		
67	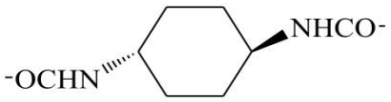	8.55	5.07
68	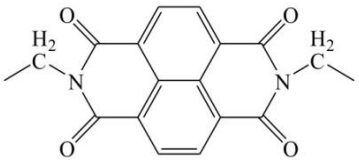	0.00037	9.43

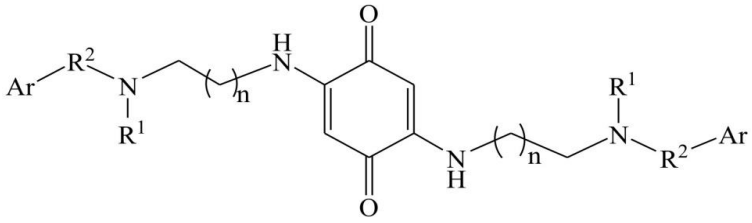

	n	Ar	R1	R2		
69	5	2-$MeOC_6H_4$	H	CH_2	0.123	6.91
70	5	2-ClC_6H4	Et	CH_2	0.593	6.23
71	5	2-$NO_2C_6H_4$	Et	CH_2	2.31	5.64

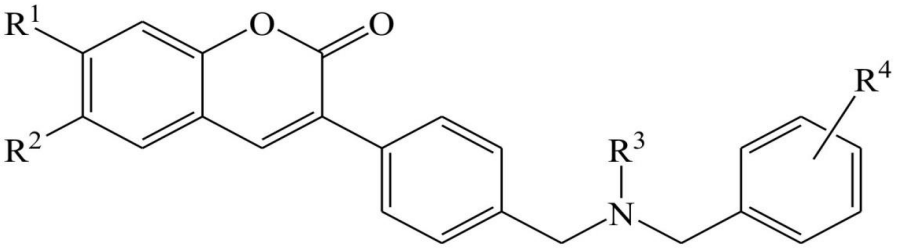

	R1	R2	R3	R4		
72	OCH_3	OCH_3	CH_3	H	0.0445	7.35
73	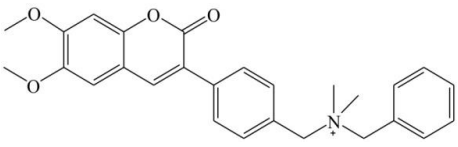				0.0105	7.98

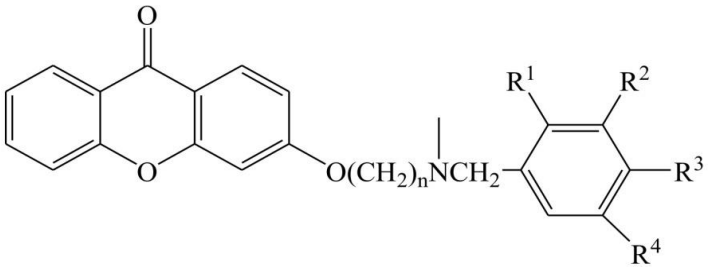

	n	R1	R2	R3	R4		
74	9	H	H	H	H	152	3.82
75	10	H	H	H	H	388	3.41
76	11	H	H	H	H	626	3.20
77	12	H	H	H	H	908	3.04
78	7	H	H	OCH_3	H	360	3.44
79	7	Cl	H	H	H	433	3.36
80	7	H	Cl	H	H	594	3.23
81	7	H	H	Cl	H	1050	2.98
82	7	CH_3	H	H	H	565	3.25
83	7	OCH_3	OCH_3	H	H	138	3.86
84	7	OCH_3	H	H	OCH_3	127	3.90
85	7	OCH_3	OCH_3	OCH_3	H	155	3.81

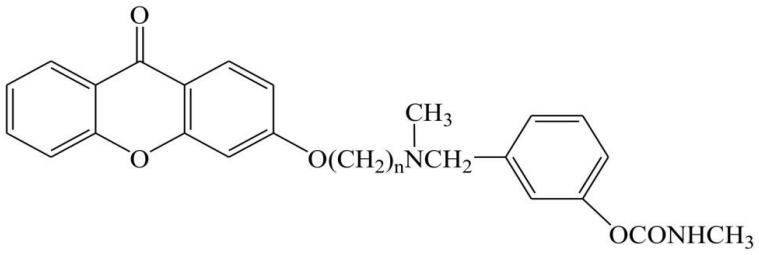

	n		
86	3	0.0003	9.52
87	7	0.00032	9.49

Appendix II

GC/MS Analysis of *Aloysia citrodora* Essential Oil

Aloysia citriodora Palau[#] Essential Oil and Fractions (V2 – V5)

GC-MS Analysis

Sample preparation

Oil (BI 21372 stored at 6°C in the dark, since Feb 2012): 1/100 dilution in diethyl ether.
Fractions analysed without dilution.

Method

GC:	Agilent 7890A
Column:	30 m x 0.25 mm i.d. x 0.25 µm DB-5MS (J. & W. Scientific)
Temp prog.:	40-300ºC @ 3ºC/min
Carrier gas:	Helium (flow: 1ml/min)
Injection temp.:	220 °C
MS:	Agilent 5975C
Source:	EI (70 eV)
Source temp.:	180 °C
Scan range:	38-600 *m/z*

[#]Synonym: *Aloysia triphylla* (L'Hér.) Britton

Table 1. Percentage composition of detected compounds (based on all detected peaks assigned as oil constituents).

Compound	**Retention time (min)**	***Aloysia* oil dried (BI 21372) Percentage composition (TIC) and [RI]***	**Fraction V2 1/3 (BI 22729) Percentage composition (TIC) and [RI]***	**Fraction V2 2/3 (BI 22730) Percentage composition (TIC) and [RI]***	**Fraction V4 1/11 (BI 22737) Percentage composition (TIC) and [RI]***	**Fraction V4 2/11 (BI 22738) Percentage composition (TIC) and [RI]***	**Fraction V4 3/11 (BI 22739) Percentage composition (TIC) and [RI]***	**RI (published)**
Salvene	7.8	0.03 [820]	Tr [820]	Nd	Nd	Tr [820]	Nd	(*Z*)-: 847 (*E*)-: 858
α-Thujene	11.7	0.07 [906]	0.11 [906]	Nd	Nd	Tr [906]	Nd	924
α-Pinene	12.0	0.44 [914]	0.82 [914]	Nd	Tr [914]	0.98 [914]	Nd	932
Camphene	12.8	Tr [931]	Tr [931]	Nd	Nd	Nd	Nd	946
Sabinene	13.8	0.92 [954]	1.52 [954]	Nd	Nd	1.68 [954]	Nd	969
β-Pinene	14.0	0.08 [959]	0.14 [959]	Nd	Nd	Nd	Nd	974
1-Octen-3-ol	14.1	0.55 [961]	Tr [961]	0.05 [961]	Nd	Nd	0.01 [961]	974
6-Methyl-5-hepten-2-one	14.4	2.37 [966]	2.42 [966]	Nd	Nd	2.40 [966]	Nd	981
Myrcene	14.6	0.20 [971]	0.32 [971]	Nd	Nd	Nd	Nd	988
α-Terpinene	15.9	0.01 [1001]	Tr [1001]	Nd	Nd	Nd	Nd	1014
Cymene	16.3	0.46 [1009]	0.49 [1009]	Nd	Nd	0.50 [1009]	Nd	*o*-: 1022 *p*-: 1020
Limonene	16.6	12.14 [1015]	20.24 [1014]	Nd	100.00 [1014]	23.08 [1014]	Tr [1014]	1024
1,8-Cineole	16.7	7.94 [1018]	11.44 [1018]	Nd	Nd	13.49 [1018]	Tr [1017]	1026
β-Ocimene	17.4	0.04 [1032]	Tr [1032]	Nd	Nd	Nd	Nd	(*Z*)-: 1032 (*E*)-: 1044
Bergamal	17.7	0.07 [1040]	Tr [1040]	Nd	Nd	Nd	Nd	1051
γ-Terpinene	18.0	0.16 [1046]	0.28 [1046]	Nd	Nd	0.29 [1046]	Nd	1054
cis-Sabinene hydrate	18.6	0.96 [1059]	0.09 [1059]	7.17 [1059]	Nd	0.70 [1059]	Tr [1059]	1065

Compound	**Retention time (min)**	***Aloysia* oil fresh (BI 21372)** **Percentage composition (TIC) and [RI]***	**Fraction V2 1/3 (BI 22729)** **Percentage composition (TIC) and [RI]***	**Fraction V2 2/3 (BI 22730)** **Percentage composition (TIC) and [RI]***	**Fraction V4 1/11 (BI 22737)** **Percentage composition (TIC) and [RI]***	**Fraction V4 2/11 (BI 22738)** **Percentage composition (TIC) and [RI]***	**Fraction V4 3/11 (BI 22739)** **Percentage composition (TIC) and [RI]***	**RI (published)**
Perillene	19.9	Tr [1089]	0.07 [1089]	Nd	Nd	Nd	Nd	1102
Linalool	20.0	0.61 [1091]	0.16 [1091]	1.43 [1091]	Nd	0.40 [1091]	Nd	1095
trans-Sabinene hydrate	20.1	0.41 [1093]	Nd	2.88 [1093]	Nd	Tr [1093]	10.23 [1093]	1098
α-Pinene oxide	20.3	0.12 [1098]	Tr [1098]	Nd	Nd	Tr [1097]	Nd	1099
cis-Rose oxide	20.5	0.06 [1102]	Tr [1102]	Nd	Nd	Nd	Nd	1106
trans-Thujone	20.9	0.03 [1111]	Tr [1111]	Nd	Nd	Nd	Nd	1112
trans-*p*-Mentha-2,8-dien-1-ol	21.1	0.48 [1115]	Tr [1115]	3.18 [1115]	Nd	Tr [1115]	12.59 [1115]	1119
α-Campholenal	21.3	0.09 [1120]	Tr [1121]	Nd	Nd	Nd	Nd	1122
cis-Limonene oxide	21.6	0.27 [1127]	0.19 [1127]	Nd	Nd	Tr [1127]	Nd	1132
cis-*p*-Mentha-2,8-dien-1-ol	21.8	0.81 [1131]	0.35 [1132]	3.06 [1131]	Nd	Nd	20.73 [1131]	1133
Verbenol	22.2	0.10 [1141]	Nd	Tr [1141]	Nd	Nd	Tr [1141]	*cis*-: 1137 *trans*-: 1140
Citronellal	22.5	0.14 [1147]	0.10 [1147]	Nd	Nd	Tr [1147]	Nd	1148
Sabina ketone	22.8	0.12 [1154]	Nd	Tr [1154]	Nd	Nd	Nd	1154
Rosefuran epoxide	23.4	0.59 [1166]	0.58 [1166]	Nd	Nd	0.13 [1166]	Nd	1173
Terpinen-4-ol	24.0	0.75 [1179]	0.51 [1179]	2.31 [1179]	Nd	0.56 [1179]	Nd	1174
trans-*p*-Mentha-1(7),8-dien-2-ol	24.3	0.30 [1186]	Tr [1186]	Tr [1186]	Nd	Nd	Tr [1186]	1187
α-Terpineol	24.7	3.27 [1195]	0.33 [1195]	24.70 [1194]	Nd	2.14 [1194]	21.19 [1194]	1186
Shisofuran	25.6	0.09 [1215]	Tr [1215]	Nd	Nd	Nd	Nd	1198
trans-Carveol	25.8	0.86 [1219]	Nd	3.48 [1219]	Nd	Tr [1219]	18.24 [1219]	1215
Nerol	26.0	0.24 [1224]	Nd	Tr [1224]	Nd	Nd	Nd	1227
Citronellol	26.1	0.10 [1227]	Nd	Nd	Nd	Nd	Nd	1223
cis-*p*-Mentha-1(7),8-dien-2-ol	26.3	0.22 [1230]	Nd	Tr [1230]	Nd	Nd	Tr [1230]	1227
cis-Carveol	26.4	0.39 [1233]	Nd	Tr [1233]	Nd	Nd	Tr [1233]	1226
Neral	26.7	2.55 [1239]	2.85 [1239]	Tr [1239]	Nd	2.08 [1239]	Nd	1235
Carvone	26.9	1.14 [1245]	1.37 [1245]	Nd	Nd	1.09 [1245]	Nd	1239
Geraniol	27.2	0.25 [1251]	Nd	Nd	Nd	Nd	Nd	1249
Piperitone	27.4	0.33 [1256]	Tr [1256]	Tr [1256]	Nd	Nd	Nd	1249
Geranial	28.1	4.03 [1270]	4.64 [1269]	Tr [1270]	Nd	3.51 [1269]	Nd	1264
Perilla aldehyde	28.4	0.13 [1279]	0.12 [1278]	Nd	Nd	Nd	Nd	1269
(*E*)-Anethole	28.9	0.35 [1289]	0.27 [1289]	Nd	Nd	Tr [1289]	Nd	1282
Thymol	29.0	0.16 [1292]	0.13 [1292]	Nd	Nd	Nd	Tr [1292]	1289
Carvacrol	29.4	0.82 [1300]	0.32 [1300]	Tr [1301]	Nd	Nd	17.01 [1301]	1298
trans-Carvyl acetate	31.0	0.09 [1335]	Tr [1335]	Nd	Nd	Nd	Nd	1339
Piperitenone	31.3	0.06 [1341]	Nd	Nd	Nd	Nd	Nd	1340
α-Cubebene	31.7	0.09 [1350]	Tr [1350]	Nd	Nd	Nd	Nd	1345
Eugenol	31.8	0.16 [1353]	Tr [1354]	Nd	Nd	Nd	Nd	1356
α-Ylangene	32.7	0.12 [1372]	0.09 [1372]	Nd	Nd	Tr [1372]	Nd	1373
α-Copaene	33.0	1.62 [1379]	2.01 [1379]	Nd	Tr [1379]	1.12 [1379]	Nd	1374

Compound	**Retention time (min)**	***Aloysia* oil fresh (BI 21372)** **Percentage composition (TIC) and [RI]***	**Fraction V2 1/3 (BI 22729)** **Percentage composition (TIC) and [RI]***	**Fraction V2 2/3 (BI 22730)** **Percentage composition (TIC) and [RI]***	**Fraction V4 1/11 (BI 22737)** **Percentage composition (TIC) and [RI]***	**Fraction V4 2/11 (BI 22738)** **Percentage composition (TIC) and [RI]***	**Fraction V4 3/11 (BI 22739)** **Percentage composition (TIC) and [RI]***	**RI (published)**
β-Bourbonene	33.3	0.96 [1387]	1.34 [1387]	Nd	Tr [1387]	0.75 [1387]	Nd	1387
Methyl eugenol	33.9	0.14 [1400]	Tr [1401]	Nd	Nd	Nd	Nd	1403
Sesquithujene	34.1	0.13 [1404]	0.12 [1404]	Nd	Nd	Nd	Nd	1405
α-Cedrene	34.7	0.67 [1418]	0.91 [1418]	Nd	Tr [1419]	0.64 [1418]	Nd	1410
(*E*)-Caryophyllene	34.9	2.07 [1421]	3.20 [1421]	Nd	Tr [1421]	2.20 [1421]	Nd	1417
β-Cedrene	35.1	0.37 [1426]	0.50 [1426]	Nd	Nd	0.34 [1426]	Nd	1419
β-Copaene	35.3	0.16 [1431]	0.21 [1431]	Nd	Nd	Tr [1430]	Nd	1430
α-Humulene	36.4	0.25 [1455]	0.31 [1455]	Nd	Nd	Nd	Nd	1452
Allo-aromadendrene	36.6	0.86 [1459]	1.22 [1459]	Nd	Tr [1459]	0.76 [1459]	Nd	1458
Acoradiene	36.9	0.25 [1467]	0.48 [1467]	Nd	Nd	Nd	Nd	α-: 1464 β-: 1469
γ-Muurolene	37.2	0.26 [1472]	0.32 [1472]	Nd	Nd	Nd	Nd	1478
Curcumene	37.4	9.17 [1478]	15.30 [1478]	Nd	Nd	12.90 [1478]	Nd	γ-: 1481 ar-: 1479
Bicyclogermacrene (+ *epi*-cubebol**)	38.1	0.49 [1492]	0.53 [1492]	*epi*-cubebol Tr [1492]	Nd	*epi*-cubebol 0.47 [1492]	Nd	1500 (1493)
α-Muurolene	38.1	0.09 [1494]	0.12 [1494]	Nd	Nd	Nd	Nd	1500
Bisabolene	38.5	0.12 [1502]	Tr [1502]	Nd	Nd	Nd	Nd	β-: 1505 (*Z*)-α-: 1506
β-Curcumene	38.6	0.16 [1504]	0.36 [1504]	Nd	Nd	Nd	Nd	1514
γ-Cadinene	38.8	0.39 [1508]	0.53 [1507]	Nd	Nd	0.17 [1507]	Nd	1513
Cubebol	38.8	0.81 [1510]	0.10 [1509]	3.44 [1510]	Nd	0.41 [1509]	Nd	1514
δ-Cadinene	38.9	0.27 [1512]	0.41 [1512]	Nd	Nd	Tr [1511]	Nd	1522
trans-Calamenene	39.1	0.14 [1515]	Tr [1514]	Nd	Nd	Tr [1514]	Nd	1521
cis-Calamenene	39.5	0.11 [1523]	Tr [1523]	Nd	Nd	Tr [1523]	Nd	1528
α-Cadinene	39.7	0.23 [1528]	Nd	Nd	Nd	Nd	Nd	1537
(*E*)-Nerolidol	40.6	0.89 [1549]	0.33 [1549]	Nd	Nd	0.32 [1549]	Nd	1561
Spathulenol	41.4	7.16 [1566]	1.33 [1564]	40.54 [1564]	Nd	7.44 [1564]	Nd	1577
Caryophyllene oxide	41.6	10.44 [1571]	15.29 [1570]	Nd	Nd	15.45 [1569]	Nd	1582
Globulol	42.6	1.29 [1593]	0.95 [1593]	Nd	Nd	1.31 [1593]	Nd	1590
τ-Cadinol[a]	43.8	1.33 [1620]	0.50 [1620]	3.46 [1620]	Nd	1.29 [1620]	Nd	-

Compounds detected in *Aloysia* oil (BI 21372) were not detected in fractions: V2 3/3 (BI 22731), V2M (BI 22732), V3M (BI 22733), V3 1/3 (BI 22734), V3 2/3 (BI 22735), V3 3/3 (BI 22736), V4 5/11 (BI 22741), V4 6/11 (BI 22742), V4 7/11 (BI 22743), V4 8/11 (BI 22744), V4 9/11 (BI 22745), V4 10/11 (BI 22746), V4 11/11 (BI 22747), V5 6/10 (BI 22753), V5 7/10 (BI 22754), V5 8/10 (BI 22755), V5 9/10 (BI 22756), V5 10/10 (BI 22757).

Tr: < 0.01 %; Nd: not detected.

*Experimental retention index (RI) value; **co-elution.

All compounds identified by comparing retention indices (calculated against an *n*-alkane series) and by comparing mass spectra with published data[1, 2], except for [a]compounds identified by comparison with published mass spectra only[1].

Table 2. Percentage composition of detected compounds (based on all detected peaks assigned as oil constituents).

Compound	**Retention time (min)**	**Fraction V4 4/11 (BI 22740)** **Percentage composition (TIC) and [RI]***	**Fraction V5 1/10 (BI 22748)** **Percentage composition (TIC) and [RI]***	**Fraction V5 2/10 (BI 22749)** **Percentage composition (TIC) and [RI]***	**Fraction V5 3/10 (BI 22750)** **Percentage composition (TIC) and [RI]***	**Fraction V5 4/10 (BI 22751)** **Percentage composition (TIC) and [RI]***	**Fraction V5 5/10 (BI 22752)** **Percentage composition (TIC) and [RI]***	**RI (published)**
Salvene	7.8	Nd	Nd	Nd	Nd	Nd	Nd	(*Z*)-: 847 (*E*)-: 858
α-Thujene	11.7	Nd	Tr [906]	Nd	Nd	Nd	Nd	924
α-Pinene	12.0	Nd	2.70 [914]	Nd	Nd	Nd	Nd	932
Camphene	12.8	Nd	Nd	Nd	Nd	Nd	Nd	946
Sabinene	13.8	Nd	4.27 [954]	Nd	Nd	Nd	Nd	969
β-Pinene	14.0	Nd	Nd	Nd	Nd	Nd	Nd	974
1-Octen-3-ol	14.1	Nd	Nd	Nd	Nd	Tr [961]	Nd	974
6-Methyl-5-hepten-2-one	14.4	Nd	Nd	Nd	7.19 [966]	Tr [966]	Nd	981
Myrcene	14.6	Nd	Nd	Nd	Nd	Nd	Nd	988
α-Terpinene	15.9	Nd	Nd	Nd	Nd	Nd	Nd	1014
Cymene	16.3	Nd	Nd	Nd	Nd	Nd	Nd	*o*-: 1022 *p*-: 1020
Limonene	16.6	100.00 [1014]	70.66 [1014]	100.00 [1014]	Nd	Nd	Nd	1024
1,8-Cineole	16.7	Nd	Nd	Nd	59.27 [1018]	Nd	Nd	1026
β-Ocimene	17.4	Nd	Nd	Nd	Nd	Nd	Nd	(*Z*)-: 1032 (*E*)-: 1044
Bergamal	17.7	Nd	Nd	Nd	Nd	Nd	Nd	1051
γ-Terpinene	18.0	Nd	Tr [1046]	Nd	Nd	Nd	Nd	1054
cis-Sabinene hydrate	18.6	Nd	Nd	Nd	Nd	9.38 [1059]	Tr [1059]	1065
Perillene	19.9	Nd	Nd	Nd	Nd	Nd	Nd	1102
Linalool	20.0	Nd	Nd	Nd	Nd	Tr [1091]	Nd	1095
trans-Sabinene hydrate	20.1	Nd	Nd	Nd	Nd	Nd	Tr [1093]	1098
α-Pinene oxide	20.3	Nd	Nd	Nd	Nd	Nd	Nd	1099
cis-Rose oxide	20.5	Nd	Nd	Nd	Nd	Nd	Nd	1106
trans-Thujone	20.9	Nd	Nd	Nd	Nd	Nd	Nd	1112
trans-*p*-Mentha-2,8-dien-1-ol	21.1	Nd	Nd	Nd	Nd	Tr [1115]	Nd	1119
α-Campholenal	21.3	Nd	Nd	Nd	Nd	Nd	Nd	1122
cis-Limonene oxide	21.6	Nd	Nd	Nd	Nd	Nd	Nd	1132
cis-*p*-Mentha-2,8-dien-1-ol	21.8	Nd	Nd	Nd	Nd	Nd	Tr [1131]	1133
Verbenol	22.2	Nd	Nd	Nd	Nd	Nd	Nd	*cis*-: 1137 *trans*-: 1140
Citronellal	22.5	Nd	Nd	Nd	Nd	Nd	Nd	1148
Sabina ketone	22.8	Nd	Nd	Nd	Nd	Nd	Nd	1154
Rosefuran epoxide	23.4	Nd	Nd	Nd	Tr [1166]	Nd	Nd	1173
Terpinen-4-ol	24.0	Nd	Nd	Nd	Nd	Tr [1179]	Nd	1174
trans-*p*-Mentha-1(7),8-dien-2-ol	24.3	Nd	Nd	Nd	Nd	Nd	Nd	1187
α-Terpineol	24.7	Nd	Nd	Nd	Nd	15.75 [1194]	100.00 [1195]	1186
Shisofuran	25.6	Nd	Nd	Nd	Nd	Nd	Nd	1198
trans-Carveol	25.8	Nd	Nd	Nd	Nd	Tr [1219]	Nd	1215
Nerol	26.0	Nd	Nd	Nd	Nd	Nd	Nd	1227

Compound	**Retention time (min)**	**Fraction V4 4/11 (BI 22740)** **Percentage composition (TIC) and [RI]***	**Fraction V5 1/10 (BI 22748)** **Percentage composition (TIC) and [RI]***	**Fraction V5 2/10 (BI 22749)** **Percentage composition (TIC) and [RI]***	**Fraction V5 3/10 (BI 22750)** **Percentage composition (TIC) and [RI]***	**Fraction V5 4/10 (BI 22751)** **Percentage composition (TIC) and [RI]***	**Fraction V5 5/10 (BI 22752)** **Percentage composition (TIC) and [RI]***	**RI (published)**
Citronellol	26.1	Nd	Nd	Nd	Nd	Nd	Nd	1223
cis-p-Mentha-1(7),8-dien-2-ol	26.3	Nd	Nd	Nd	Nd	Nd	Nd	1227
cis-Carveol	26.4	Nd	Nd	Nd	Nd	Nd	Nd	1226
Neral	26.7	Nd	Nd	Nd	Tr [1239]	8.51 [1239]	Nd	1235
Carvone	26.9	Nd	Nd	Nd	2.30 [1246]	Nd	Nd	1239
Geraniol	27.2	Nd	Nd	Nd	Nd	Nd	Nd	1249
Piperitone	27.4	Nd	Nd	Nd	Nd	Nd	Nd	1249
Geranial	28.1	Nd	Nd	Nd	Nd	21.83 [1270]	Nd	1264
Perilla aldehyde	28.4	Nd	Nd	Nd	Nd	Nd	Nd	1269
(*E*)-Anethole	28.9	Nd	Nd	Nd	Nd	Nd	Nd	1282
Thymol	29.0	Nd	Nd	Nd	Nd	Nd	Nd	1289
Carvacrol	29.4	Nd	Nd	Nd	Nd	Tr [1301]	Nd	1298
trans-Carvyl acetate	31.0	Nd	Nd	Nd	Nd	Nd	Nd	1339
Piperitenone	31.3	Nd	Nd	Nd	Nd	Nd	Nd	1340
α-Cubebene	31.7	Nd	Nd	Nd	Nd	Nd	Nd	1345
Eugenol	31.8	Nd	Nd	Nd	Nd	Nd	Nd	1356
α-Ylangene	32.7	Nd	Nd	Nd	Nd	Nd	Nd	1373
α-Copaene	33.0	Nd	Tr [1379]	Nd	Nd	Nd	Nd	1374
β-Bourbonene	33.3	Nd	Tr [1387]	Nd	Nd	Nd	Nd	1387
Methyl eugenol	33.9	Nd	Nd	Nd	Nd	Nd	Nd	1403
Sesquithujene	34.1	Nd	Nd	Nd	Nd	Nd	Nd	1405
α-Cedrene	34.7	Nd	Tr [1418]	Nd	Nd	Nd	Nd	1410
(*E*)-Caryophyllene	34.9	Nd	3.60 [1421]	Nd	Nd	Nd	Nd	1417
β-Cedrene	35.1	Nd	Nd	Nd	Nd	Nd	Nd	1419
β-Copaene	35.3	Nd	Nd	Nd	Nd	Nd	Nd	1430
α-Humulene	36.4	Nd	Tr [1455]	Nd	Nd	Nd	Nd	1452
Allo-aromadendrene	36.6	Nd	Tr [1459]	Nd	Nd	Nd	Nd	1458
Acoradiene	36.9	Nd	Nd	Nd	Nd	Nd	Nd	α-: 1464 β-: 1469
γ-Muurolene	37.2	Nd	Nd	Nd	Nd	Nd	Nd	1478
Curcumene	37.4	Nd	18.77 [1478]	Nd	Nd	Nd	Nd	γ-: 1481 ar-: 1479
Bicyclogermacrene (+ *epi*-cubebol**)	38.1	Nd	Nd	Nd	Nd	Nd	Nd	1500 (1493)
α-Muurolene	38.1	Nd	Nd	Nd	Nd	Nd	Nd	1500
Bisabolene	38.5	Nd	Nd	Nd	Nd	Nd	Nd	β-: 1505 (*Z*)-α-: 1506
β-Curcumene	38.6	Nd	Nd	Nd	Nd	Nd	Nd	1514
γ-Cadinene	38.8	Nd	Tr [1507]	Nd	Nd	Nd	Nd	1513
Cubebol	38.8	Nd	Nd	Nd	Nd	Tr [1510]	Nd	1514
δ-Cadinene	38.9	Nd	Tr [1512]	Nd	Nd	Nd	Nd	1522
trans-Calamenene	39.1	Nd	Nd	Nd	Nd	Nd	Nd	1521

Compound	Retention time (min)	Fraction V4 4/11 (BI 22740) Percentage composition (TIC) and [RI]*	Fraction V5 1/10 (BI 22748) Percentage composition (TIC) and [RI]*	Fraction V5 2/10 (BI 22749) Percentage composition (TIC) and [RI]*	Fraction V5 3/10 (BI 22750) Percentage composition (TIC) and [RI]*	Fraction V5 4/10 (BI 22751) Percentage composition (TIC) and [RI]*	Fraction V5 5/10 (BI 22752) Percentage composition (TIC) and [RI]*	RI (published)
cis-Calamenene	39.5	Nd	Nd	Nd	Nd	Nd	Nd	1528
Nerolidol	40.6	Nd	Nd	Nd	Nd	Nd	Nd	(*E*)-: 1561 (*Z*)-: 1531
Spathulenol	41.4	Nd	Nd	Nd	Nd	44.53 [1564]	Nd	1577
Caryophyllene oxide	41.6	Nd	Nd	Nd	31.24 [1569]	Nd	Nd	1582
Globulol	42.6	Nd	Nd	Nd	Nd	Nd	Nd	1590
τ-Cadinol[a]	43.8	Nd	Nd	Nd	Nd	Tr [1620]	Nd	-

Compounds detected in *Aloysia* oil (BI 21372) were not detected in fractions: V2 3/3 (BI 22731), V2M (BI 22732), V3M (BI 22733), V3 1/3 (BI 22734), V3 2/3 (BI 22735), V3 3/3 (BI 22736), V4 5/11 (BI 22741), V4 6/11 (BI 22742), V4 7/11 (BI 22743), V4 8/11 (BI 22744), V4 9/11 (BI 22745), V4 10/11 (BI 22746), V4 11/11 (BI 22747), V5 6/10 (BI 22753), V5 7/10 (BI 22754), V5 8/10 (BI 22755), V5 9/10 (BI 22756), V5 10/10 (BI 22757).
Tr: < 0.01 %; Nd: not detected.
*Experimental retention index (RI) value; **co-elution.
All compounds identified by comparing retention indices (calculated against an *n*-alkane series) and by comparing mass spectra with published data[1, 2], except for [a]compounds identified by comparison with published mass spectra only[1].

References

[1] NIST 08. (2008) NIST/EPA/NIH Mass Spectral Database. National Institute of Standards and Technology, Gaithersburg, USA.

[2] Adams R.P. (2007) Identification of Essential Oil Components by Gas Chromatography / Mass Spectroscopy. Allured Publishing Corporation, Illinois, USA.

Appendix III

SPE of *Aloysia Citrodora* Essential Oil

Sample ID:	v1
Solvent A:	Hexane
Solvent B:	Diethyl Ether
Column:	SF10-4g
Column Station:	1
Start Time:	11/9/2011 10:36:41 PM
Detectors:	UV: 254nm, 300nm, 399nm, 200nm

Agilent Technologies

AU Graph

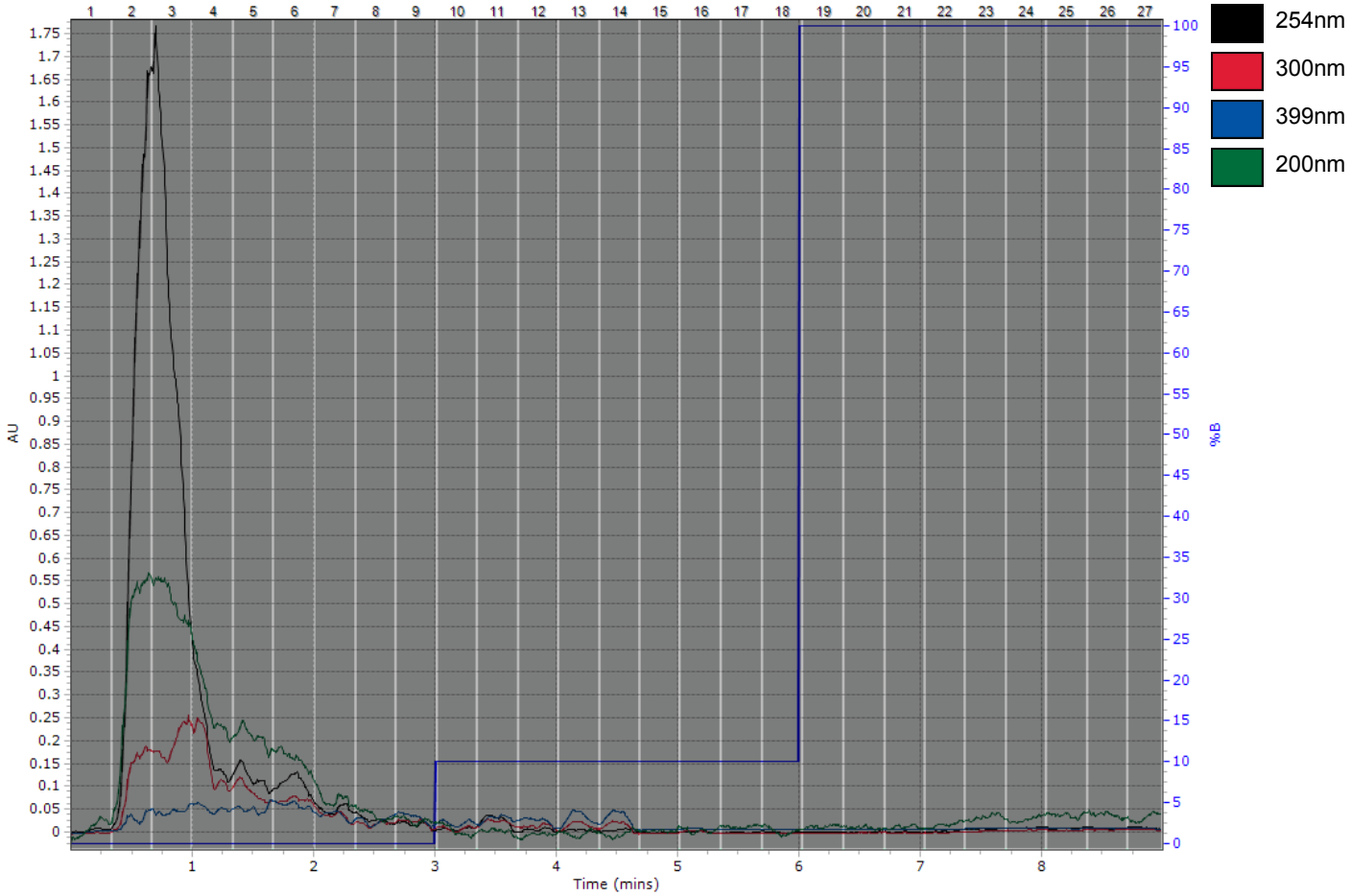

Gradient Graph

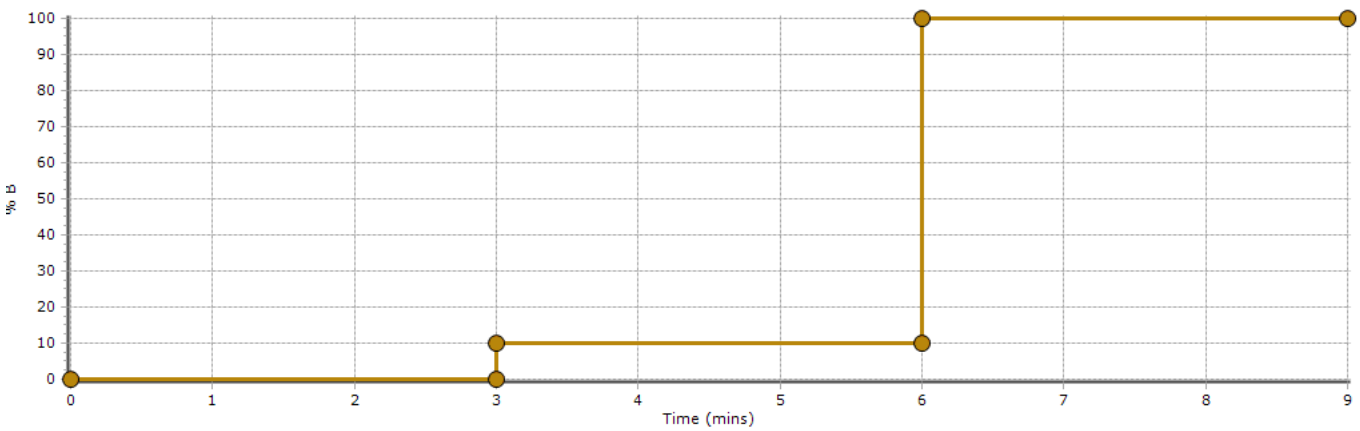

Solvent Details

%B	Time	%B	Time
0	00:00	10	06:00
0	03:00	100	06:00
10	03:00	100	09:00

Tube Map

Rack: 1 **18 x 150 mm (1)**

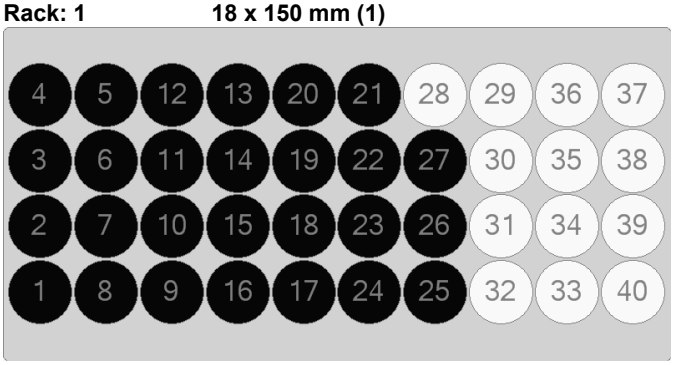

Rack: 1 **Instance: 1** **18 x 150 mm**

Peak	Tube Number	Volume (CV)	Volume (ml)
1	1	1.00	6.00
1	2	1.00	6.00
1	3	1.00	6.00
1	4	1.00	6.00
1	5	1.00	6.00
1	6	1.00	6.00
1	7	1.00	6.00
1	8	1.00	6.00
1	9	1.00	6.00
1	10	1.00	6.00
1	11	0.90	5.40
1	12	0.90	5.40
1	13	1.00	6.00
1	14	1.00	6.00
1	15	1.00	6.00
1	16	0.90	5.40
1	17	1.00	6.00
1	18	1.00	6.00
1	19	1.00	6.00
1	20	1.00	6.00
1	21	1.00	6.00
1	22	1.00	6.00
1	23	1.00	6.00
1	24	1.00	6.00
1	25	1.00	6.00
1	26	1.00	6.00
1	27	0.90	5.40
	Total:	**26.60**	**159.60**

***Aloysia citrodoria* Essential Oil and Fractions (L1, L2, L3)**

GC-MS Analysis

Sample preparation

Oil: 1/100 dilution in diethyl ether.

Fractions analysed without dilution.

Method

GC: Perkin-Elmer AutoSystem XL

Column: 30 m x 0.25 mm i.d. x 0.25 µm DB-5MS (J. & W. Scientific)

Temp prog.: 40-300ºC @ 3ºC/min

Carrier gas: Helium (flow: 1ml/min)

Injection temp.: 220 °C

MS (quadrupole): Perkin-Elmer TurboMass (quadrupole)

Source: EI (70 eV)

Source temp.: 180 °C

Scan range: 38-600 m/z

Scan time: 0.50 s

Inter-scan delay: 0.20 s

	Aloysia Percentage composition	**Fraction I** 100% Pet Ether Percentage composition	**Fraction II** 90% PetEther 10% DiethylEther Percentage composition	**Fraction III** 100% DiethylEther Percentage composition
Salvene	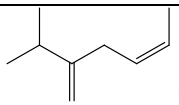 0.03	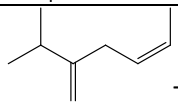 Tr	0	0
α-Thujene	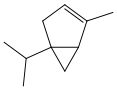 0.07	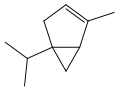 0.11	0	
α-Pinene	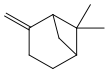 0.44	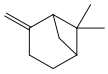 0.82	0	
Camphene	 Tr	 Tr	0	
Sabinene	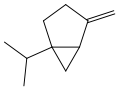 0.92	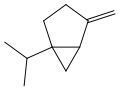 1.52	0	
β-Pinene	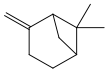 0.08	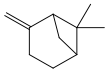 0.14	0	
1-Octen-3-ol	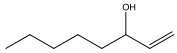 0.55	Tr	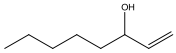 0.05	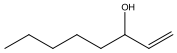 Tr
6-Methyl-5-hepten-2-one	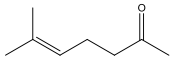 2.37	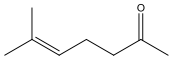 2.42	0	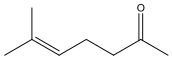 7.19
Myrcene	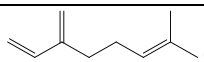 0.20	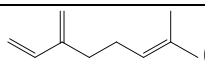 0.32	0	
α-terpinene	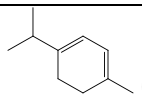 0.01	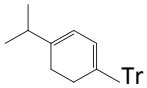 Tr	0	
Cymene	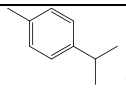 0.46	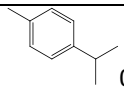 0.49	0	
Limonene	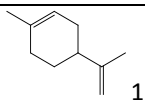 12.14	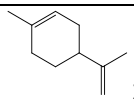 20.24	0	
1,8-Cineole	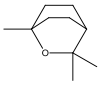 7.94	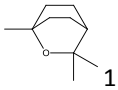 11.44	0	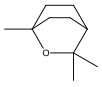 59.27
β-Ocimene	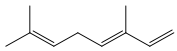 0.04	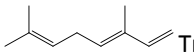 Tr	0	
Bergamal	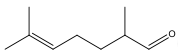 0.07	Tr	0	
γ-Terpinene	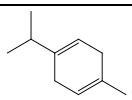 0.16	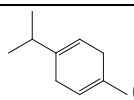 0.28	0	
cis Sabinene hydrate	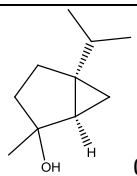 0.96	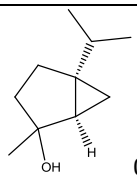 0.09	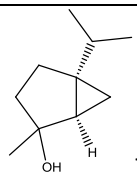 7.17	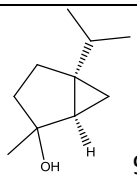 9.38
Perillene	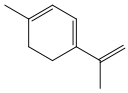 Tr	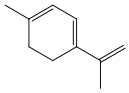 0.07	0	
Linalool	0.61	0.16	1.43	Tr

trans Sabinene hydrate	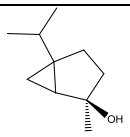 0.41	0	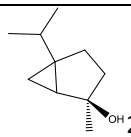 2.88	
α-Pinene oxide	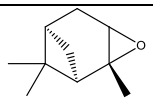 0.12	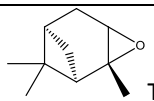 Tr	0	
cis-Rose oxide	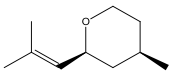 0.06	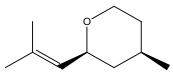 Tr	0	
Trans-Thujone	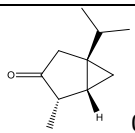 0.03	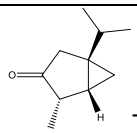 Tr	0	
trans-p-Mentha-2,8-dien-1-ol	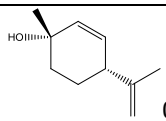 0.48	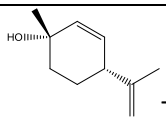 Tr	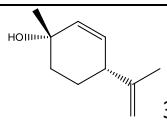 3.18	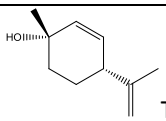 Tr
α-Campholenal	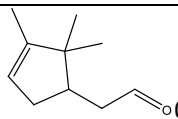 0.09	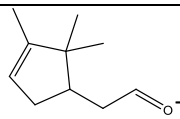 Tr	0	
cis-Limonene oxide	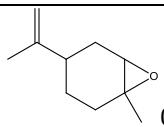 0.27	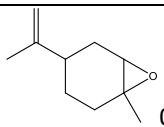 0.19	0	
cis-p-Mentha-2,8-dien-1-ol	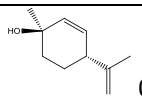 0.81	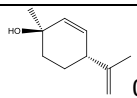 0.35	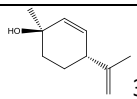 3.06	
verbenol	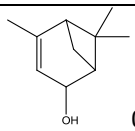 0.10	0	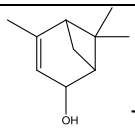 Tr	
Citronellal	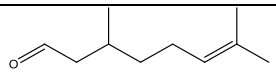 0.14	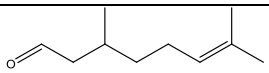 0.10	0	
Sabina ketone	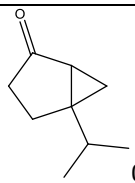 0.12	0	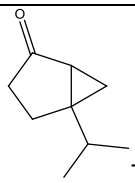 Tr	
rosefuran epoxide	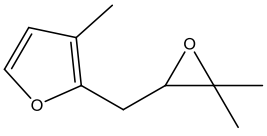 0.59	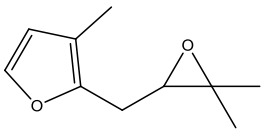 0.58	0	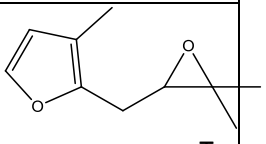 Tr
Terpinen-4-ol	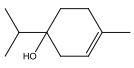 0.75	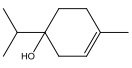 0.51	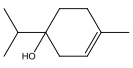 2.31	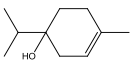 Tr

trans-p-Mentha-1(7),8-dien-2-ol	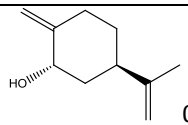 0.30	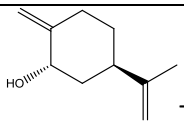 Tr	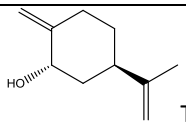 Tr	
α-Terpineol	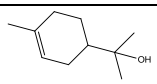 3.27	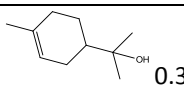 0.33	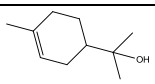 24.70	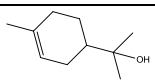 15.75
Shisofuran	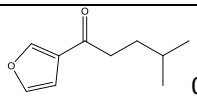 0.09	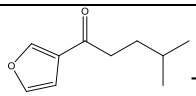 Tr	0	
trans-Carveol	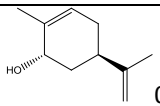 0.86	0	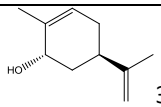 3.48	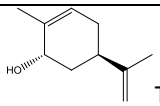 Tr
Nerol	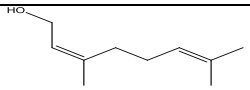 0.24	0	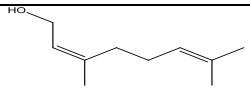 Tr	
Citronellol	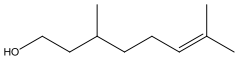 0.10	0	0	
cis-p-Mentha-1(7),8-dien-2-ol	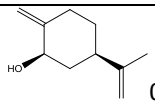 0.22	0	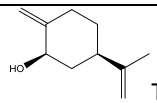 Tr	
cis−carveol	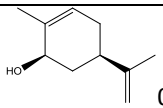 0.39	0	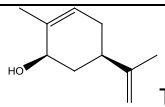 Tr	
Neral	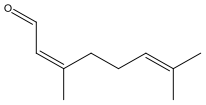 2.55	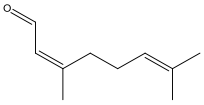 2.85	Tr	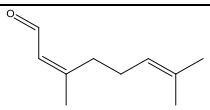 8.51
carvone	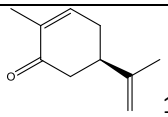 1.14	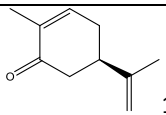 1.37	0	
Geraniol	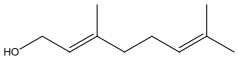 0.25	0	0	
Piperitone	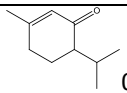 0.33	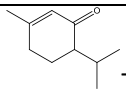 Tr	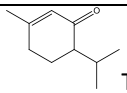 Tr	
Geranial	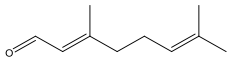 4.03	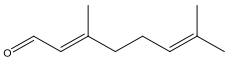 4.64	Tr	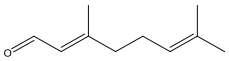 21.83
Perilla aldehyde	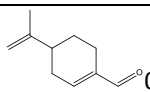 0.13	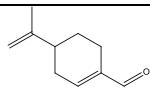 0.12	0	
(E)-Anethole	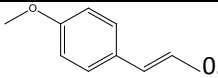 0.35	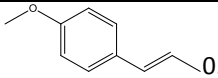 0.27	0	
Thymol	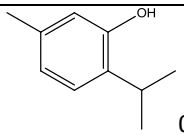 0.16	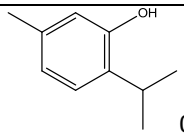 0.13	0	

Carvacrol	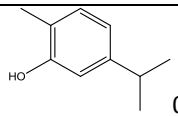 0.82	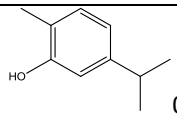 0.32	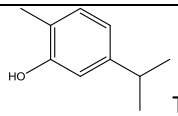 Tr	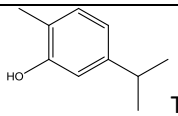 Tr
trans-Carvyl acetate	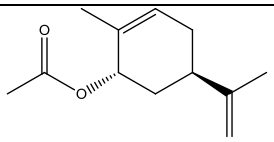 0.09	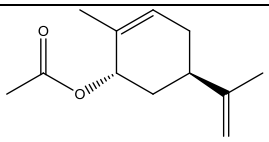 Tr	0	
Piperitenone	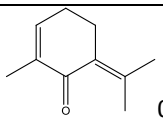 0.06	0	0	
α-Cubebene	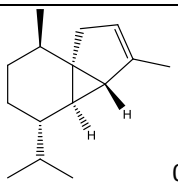 0.09	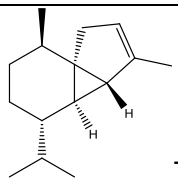 Tr	0	
Eugenol	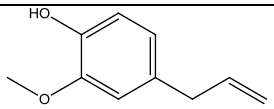 0.16	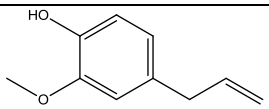 Tr	0	
α-Ylangene	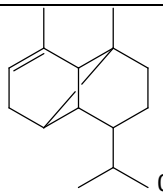 0.12	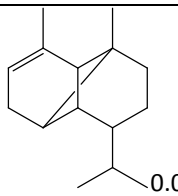 0.09	0	
α-Copaene	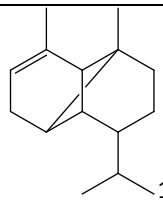 1.62	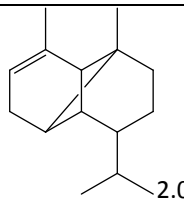 2.01	0	
β-Bourbonene	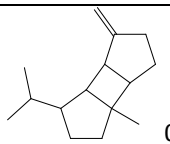 0.96	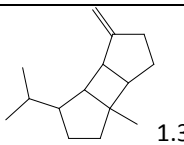 1.34		
Methyl eugenol	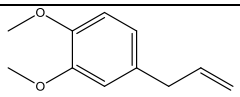 0.14	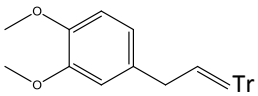 Tr		
Sesquithujene	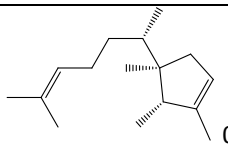 0.13	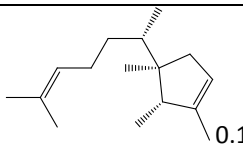 0.12		
α-Cedrene	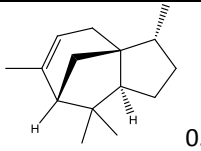 0.67	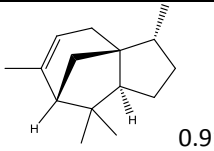 0.91		

(*E*)-Caryophyllene	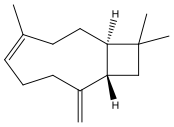 2.07	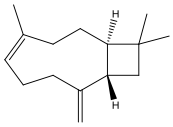 3.20		
β-Cedrene	0.37	0.50		
β-Copaene	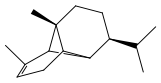 0.16	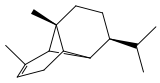 0.21		
α-Humulene	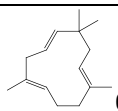 0.25	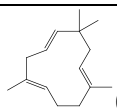 0.31		
Allo-aromadendrene	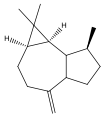 0.86	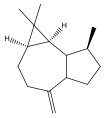 1.22		
Acoradiene	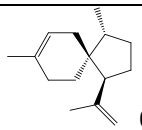 0.25	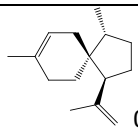 0.48		
γ-Muurolene	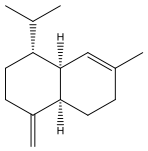 0.26	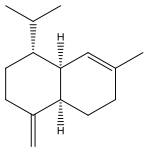 0.32		
Curcumene	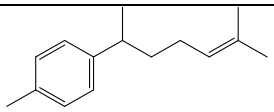 9.17	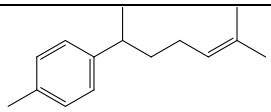 15.30		
Bicyclogermacrene (+ *epi*-cubebol**)	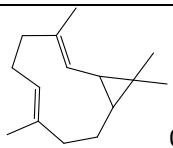 0.49	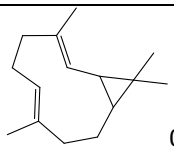 0.53	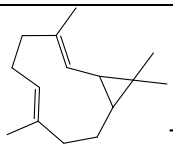 Tr	
α-Muurolene	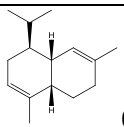 0.09	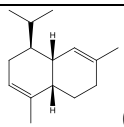 0.12		
Bisabolene	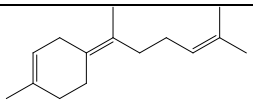 0.12	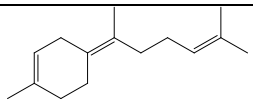 Tr		
β-Curcumene	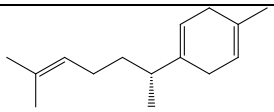 0.16	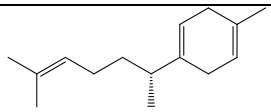 0.36		
γ-Cadinene	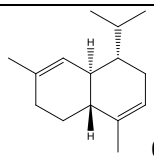 0.39	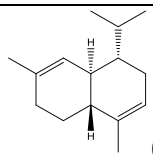 0.53		

Cubebol	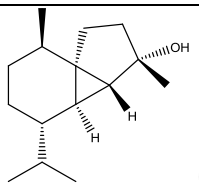 0.81	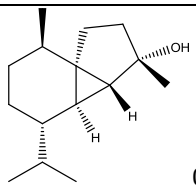 0.10	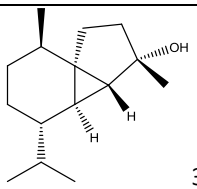 3.44	Tr
δ-Cadinene	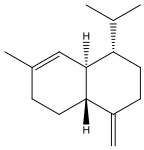 0.27	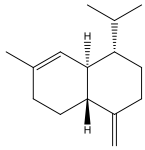 0.41		
trans-Calamenene	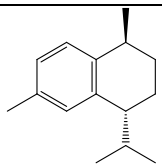 0.14	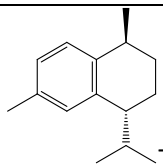 Tr		
cis-Calamenene	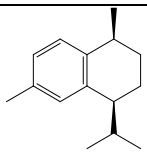 0.11	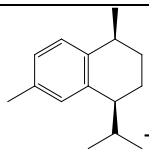 Tr		
α-Cadinene	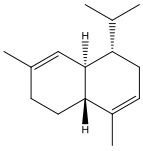 0.23	0		
(*E*)-Nerolidol	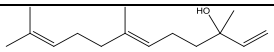 0.89	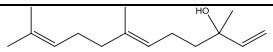 0.33		
Spathulenol	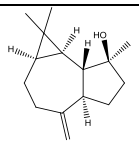 7.16	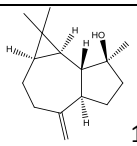 1.33	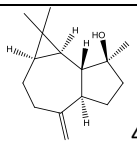 40.54	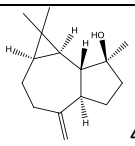 44.53
Caryophyllene oxide	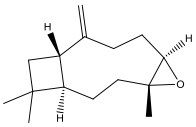 10.44	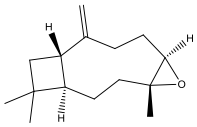 15.29		
Globulol	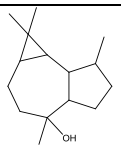 1.29	 0.95		
τ-Cadinol	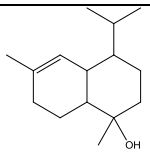 1.33	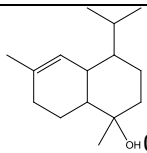 0.50	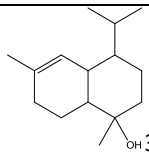 3.46	Tr

Appendix IV

SPE of *Lavandula angustifolia* Essential Oil

Sample ID:	Lav
Solvent A:	Pet Ether
Solvent B:	Diethyl Ether
Column:	SF10-4g
Column Station:	1
Start Time:	3/10/2010 6:12:37 PM
Detectors:	UV: 254nm, 300nm, 399nm, 200nm

AU Graph

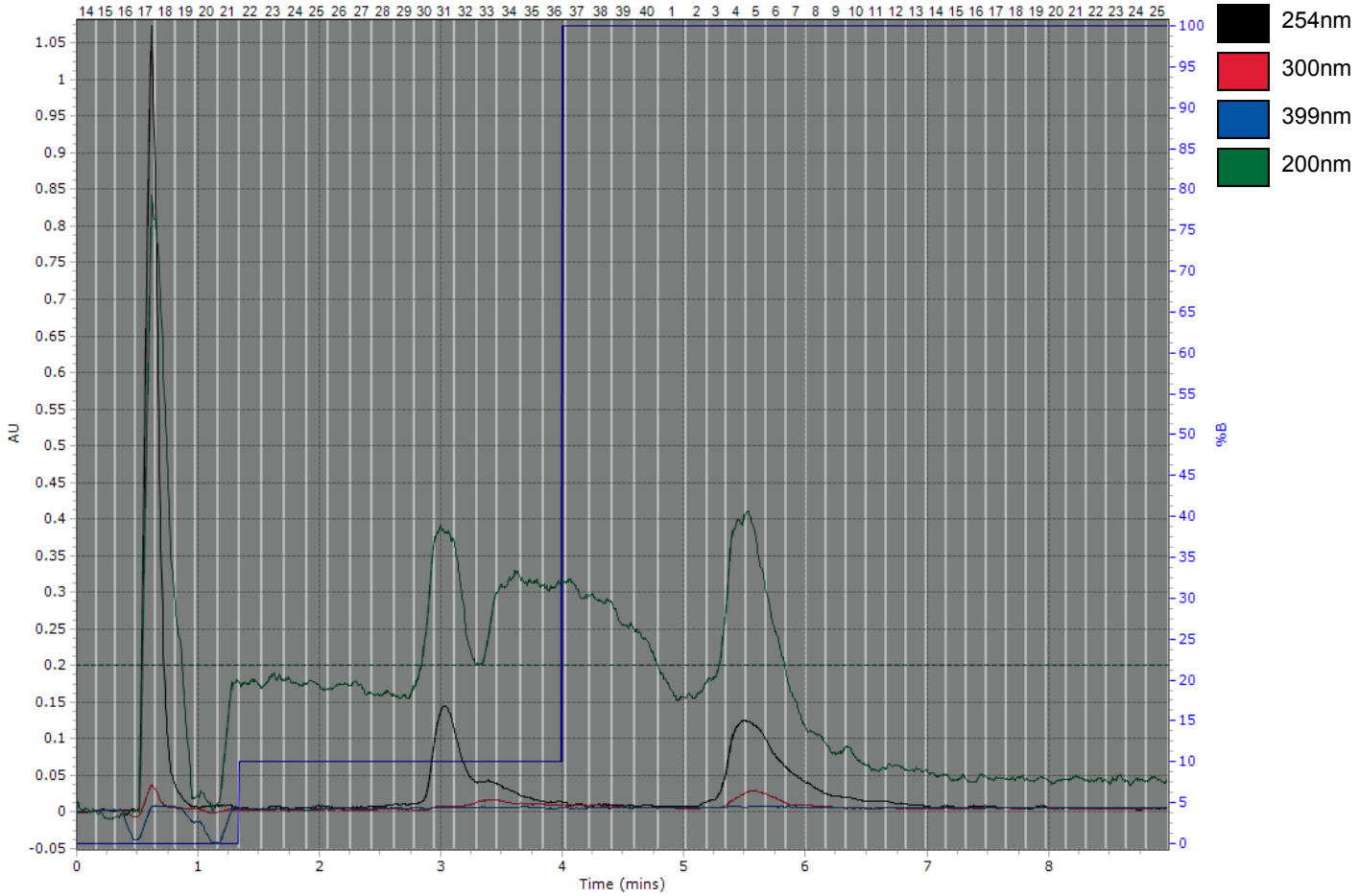

Gradient Graph

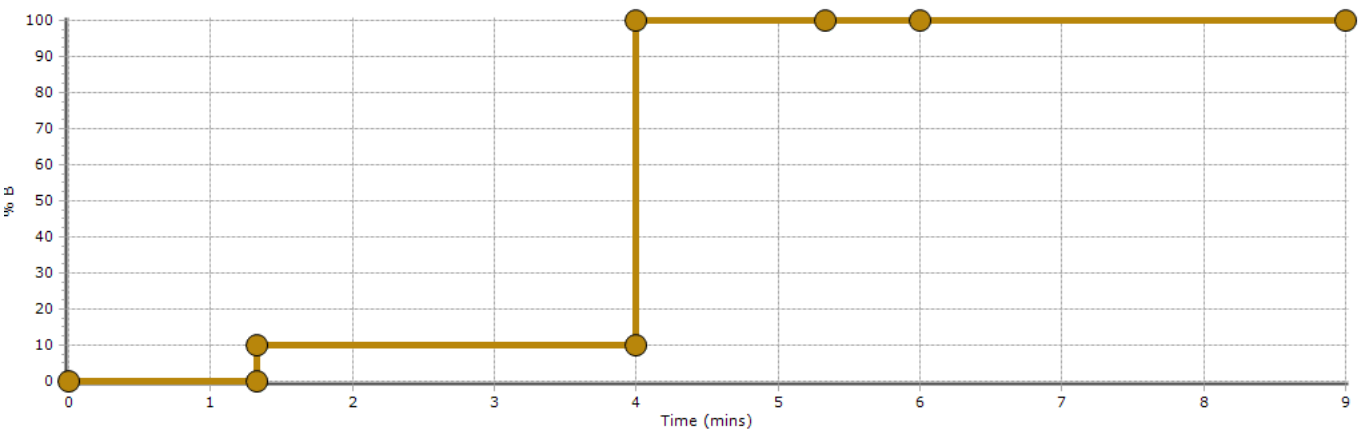

Solvent Details

%B	Time	%B	Time
0	00:00	100	04:00
0	01:20	100	05:20
10	01:20	100	06:00
10	04:00	100	09:00

Tube Map

Rack: 2 **Instance: 1**

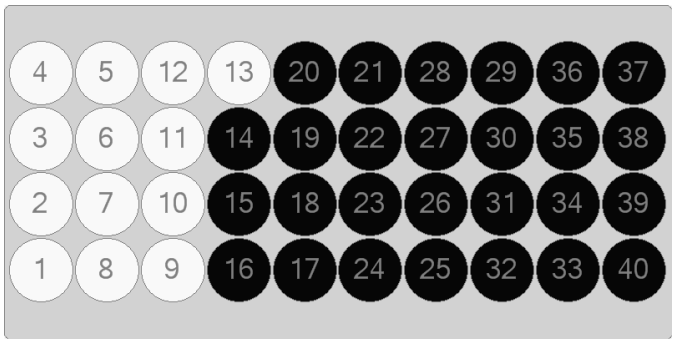

Rack: 3 **Instance: 1**

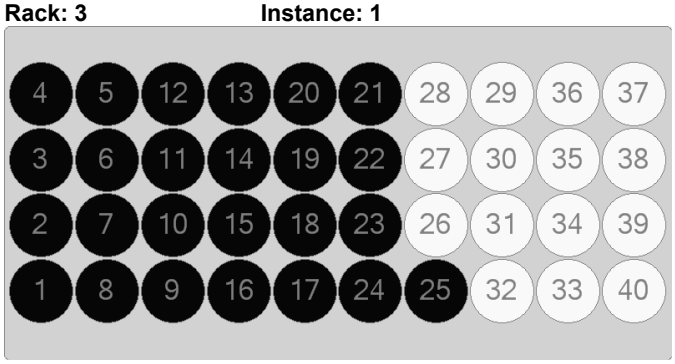

Rack: 2 **Instance: 1**

Peak	Tube Number	Volume (CV)	Volume (ml)
1	14	0.50	3.00
1	15	0.50	3.00
1	16	0.50	3.00
1	17	0.40	2.40
1	18	0.40	2.40
1	19	0.40	2.40
1	20	0.50	3.00
1	21	0.50	3.00
1	22	0.50	3.00
1	23	0.50	3.00
1	24	0.50	3.00
1	25	0.40	2.40
1	26	0.50	3.00
1	27	0.50	3.00
1	28	0.60	3.60
1	29	0.50	3.00
1	30	0.50	3.00
1	31	0.50	3.00
1	32	0.50	3.00
1	33	0.40	2.40
1	34	0.60	3.60
1	35	0.60	3.60
1	36	0.50	3.00
1	37	0.60	3.60
1	38	0.60	3.60
1	39	0.50	3.00
1	40	0.60	3.60

Rack: 3 **Instance: 1**

Peak	Tube Number	Volume (CV)	Volume (ml)
1	1	0.70	4.20
1	2	0.50	3.00
1	3	0.50	3.00
1	4	0.50	3.00
1	5	0.50	3.00
1	6	0.50	3.00
1	7	0.40	2.40
1	8	0.50	3.00
1	9	0.50	3.00
1	10	0.40	2.40
1	11	0.40	2.40
1	12	0.40	2.40
1	13	0.50	3.00
1	14	0.50	3.00
1	15	0.50	3.00
1	16	0.50	3.00
1	17	0.50	3.00
1	18	0.50	3.00
1	19	0.50	3.00
1	20	0.50	3.00
1	21	0.50	3.00
1	22	0.50	3.00
1	23	0.40	2.40
1	24	0.40	2.40
1	25	0.60	3.60
	Total:	**25.80**	**154.80**

Lavandula angustifolia Mill. Essential Oil and Fractions (L1, L2, L3)

GC-MS Analysis

Sample preparation

Oil: 1/100 dilution in diethyl ether.

Fractions analysed without dilution.

Method

GC: Perkin-Elmer AutoSystem XL

Column: 30 m x 0.25 mm i.d. x 0.25 µm DB-5MS (J. & W. Scientific)

Temp prog.: 40-300ºC @ 3ºC/min

Carrier gas: Helium (flow: 1ml/min)

Injection temp.: 220 °C

MS (quadrupole): Perkin-Elmer TurboMass (quadrupole)

Source: EI (70 eV)

Source temp.: 180 °C

Scan range: 38-600 m/z

Scan time: 0.50 s

Inter-scan delay: 0.20 s

	Lavender Oil Percentage composition	**Fraction I** 100%Pet Ether Percentage composition	**Fraction II** 90% PetEther 10% DiethylEther Percentage composition	**Fraction III** 100% DiethylEther Percentage composition
Tricyclene	 Tr	 0.1	0	0
α-Thujene	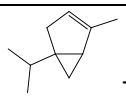 Tr	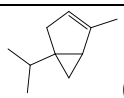 0.3	Tr	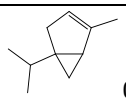 0.1
α-Pinene	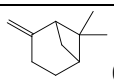 0.1	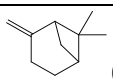 0.7	Tr	Tr
Camphene	 0.1	 0.8	0	0
Sabinene	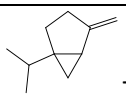 Tr	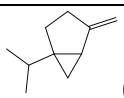 0.2	0	0
β-Pinene	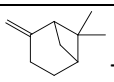 Tr	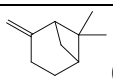 0.2	0	0
1-Octen-3-ol	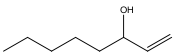 0.4	0	Tr	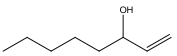 1.4
3-Octanone	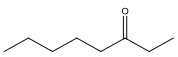 0.1	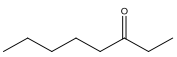 0.1	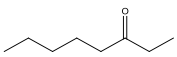 0.1	Tr
Myrcene	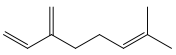 0.5	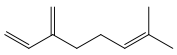 2.6	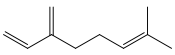 0.1	Tr
α-Phellandrene	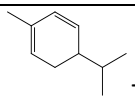 Tr	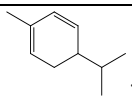 Tr	0	0
2-δ-Carene	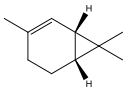 0.3	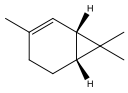 2.1	0	0
Hexyl acetate	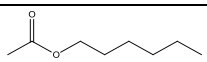 0.1	Tr	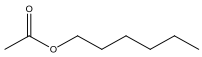 0.1	0
***p*-Cymene**	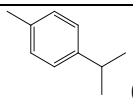 0.1	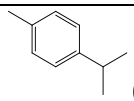 0.6	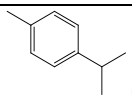 0.1	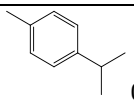 0.1
***o*-Cymene**	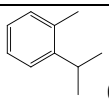 0.3	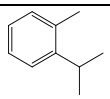 1.5	Tr	Tr
Limonene	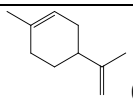 0.8	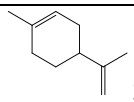 2.8	Tr	Tr
β-Phellandrene	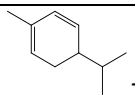 Tr	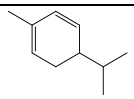 1.8	0	Tr
1,8-Cineole	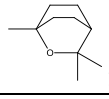 1.4	0	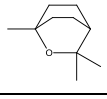 2.5	Tr
(*Z*)-β-Ocimene	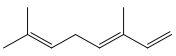 2.6	13.8	0.2	0.2
(*E*)-β-Ocimene	1.5	8.3	0.1	0.2
γ-Terpinene	0.1	0.4	0	0
***trans*-Linalool oxide**	0.1	0	0	0.3

Terpinolene	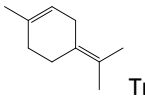 Tr	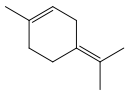 0.5	0	0
***cis*-Linalool oxide (furanoid)**	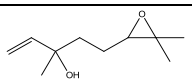 0.1	0	0	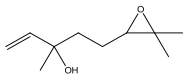 0.1
Dehydro-linalool	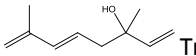 Tr	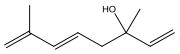 Tr	0	0
Perillene	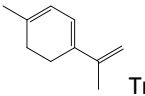 Tr	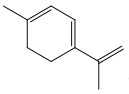 Tr	0	0
Linalool	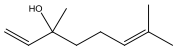 40.4	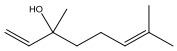 0.4	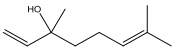 30.9	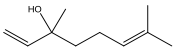 66.2
1-Octen-3-ylacetate	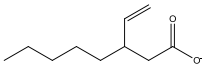 1.0	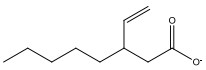 0.6	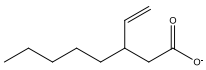 1.2	0
Allo-ocimene	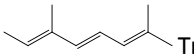 Tr	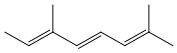 0.2	0	0
***trans*-Sabinol**	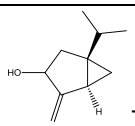 Tr	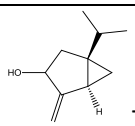 Tr	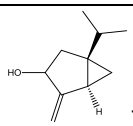 Tr	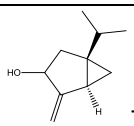 Tr
Camphor	 0.3	0	 0.4	Tr
3-Neo / 3-Neoiso-thujanol	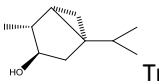 Tr	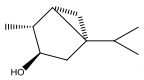 Tr	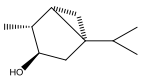 Tr	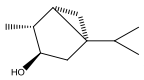 Tr
Borneol	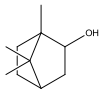 0.8	0	0	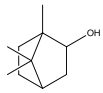 2.7
Terpinen-4-ol	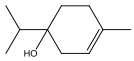 3.1	Tr	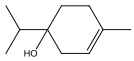 2.7	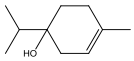 1.4
Cryptone	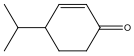 0.4	0	0	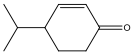 1.2
Hexyl butanoate	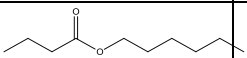 0.1	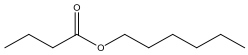 0.3	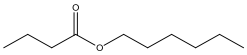 0.1	0
α-Terpineol	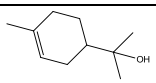 1.7	Tr	Tr	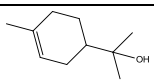 4.8
Isobornyl formate	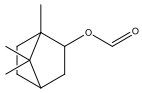 0.2	0.1	0	0
Cumin aldehyde	0.2	0	0.2	0
Linalyl acetate	30.2	17.5	49.8	0.1
Tetrahydro-lavandulylacetate	Tr	Tr	Tr	0.1
Lavandulyl acetate	2.0	0.4	3.2	0.1
Hexyl tiglate	Tr	Tr	0	0

Neryl acetate	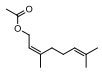 0.4	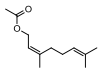 0.1	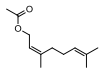 0.6	0
α-Copaene	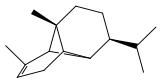 Tr	0	0	0
Linalyl isobutanoate	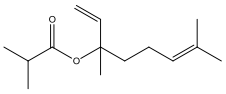 0.8	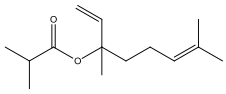 0.1	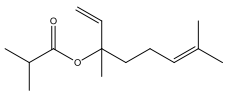 0.1	0
β-Bourbonene	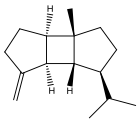 0.8	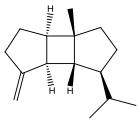 0.1	0	0
7-*epi*-Sesquithujene	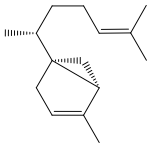 0.1	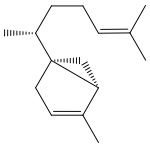 0.2	0	0
***cis*-α-Bergamotene**	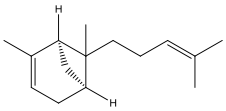 Tr	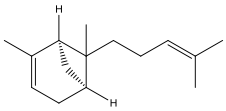 0.1	0	0
(*E*)-Caryophyllene	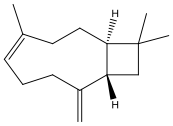 4.9	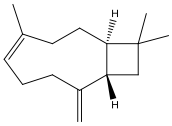 20.7	Tr	0
***trans*-α-Bergamotene**	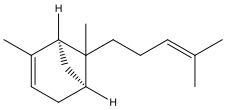 0.2	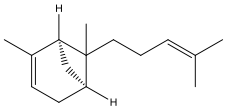 0.7	0	0
(*E*)-β-Farnesene	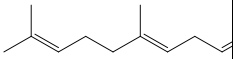 1.5	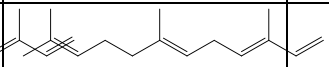 6.3	0	0
γ-Muurolene	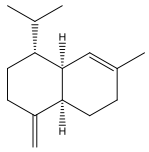 0.5	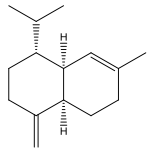 2.1	0	0
γ-Cadinene	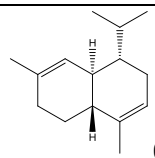 0.2	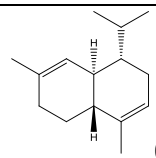 0.8	0	0
Caryophyllene oxide	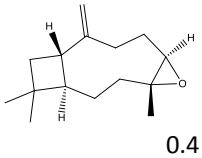 0.4	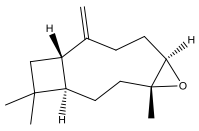 0.1	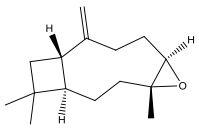 0.4	0